3D seismic architecture of Pleistocene submarine channels and lobe complexes in the thin-skin deformed slope of the Levantine Basin

Master Thesis in Petroleum Geoscience

Evangelos Kaikas

Department of Earth Science

University of Bergen

June, 2013

ABSTRACT

The current study describes the architecture of Pleistocene-Holocene depositional features that is affected by the underlying structurally topography. The study area is located offshore Israel, at the Levantine Basin of the southeastern Mediterranean sea and is part of the eastern Nile's middle to lower submarine fan at depth of approximately 1200 m. The underlying topography in the study area is controlled by thin-skinned tectonic deformation resulted from the underlying mobile Messinian salt sequence.

Previous work in the area of study has delineated several turbidite channel levee systems that are fed and has described in details qualitatively and quantitatively the most well illustrated depositional features in terms of interaction between the evolution of the depositional systems and the surrounding structures. This study is focused on the turbidite systems that have not been mentioned before or if they have been mentioned and they have not been described in details.

The analysis of the data is based on the seismic interpretation of 3D HR seismic data and the extraction of attribute maps that cover an area of 1400 km^2. Based on the attribute maps in combination with the seismic lines, qualitative and quantitative measurements took place for the main depositional elements of interesting, with the small scale lower submarine fan turbidite channel levee complexes to be the dominant sedimentary features in the area.

The depositional system of the study consists of five different seismic Facies with Facies 1: channel fill deposits (HAR's), Facies 2: channel levee deposits, Facies 3: mass transport deposits, Facies 4: frontal splays or crevasse splay deposits (HARP's) and Facies 5: hemipelagic or sheet like turbidite deposits. The oldest system consists of a channel system while the most recent depositional feature is a turbidite channel system which ends up to frontal splay deposits.

Based on the observations from the interaction between the depositional features and the deformed structures in the study area four models were created and an attempt to interpret external factors that control the stratigraphy of the Syn-tectonic sequence such as sea-level flunctuations took place.

ACKNOWLEDGEMENTS

Contents

1. Introduction

1.1 The aim of the present study

The purpose of the present study is focused on the interaction between the depositional systems consist of submarine channels and frontal splay deposits and the underlying structures of the deep Levantine Basin that are deformed from thin-skinned tectonics. Previous workers have describe the turbidite channels of the northern part of the area covered by the dataset in details, however, a detailed analysis of the southern most part has not been described in details and some of the depositional features described were unknown prior to this study.

Based on the integrated seismic facies analysis the thesis intends to analyze the following:

1) To perform a detailed seismic facies analysis of the different depositional systems of deep water settings through the study area of main focus by dividing the Pleistocene sequence into five subsequences.

2) To describe the interaction between the evolution of the submarine channels and the surrounding deformed by salt tectonics structures.

3) To infer the factors controlling the transport and deposition of the different depositional systems described from the facies through a sequence stratigraphic framework.

1.2 The study area

The Levantine basin *(Figure 1.1)* occupies a considerable part of the southeastern Mediterranean Sea and is considered as a relic of the Mesozoic Neo-Tethys ocean (Garfunkel, 2004). It is bounded *(Figure 1.1)* to the north by the subduction zone and transform fault of the Cyprian Arc plate boundary of the southern edge of Eurasia, to the south by the continental margins of Egypt and Sinai where the north eastern segment of the Nile deep sea fan is located and all together constitute the northeastern edge of the African plate, to the east by the passive continental margins of Israel, Lebanon and Syria and the Eratosthenes Seamount west (Vidal et al., 2000).
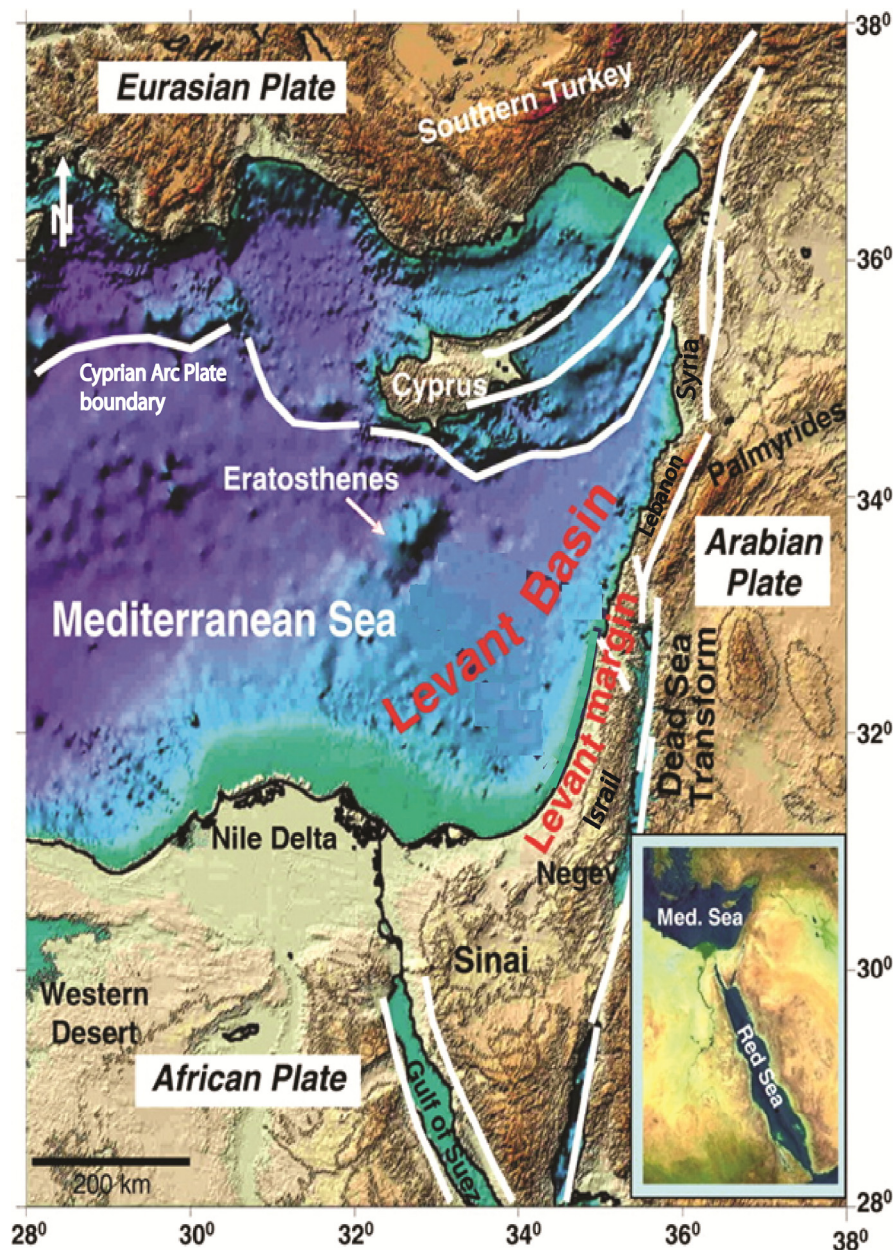
Figure 1.1: *The Levantine basin with the boundaries (the thick white line represent the plate boundaries) (modified from Gardosh et al., 2010).*

2

From the deep Levant basin the segment of main focus where the data are derived from belongs to an easternmost segment of the middle to lower fan region of the Nile deep sea fan complex (***Figure 1.2***) located offshore Israel, a few tens of kilometers away from the W-NW dipping slope of the Israil's passive margin (Folkman and Mart 2008) and approximately 120 km from the north shoreline of Sinai on the N-NE dipping slope of the Sinai passive margin (Mascle et al., 2000; Segev et al., 2006).
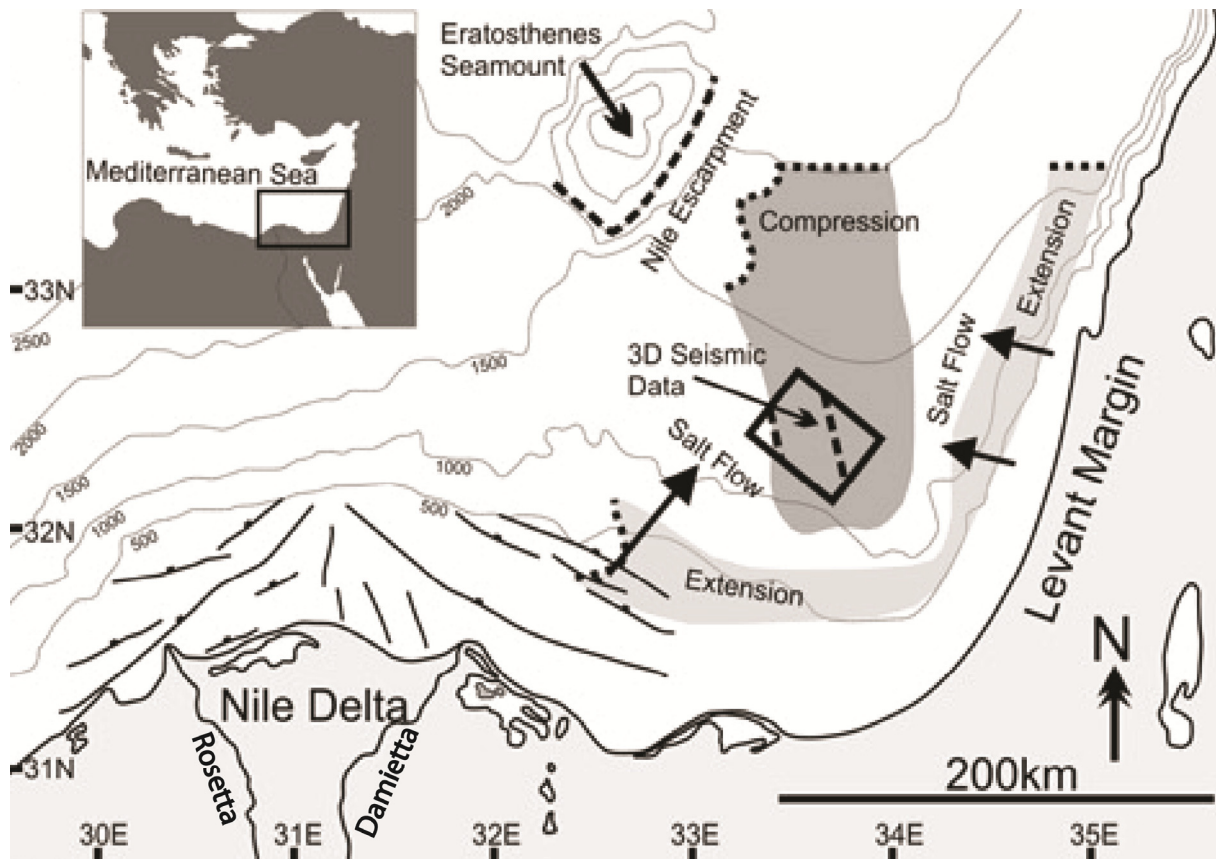
Figure 1.2: *The location and geological setting of the Gal_C 3D seismic survey used in this study (modified by Clark and Cartwright, 2011).*

The segment covers an area of 1400 km^2 and it is located at water depths of about 1000 to 1400 m where the seabed has a gentle gradient of approximately 0.45 degrees to the N-NE (Folkman and Mart 2008), 0.38 degrees at the downslope direction and 0.02 degrees in the cross slope direction (Clark and Cartwright, 2009). The area is dominated by a dense network of submarine channels that are fed from the Damietta (***Figure 1.2***) branch of the Nile (Folkman and Mart 2008) and have been developed in the deep-water compressional province of fold and thrust belt setting of the Levant basin where compressional deformation is driven by the up-dip collapse of the Nile cone to the south west in combination with the eastwards collapse of the Levant margin (Clark and Cartwright, 2011) above the ductile Messinian evaporites (Clark and Cartwright, 2009) that forming the detachment layer.

2. Deep marine depositional environments

2.1 Definition

As a deep marine environment in the modern oceans the term refers to the seaward from the shelf break (200 m depth) bathyal sedimentary environments from the continental slope, rise to the basin floor (*Figure 2.1*). However the depth threshold from the shallow to the deep water environments is different from place to place (Shanmugam, 2006). The continental rise, which represents that part of the continental margin between continental slope and abyssal plain, is included under the broad term "basin."
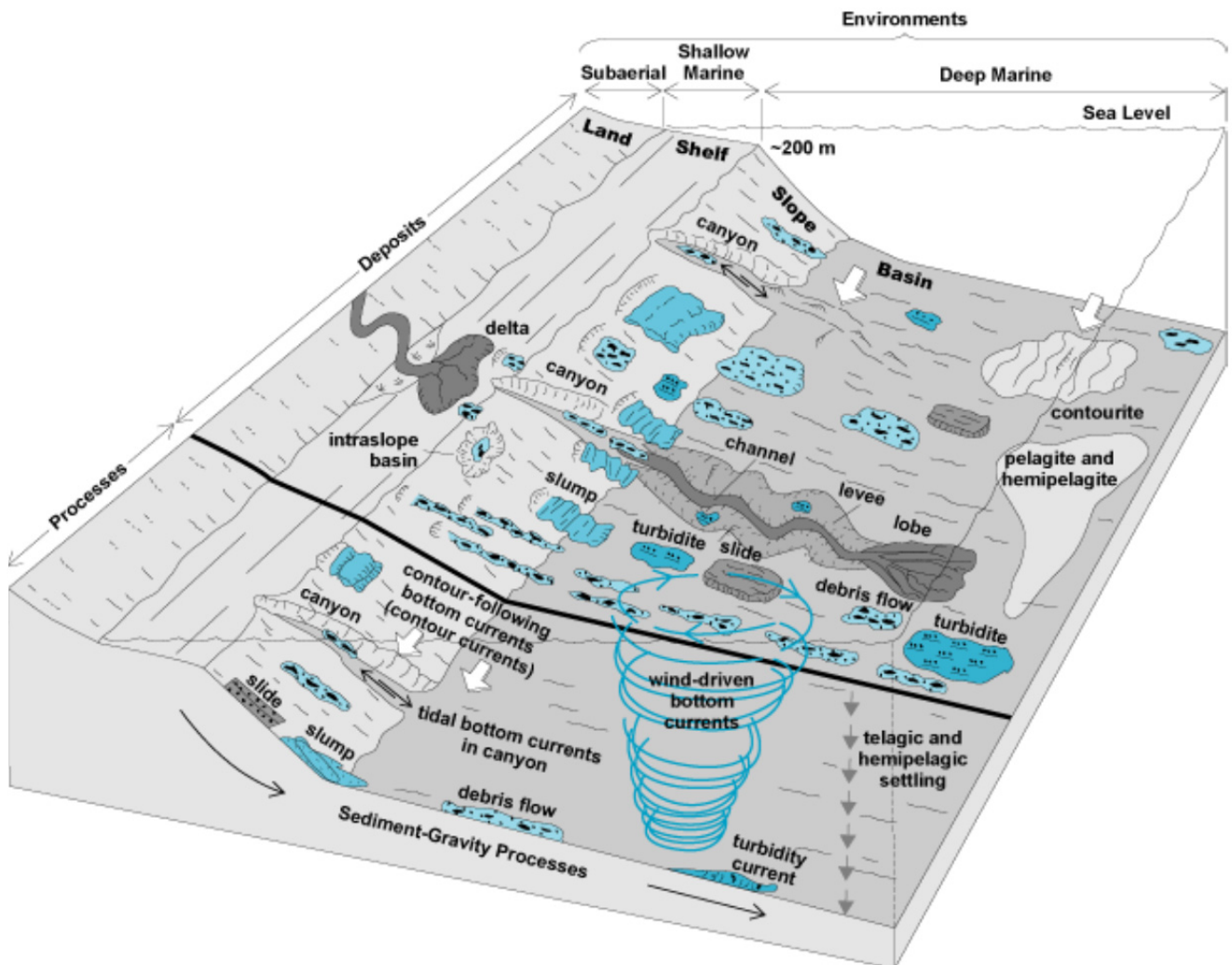
Figure 2.1: Slope and basin deep marine depositional environments (Shanmugam, 2006).

The rapid development of the knowledge for the deep marine sedimentary started in the mid 1980's. The initiation of the deep water research was the result of a communication disruption when the communication cables between the North America (on the southern margin of the

Grand Banks-east coast of Canada) and Europe were successively deactivated in an offshore direction after an earthquake on 18 of November 1929 (Heezen and Ewing, 1952).

2.2 Controlling factors

The deep marine environments are controlled by three major factors *(Figure 2.2)*: tectonics, fluctuations of global relative sea level and climate which controls the sediment flux, the nature and composition of the sediment supply in the system (Reading and Richards, 1994). The interplay of these various factors determines accommodation space and sediment supply in the deep-water which influences the systems' facies association and depositional elements. Based on these processes the deep marine environments have been classified based on the morphology and their dominant grain size of the submarine fans that they consist from. From the twelve different types of classification the sedimentary system that represents the study area belongs to the category of the point source submarine fan mud rich systems.
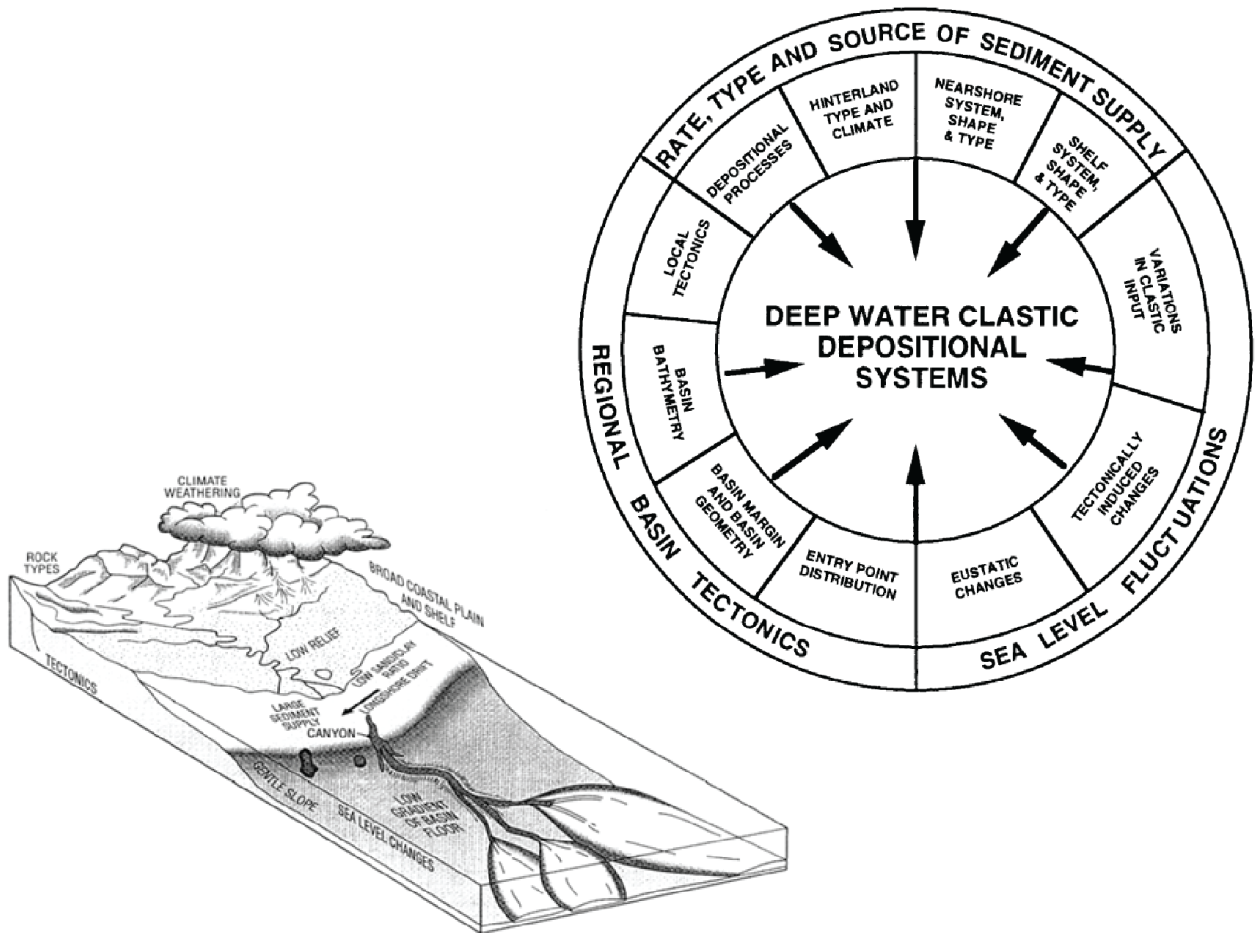
Figure 2.2: The main factors controlling the deep water deposition (Bouma, 2001, Richards et al., 1998).

2.3 Deep water processes and deposits

2.3.1 Mass Transport Deposits

Mass transport deposits (***Figure 2.3***) cover areas of thousands square kilometers when they are resulted from instability processes near the shelf edge or the upper basin margin part and smaller scale deposits when they occur in a basin by local slope failure (Moscardelli and Wood, 2008). These deposits have internal content of slumps, slides and gravity-flows and where they occur, they are indicators of changes of the basin sedimentation.

The mass-movements of coherent to semi cohesive masses that can travel up to hundreds of kilometers are subdivided based on their intensity and internal deformation to slides and slumps. These types of deposits occur when the gravity exceeds the tensile strength of the sediments, they travel hundreds of kilometers and stop when the frictional force exceeds the gravitational (Mulder and Alexander, 2001). Mass-movement deposits are separated from the gravity flows based on their internal deformation which is higher for the gravity flows (Middleton & Hampton 1973).
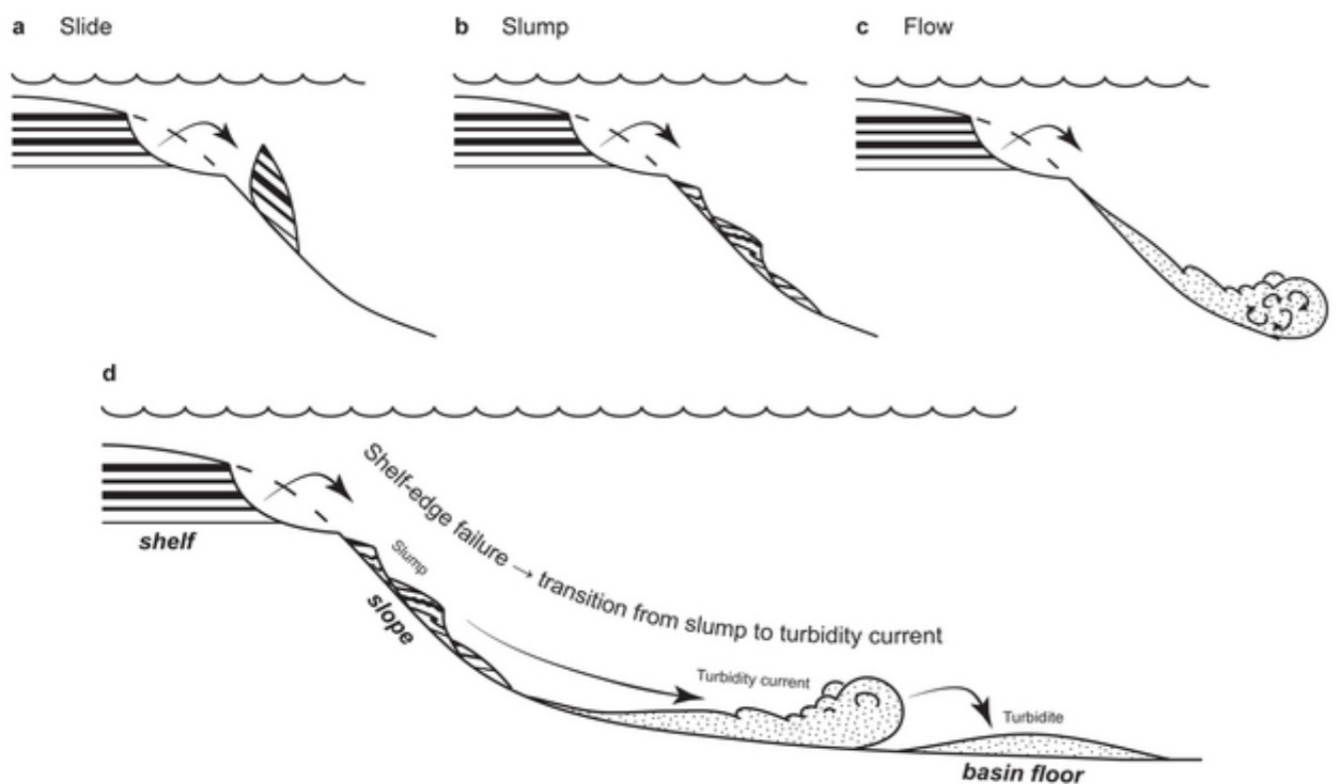
Figure 2.3: *Types of mass transport deposits based on the degree of internal deformation (Middleton & Hampton 1973).*

2.3.2 Sediment gravity flows and their deposits

Sediment gravity flows (*Figure 2.4*) are the main flows of mass-movement processes for deep water sedimentation of sand and gravel (Middleton & Hampton 1973). Silt and clay can be as well the result of sediment gravity flows but their main driving force is the suspension form the water column.
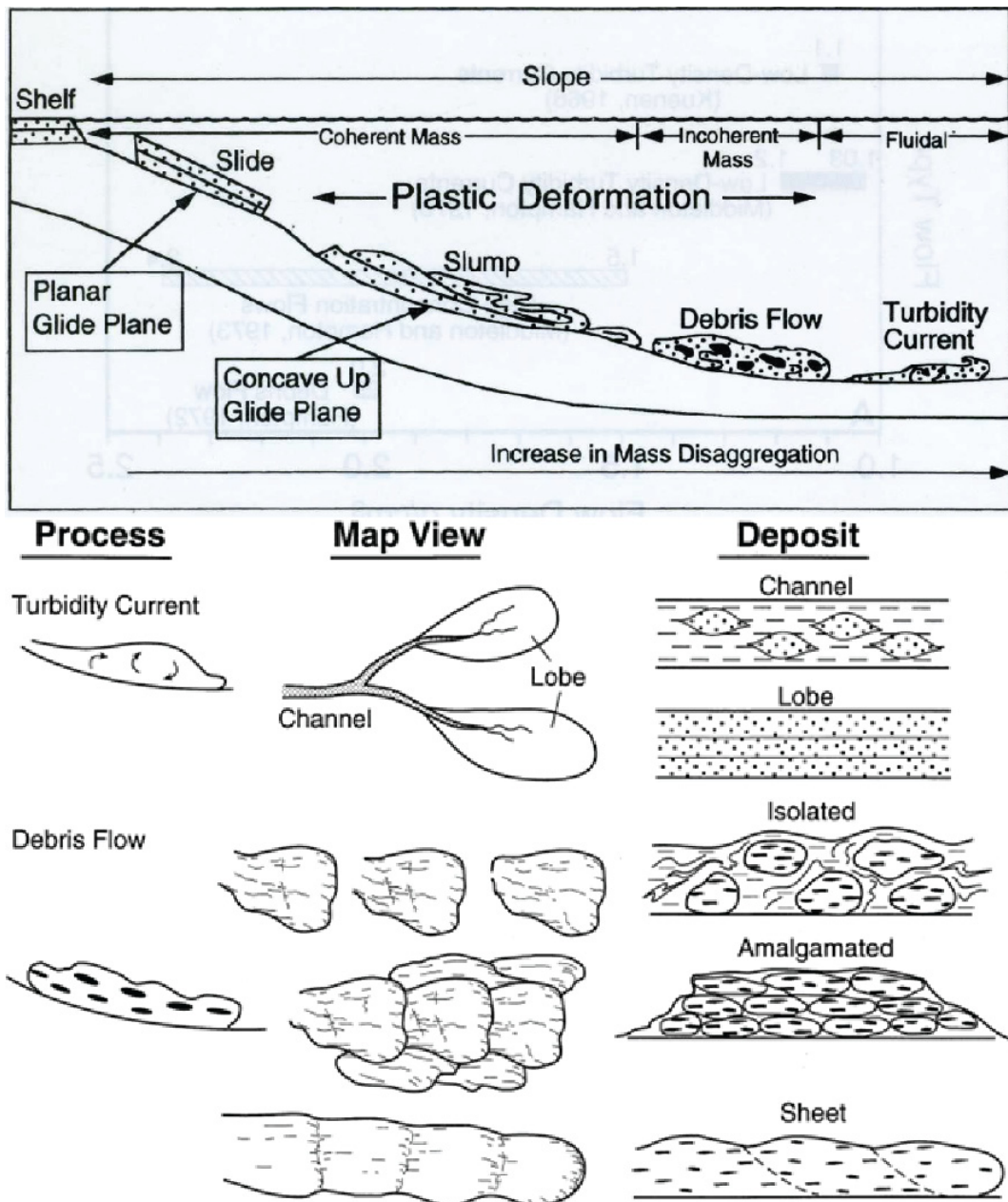
Figure 2.4: *Sediment gravity flows and their deposits (Shanmugam, 1996, 2000).*

The gravity currents occur because of the density contrast of a moving fluid of higher density because of suspended sediment and the surrounding less dense fluid that is displaced.

Sediment gravity flows have been divided into the following four end members based on the maintaining of the density contrast and the mechanism of suspended sediments: turbidity currents, debris flows, grain flows and fluidized/liquified flows (Mulder and Alexander, 2001).

Debris flows can travel over tens of kilometers and are cohesive mud flows which have the same order of phase magnitude between the volume of the solid and the fluid (Mulder and Alexander, 2001) and their deposits are characterized a sheet to lobe external geometry with steep margins. Their deposits range from mud to sand rich with a disorganized and poorly sorted character (Nemec and Steel, 1984).

Turbidity currents *(Figure2.5)* are frictional flow currents that are characterized from the head which is the most sediment rich part of the flow, the body and the tail (Kneller and Buckee, 2000). The responsible for the initiation of turbidity currents force is a function of the slopes angle and length, the thickness of the suspension currents and the difference in density between the surrounding water and the suspension.
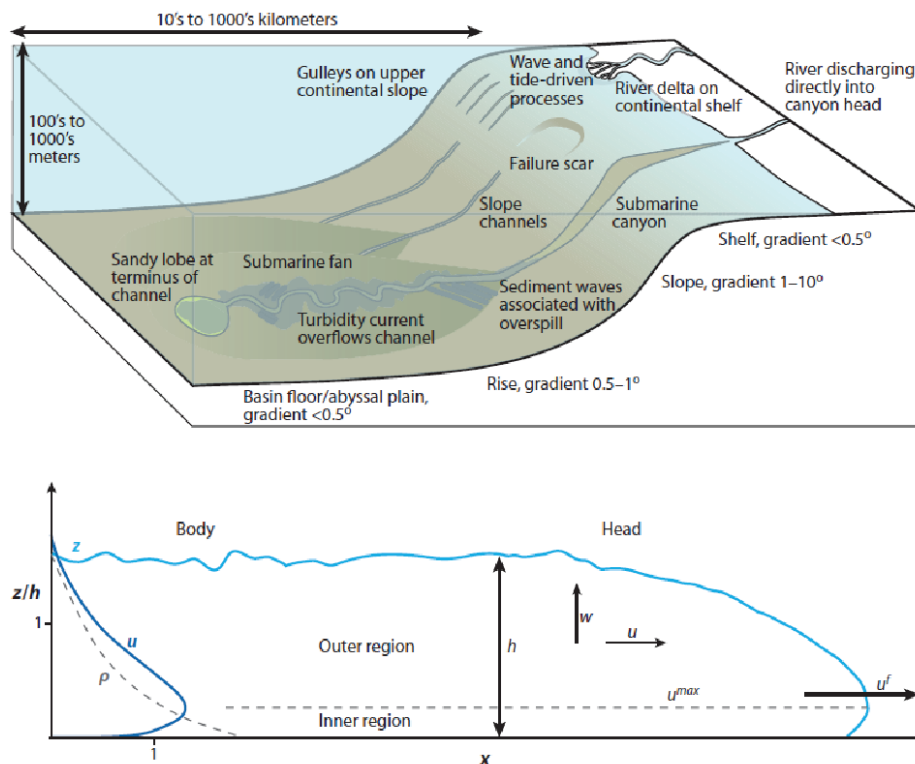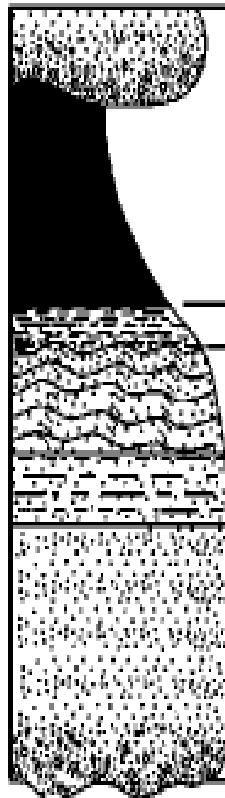
Figure 2.5: Turbidity current (Meiburg and Kneller, 2010).

"Confined turbidite systems are those deepwater clastic depositional systems whose development has been fundamentally constrained by pronounced basin-floor topography" (Lomas and Joseph, 2004). The turbidite facies have been desribed since 1962 from Bouma who linked the sequence of the structures and their origin from turbidity currents and is known as the Bouma sequence *(Figure2.6)*. The facies model of a turbidite consists of an ascending order of vertical sequence of structures that has been subdivided into the five

internal divisions: Division a (lower part)-Ta which is basal normally graded or massive, Division b-Tb which is lower parallel laminated, Division c-Tc which with current ripples and is convolute laminated, Division d-Td which is upper parallel laminated and Division e (upper part)-Te which is uppermost pelitic

Grain Size		Bouma (1962) Divisions	Middleton and Hampton (1973)	Lowe (1982)	This study
Mud	Te	Laminated to homogeneous	Pelagic and low - density turbidity current	Pelagic and hemipelagic	Pelagic and hemipelagic
Sand-silt	Td	Upper parallel laminae	Turbidity current	Low-density turbidity current	Bottom-current reworking
	Tc	Ripples wavy, or convoluted laminae			
	Tb	Plane parallel laminae			
Sand to granule at base	Ta	Massive, graded		High-density turbidity current	Sandy debris flow (Turbidity current, if graded)

Figure 2.6: The classic Bouma sequence and the conventional interpretations (Shanmugam, 1997).

Basin floor depositional elements

"Elements are the basic mapable components of both modern and ancient turbidite systems and are characterized by a distinctive assemblage of facies and facies associations" (Mutti and Normark, 1991). Turbidite deposits are observed on the basin floor and based on Posamentier and Kolla, (2003) they are consisted from the following five key elements: 1) turbidite levee channels, 2) channel overbank deposits, 3) frontal splays, 4) crevasse splays and 5) debris flows (*Figure2.7*).
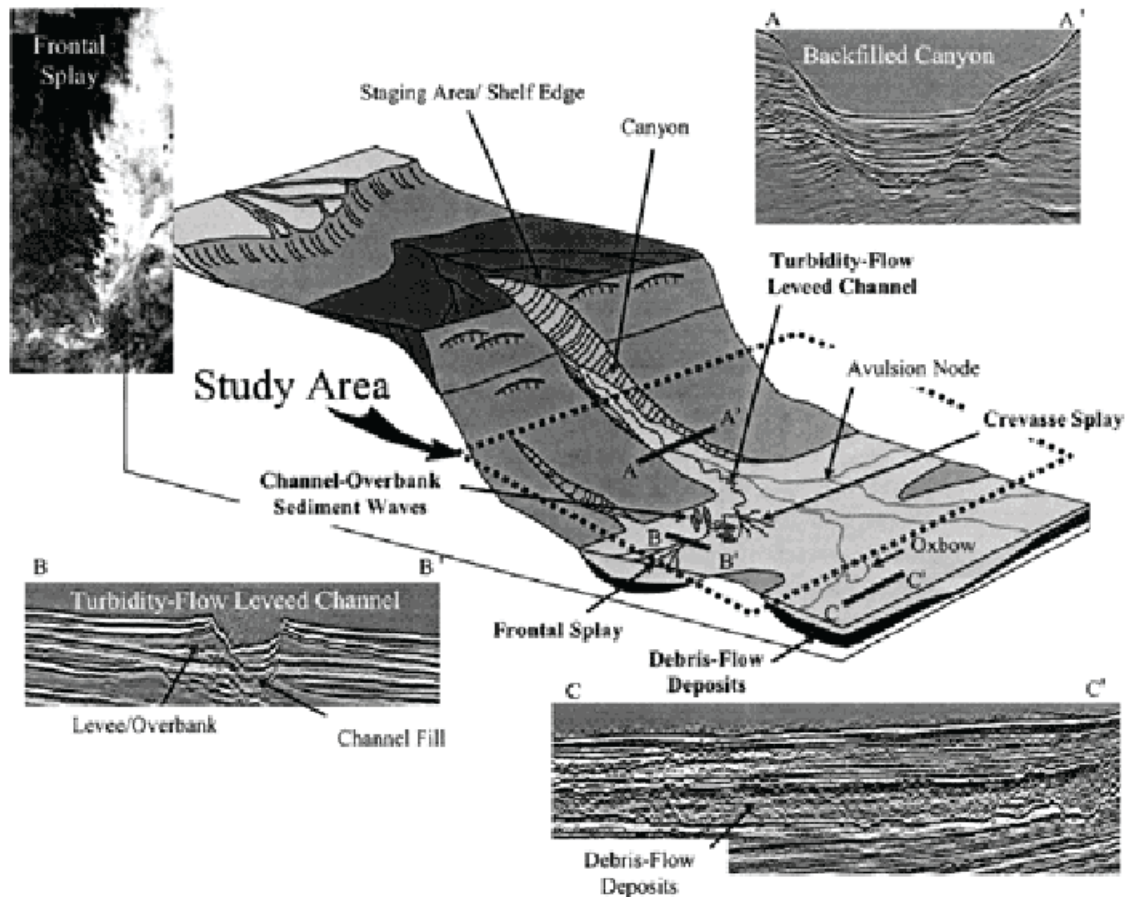
Figure 2.7: *The main elements of the basin floor turbidite deposits (Posamentier and Kolla, 2003).*

The turbidity systems represent highly confined channels that end to be unconfined from up-flow to down-flow respectively (Posamentier and Kolla, 2003). In the up-flow part of the turbidity system the flow is confined and erosion occurs, further down-slope the confinement is decreased and deposition occurs with the subsequent levee development and at the transition zone when the flow is unconfined the channel pass to a lobe (Lomas and Joseph, 2004).

Based on variations in the volume and the caliber of the sediment load the turbidite systems can be subgrouped into the following three types of turbidite systems: 1) deposits consisted mainly of thick-bedded, unchannelized sandstone lobes and sheets, 2) deposits consist of channelized sandstones with associated thin to thick bedded lobes and mud rich deposits consisting of small scale sandstone channel fills and thick mudstone and siltstone levee/overbank deposits (Mutti, 1985).

Overbank/Levee deposits

These deposits are thin bedded fine grained, are located adjacent to the main turbidite channel and are laterally extensive. They can be subdivided into two types with the first one to be related with positive relief along the active channel margins where the levee relief is negative and the distal parts without major relief (Mutti and Normark, 1987).

10

Crevasse splays

Crevasse splays are formed along the outer channel bends and occur when the levees of a channel breached. At the area of the channel breached the crevasse splays transferred through the crevasse channel (Posamentier and Kolla, 2003).

 Channel-lobe transition zone

The transition (*Figure 2.7*) occurs when the turbidity currents pass from a high gradient area of channelized and confined conditions to a gentler slope unconfined area (Mutti and Normark, 1987). This zone reflects the hydraulic jump that transforms the turbidity current through erosion caused from the increased turbulence and deposition. The hydraulic jump in that area except of the erosion produces as well dilution and enlargement of the flow (Ravenne and Beghin, 1983).

Depositional Lobes

Lobes are deposited in the proximal part of the basin floor and represent the maximum down-current extent of the transported to the basin sand. They have channels without levees and the turbidity currents in combination with the size of the basin and the system control their extend (Mutti, 1985).

The depositional lobes can be further subdivided into the following three architectural elements (Meyer and Ross, 2007):

1) Deep channels that have locally steep margins, incision up to a few of ten of meters and they are the main sediment supply conduit of the depositional lobe.

2) Shallow channels that form a distributive network located down-flow of the deep channels and have a scour with a depth of a few meters.

3) Downflow of the shallow channels the flow becomes unconfined which results in high deposition rate and the formation of a frontal splay.

2.3.3 Submarine fans

Submarine fans are defined as '' terrigenous, cone or fan shaped deposits located seaward of large rivers and submarine canyons.'' (Gary et al., 974). They are consisted from mass movements with the most dominant to be the turbidites. The mass-movement flows are affected by the seabed topography (Kneller and Mc Caffrey, 1999) and during the deposition of the submarine fan can be transformed from slides and slumps to sediment-gravity-flows as their fluid content is increased from proximal (shelf edge) to the distal (basin-floor) respectively (Fischer 1983).

Submarine fans have been subdivided into upper fan, middle fan and lower fan form proximal to distal respectively based on their sediment erosion and deposition spatial patterns

(Pirmez et al 2000). The upper part belongs to the uppermost slope and is characterized by erosion and sediment bypass, the middle part is an area of deposition resulted from flow expansion because of flow unconfinment and the lower part which is located to the basin floor, is characterized from decrease of deposition (Pirmez et al, 2000).

The deep sea fans are subdivided based on their grain size (from gravel to mud) and the deep-marine fan of this study belongs to the category of the mud rich deep sea fans (*Figure 2.8*) which are fed from point sources of major rivers. The transportation of the sediments occurs from pro-delta sediment gravity flows or from concentrated suspension currents from the river (Reading and Richards, 1994). This category of submarine fans is consider to represent decrease in grain size, slope gradient, flow frequency and channel migration.
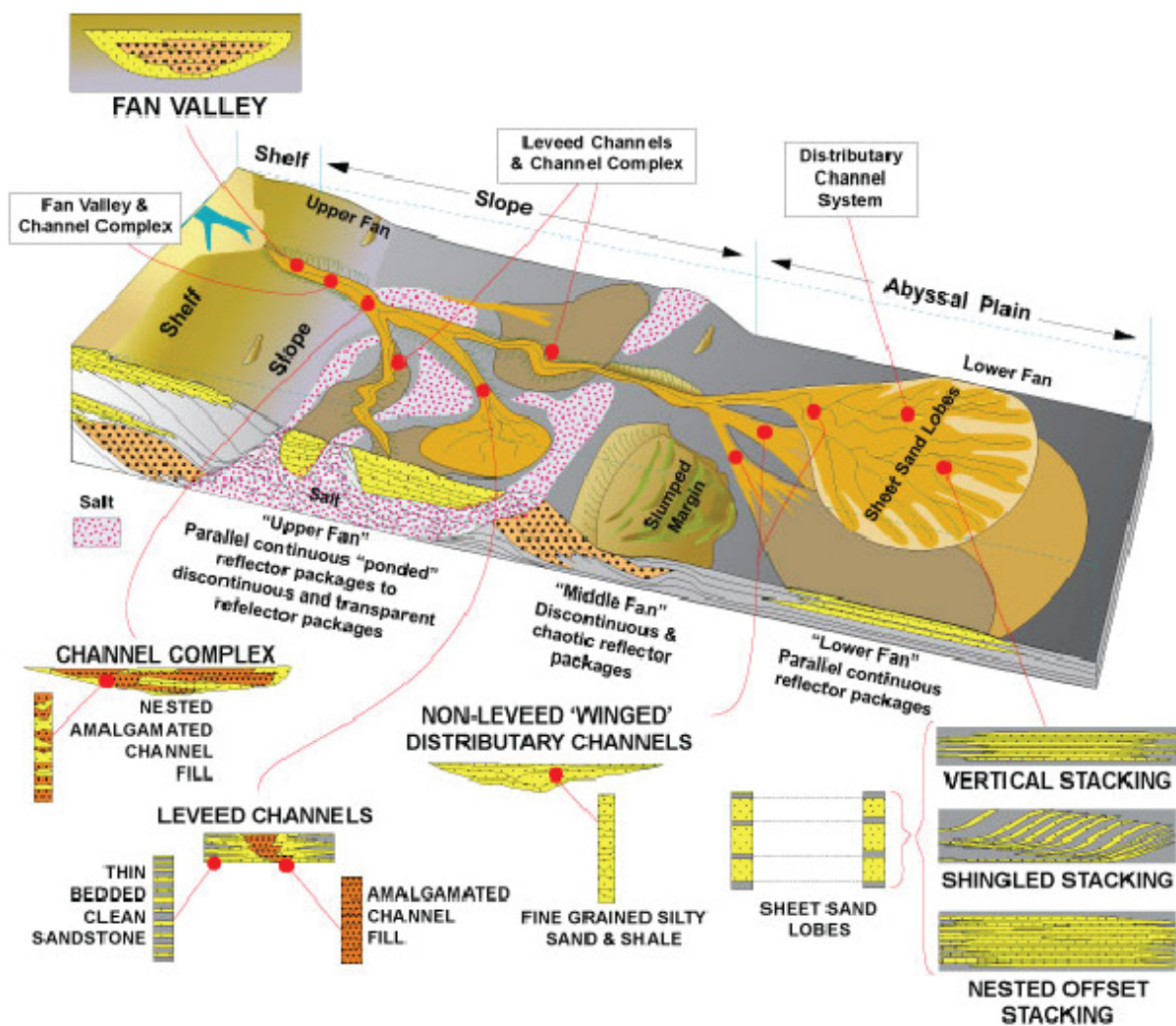
Figure 2.8: Mud rich fine grained submarine fan (DeVay et al, 2000).

2.3.4 Submarine channels

"Channels are elongate negative relief features produced and maintained by turbidity current flow and represent major relative long term pathways for sediment transport" (Normark 1970) while Mutti (1977) defined a submarine channel as a long-term conduit for the down-slope transport of sediment. On modern submarine fans there are two types of channels: the primary sediment feeder systems of large leveed valleys and smaller un-leveed distributary channels (Normark 1970).

Channel fill

There are three types of channel fill deposits *(Figure 2.9)*: 1) erosional channel fill deposits where basal coarse grained deposits are overlain by finer channel abandoned deposits. 2) depositional channel fill deposits that infill the channel after its main activity process. 3) Mixed type deposits which are a combination of the two types that have been mentioned (Mutti and Normark, 1987).

A. Erosional

B. Erosional/depositional (mixed)

C. Depositional

Figure 2.9: *Channel fill deposits (Mutti and Normark, 1987).*

Contrasting low sinuosity fan channels producing sheet sands by lateral migration with high sinuosity channels with abundant spillover producing ribbon sands in an aggrading package of levee deposits. The channel deposits can be divided into two end members, erosional and aggradational. Erosional channel deposits tend to occur on smaller fans and are usually low sinuosity channels with low levees transporting coarse sediment at down relatively steep slopes, avulsion is frequent and locally is achieved a high degree of channel deposition density. Aggradational channel deposits are high sinuosity channels with large levees on gentler slopes (Clark & Pickering, 1996).

2.3.5 Submarine channel development affected by seabed deformation

The interaction of submarine turbidity channel evolution on their flow downslope and the surrounding deformed topography have been documented by several authors (Clark and Cartwright, 2011,2009; Mayall et al., 2010, Cross et al., 2009; Gee and Gawthorpe, 2006, Ferry et al., 2005, Huyghe et al., 2004, Smith, 2004).

The different patterns of channel development are the result of channel structure interactions through the following four end members (***Figure 2.10-1)*** (Clark and Cartwright, 2009): confinement, blocking, diversion and deflection.

 Confinement results in restriction of the channel, its levees and lateral migration because of pre-dated from the channel structures that are inactive. The degree of confinement depends on the scale and number of the surrounding structures and in the case of non-active structures can be decreased with aggradation of the channel.

Blocking occurs when the flow of a submarine channel downslope is prevented by the uplift and the orientation of a structure relative to the channel flow which results in blocking and backfilling. Blocking of the channel system can occur as well at enclosed intra slope basins because of the growth of coalescing structures.

Deflection occurs when the structure that grows on the same time with the channel's development (Clark and Cartwright, 2009) is of a small scale (less than 5 km) (Mayall et al., 2010) but in the case of increase in the relative rate of the structure's growth in combination with decrease in channel erosion and deposition can create transition from deflection to blocking (Clark and Cartwright, 2011). Opposite if the relative rate of the growth uplift of the structure is smaller than the relative rate of channel erosion, the channel will maintain it's original flow path direction downslope by cutting across the structure.

Diversion is the lateral shifting of the channel flow path around a large-scale (more than 5 km) (Mayall et al., 2010) slope inactive pre-existed structure (Clark and Cartwright, 2009) which is and can be accompanied by resuming of the initial flow path after the channel have passed the structure. The channels can be inhibited by large-scale structures and flow parallel to the slope over long distances (Mayall et al., 2010).

The channel development affected of deformation has been described as well in terms of levee geometries *(Figure 2.10- 2)* (Clark and Cartwright, 2011). The levee of confined channels, when the deformation and channel development are on the same time, are illustrated as tilted reflections that progressively rotate towards the base of the levee package while the levee are illustrated as onlap reflections on the flank of the structure when the structure pre-dates the channel development. In the case of unconfinement, the levee reflectors downlap onto the pre-channel development while when there is structure that post-dates the levee development then the levee is folded and incorporated on the crest of the growing structure.
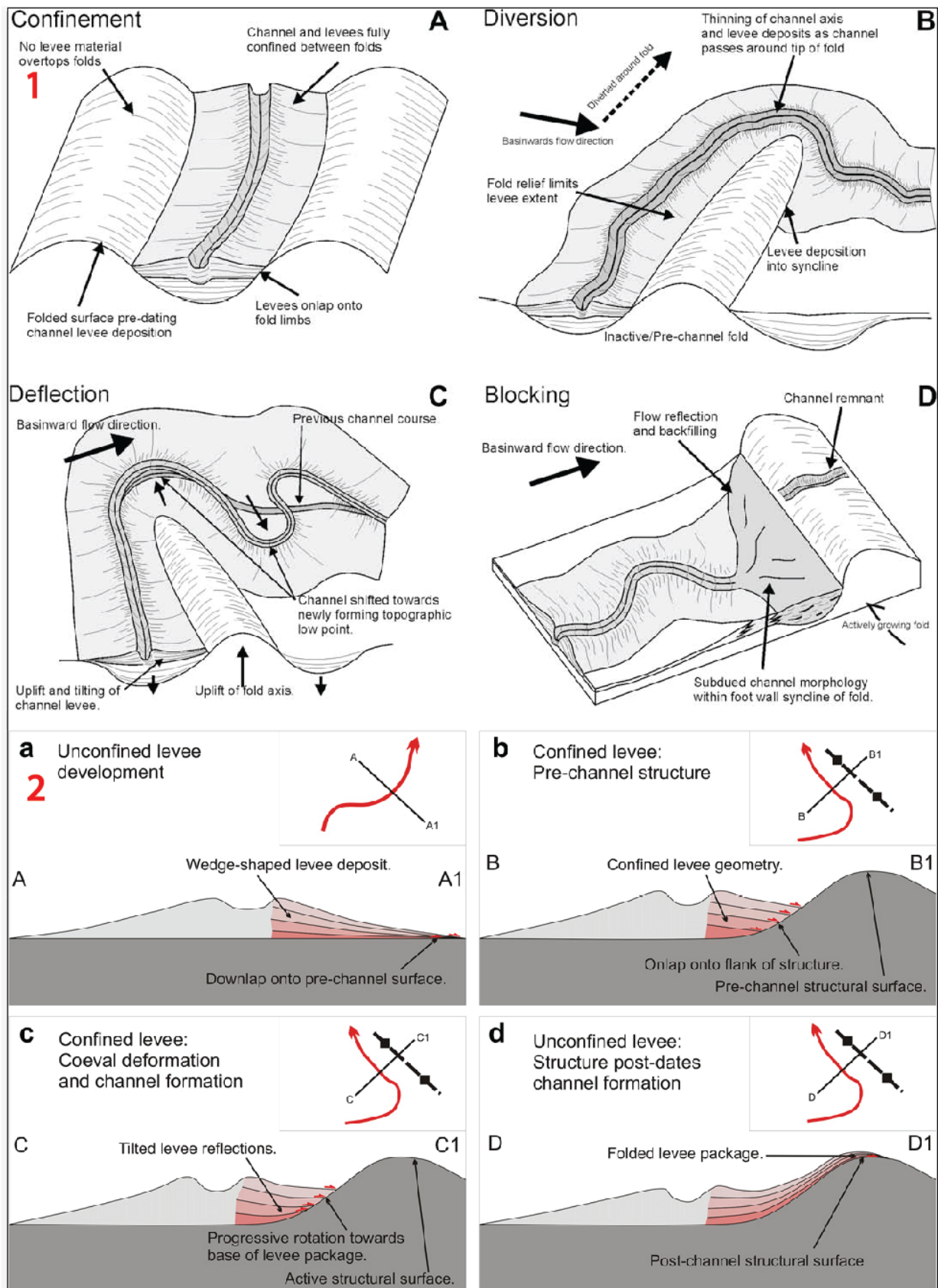
Figure 2.10: *Interactions between channel development and deformation based on1) four end members (from Clark and Cartwright, 2009) and 2) levee geometries (from Clark and Cartwright, 2011)*

Stratigraphy of deep water settings

An ideal model of a deep-water sequence based on Posamentier and Kolla (2003) consists of one cycle of relative sea level change with the initiation of the cycle during relative sea level fall and the ending during the relative sea level rise with the an idealized depositional sequence (*Figure 2.11*) consists of mass transport deposits on the base on the base, capped with turbidite deposits subdivided into the upper channel levee complex and the lower part consists of frontal splay deposits. Another mass transport deposit overlain the channel levee complex and the sequence ends with a condensed section of sediments deposited through suspension from the water column.
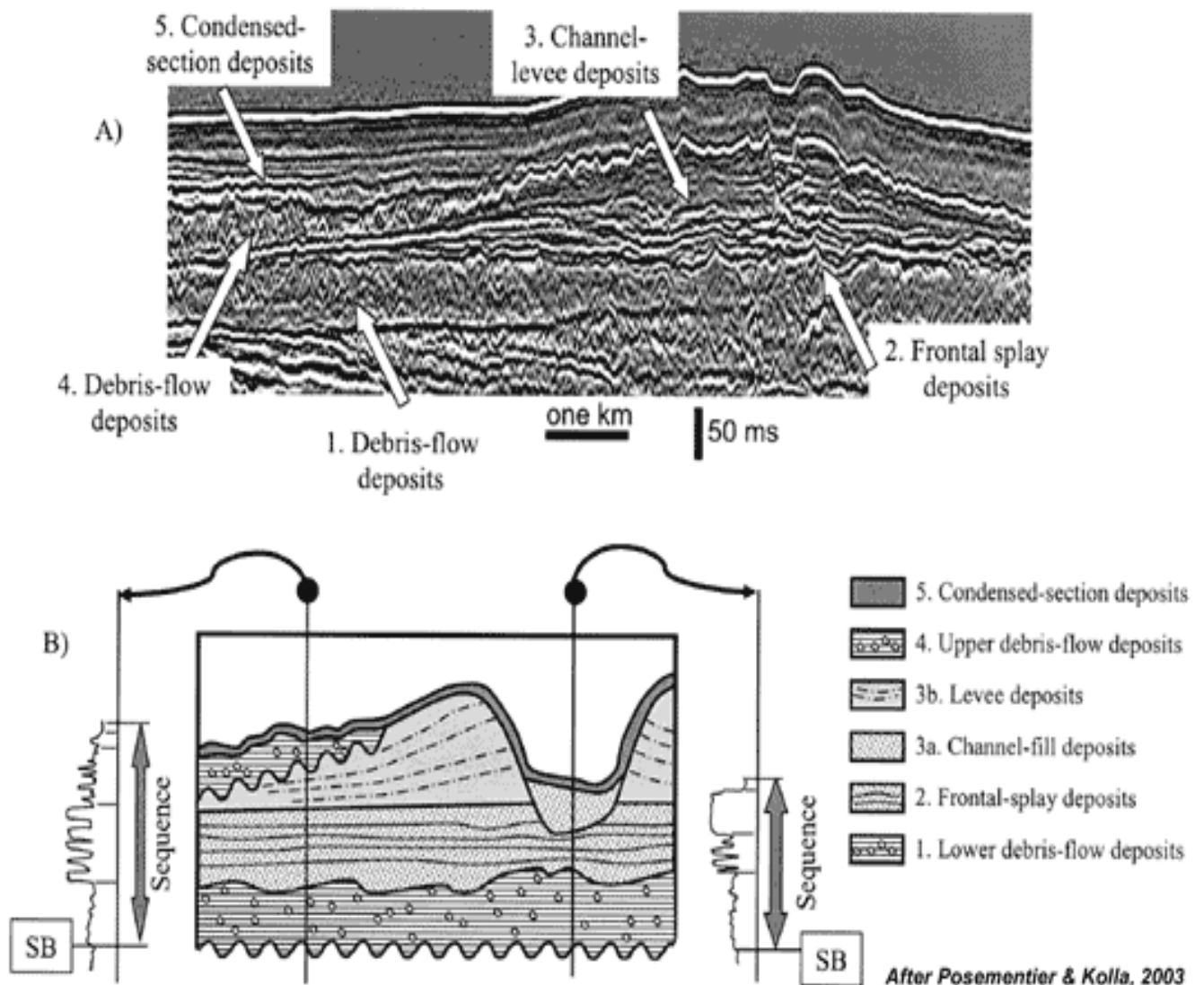
Figure 2.11: A) *Seismic profile representing the stratigraphic succession of a deep water sequence and B) the resulted interpretation model (Posamentier and Kolla, 2003).*

3. Regional geology

3.1. Historical evolution of the basin

The basin is located at an area with complex tectonic regime resulted from the interaction of four plate *(Figure 3.1)*. The north-north west moving Arabian plate, the northward moving African plate, the westwards moving Anatolian plate and the postulated Sinai sub-plate (Mascle et al., 2000).These plates interact forming a complex tectonic environment and make the basin and its margins key areas for understanding the geodynamic evolution of the eastern Mediterranean (Mascle et al., 2000).
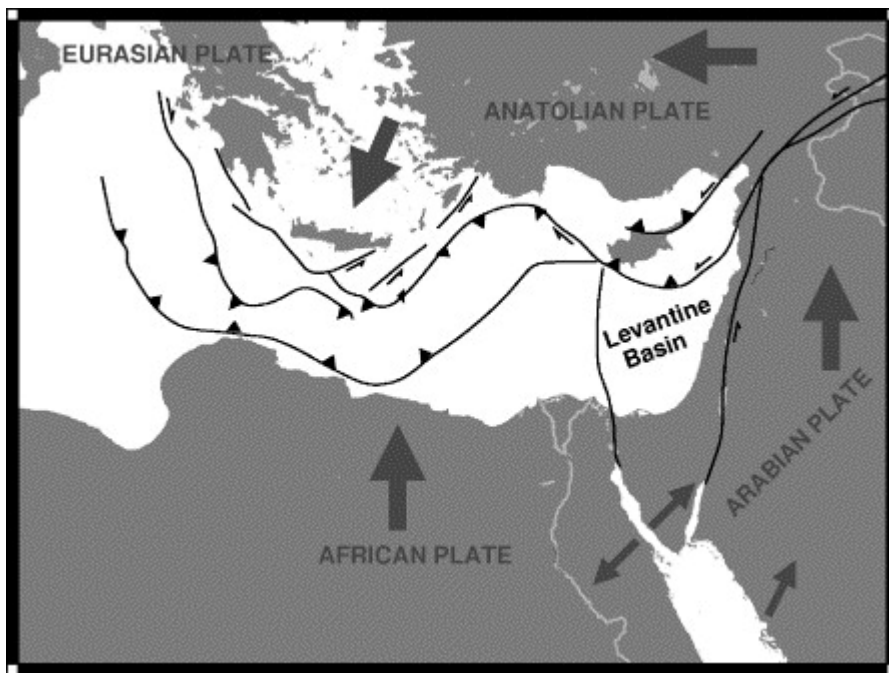

Figure 3.1: *Simplified tectonic map of the Eastern Mediterranean Sea. Arrows indicate the sense of plate motion, half arrows indicate transform/strike-slip faults (Netzeband G.L. et al., 2006).*

During the initial break-up of the Pangea from Early Permian to Middle Jurassic a sequence of rifting events resulted to the formation of the basin and the adjacent margin. At the late Cretaceous the development of the Syrian Arc Fold belt with combination of compression resulted in the creation at the Levant Margin of a fold series with NE-SW direction (Garfunkel, 1998).

14 Ma ago the Mesozoic Neotethys lost its connection to the Indo-Pacific Ocean in Middle Miocene (Gvirtzman and Buchbinder, 1987). The combination of different factors such as climatic conditions, sea level change and tectonic uplift during Late Miocene (5,3-5,9 Ma ago) resulted to a narrowing of the western passage of the Mediterranean sea to the Atlantic ocean followed by the Messinian Salinity Crisis (Hsu et al., 1978). The subsequent

rise in the salt concentration finally lead to precipitation with a sea level drop about 800-1300 m and the creation of up to 2 km of evaporites deposited during that time (Druckman et al., 1995). Erosion along the marginal areas of the Levant Basin accompanied the events that mentioned above (Garfunkel and Almagor, 1987).

Increased rate of sediment influx and deposition derived from the Nile delta to the south west took part during Pliocene (Mart and Ben Gai, 1982, Tibor et al., 1992) with combination of huge water masses, resulted to the loading of the Messinian evaporites with subsequent subsidence of the Messinian sequence (Ben-Gai, 2005) which created a critical slope angle and was the main driving force for the thin skinned salt tectonics (Gradmann et al., 2005).

3.2 Structural regime

The post-Messinian sequence of the study area has been deformed because of the combination of tilting induced collapse of the Levant Margin and the basin-ward spreading of the Nile cone resulted from gravity collapse on the ductile Messinian evaporites

The ductile Messinian evaporites have been deformed from the combination of tilting induced collapse of the Levant Margin and the basinward spreading of the Nile cone resulted from gravity collapse (Loncke et al., 2006). This deformation affects the overling Post-Messinian sequence with the development of a set of thin-skinned strike slip faults and linked compressional (down-dip) and extentional (up-dip) domains (Rowan et al., 2004).

The strike slip faults of the Post-Messinian sequence can be traced from the top of the evaporitic sequence to the present day seafloor and represented from two dominant trends, northeast-southwest set of dextral strike-slip faults which are obscured by seabed submarine channels and an east-west trending set with sinistral displacement that reaves the seafloor (Clark and Cartwright, 2009). At zones of local transtension the strike-slip fault sets are characterized from the development of small scale pull-apart structures while small scale pop-up structures can be observed in zones of transpression (Clark and Cartwright, 2009).

A northwest-southeast trending fold belt (*Figure 3.2*) in the study area is associated with thrust faults with a dominant vergance towards the north-east. The folds have a symmetrical detachment fold style at the lateral tips of the individual thrusts (Higgins et al., 2007). The folds are characterized from a transported detachment fold style towards the centre

of many thrusts along strike (Mitra, 2002). That type of folds is associated with the development of depressions within the footwall and hanging wall synclines.
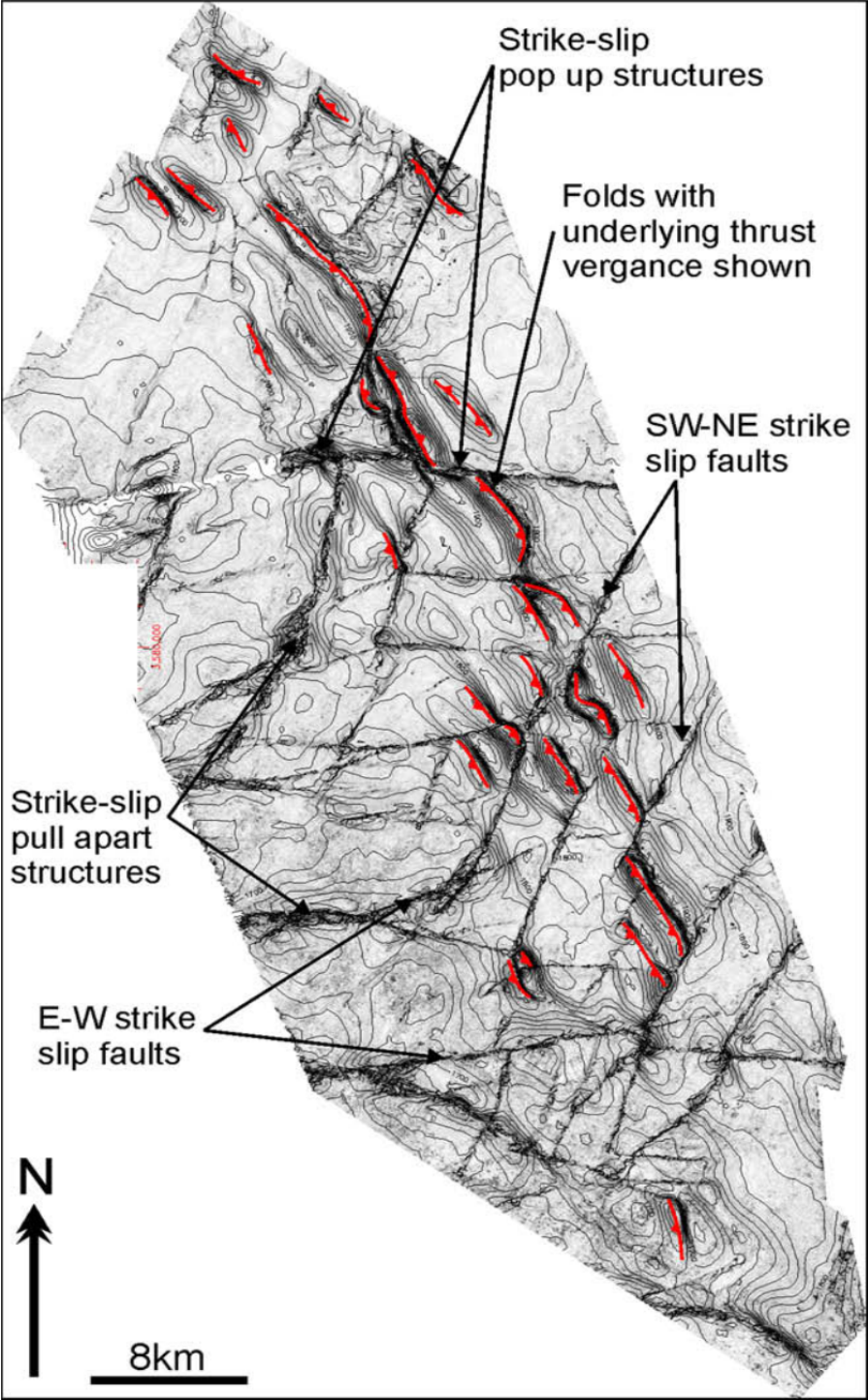
Figure 3.2: *The NW-SE trending fold belt and the strike slip fault structures of the study area (Clark and Cartwright, 2009).*

3.3 The Nile delta

The Nile's delta is concerned as arc shaped with a triangle plan view and erosive outer edges. It belongs to world class river deltas with an extension that covers an area of 240 km across the Mediterranean coastline and river length 160 km. The delta in the ancient times was divided on land to seven distributaries but in the present days due to climatic and tectonic processes it is divided only into two main active deltaic distributaries that correspond to two of the seven older, the Rosetta to the western delta and the Damietta to the eastern delta (*Figure 3.3*) that drain the area and flow to the Mediterranean sea (UNU, 1983).
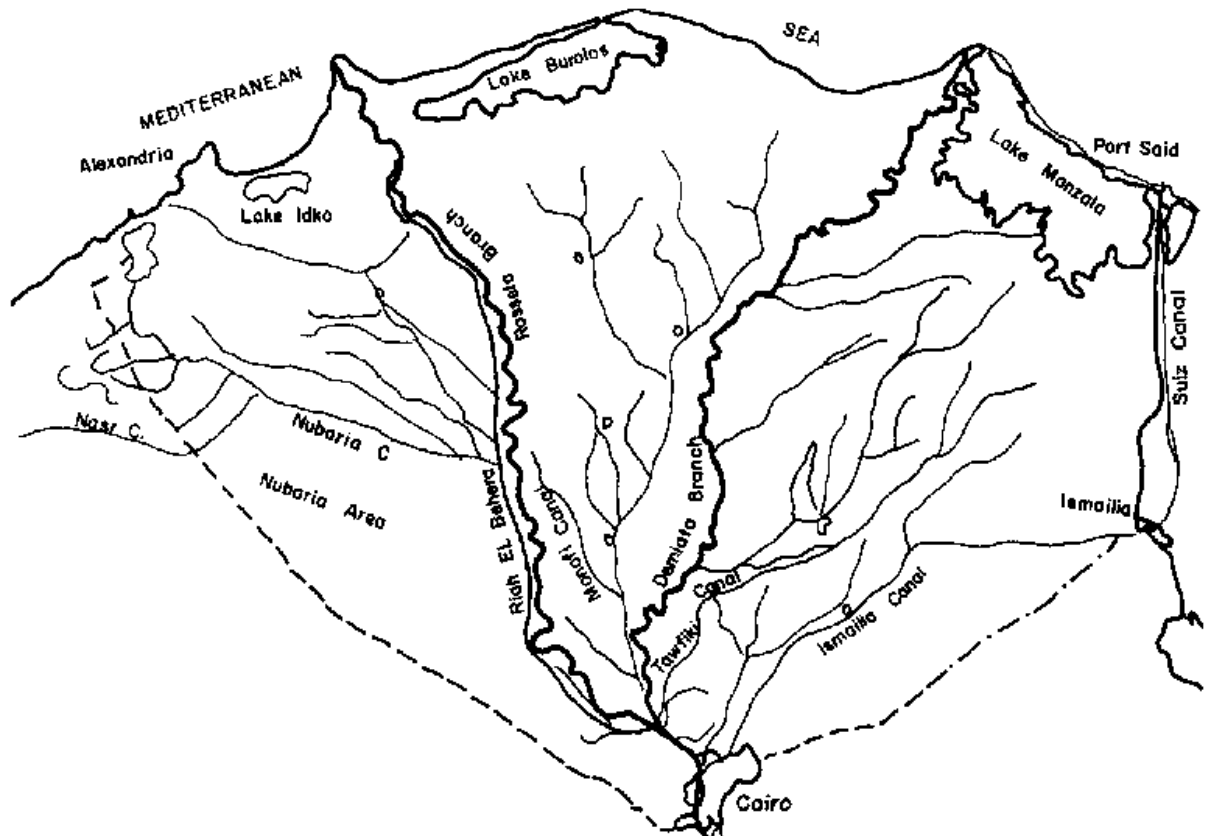
Figure 3.3: The Nile Delta and the two main distributaries Rosetta (western part) and Damietta (eastern part) (adapted from UNU, 1983).

3.4 The Nile deep sea fan

The development of the fan started by the influx of clastic sediments from the Nile River at the end of the Messinian Salinity crisis, during the latest Miocene and continue to evolve during the Holocene (Loncke et al., 2006). The Nile's deep sea fan *(Figure 3.4)* is a passive margin fan that covers part of an older passive margin formed in Jurassic and early Cretaceous during successive rifting episodes (Hirsch et al., 1995). The thick sedimentary wedge that forms the deep sea fan covers an area of approximately 100,000 km^2 with a

maximum thickness of approximately 4 km than thinning progressively towards the deeper areas of the south eastern Mediterranean Sea (Segev et al., 2006).
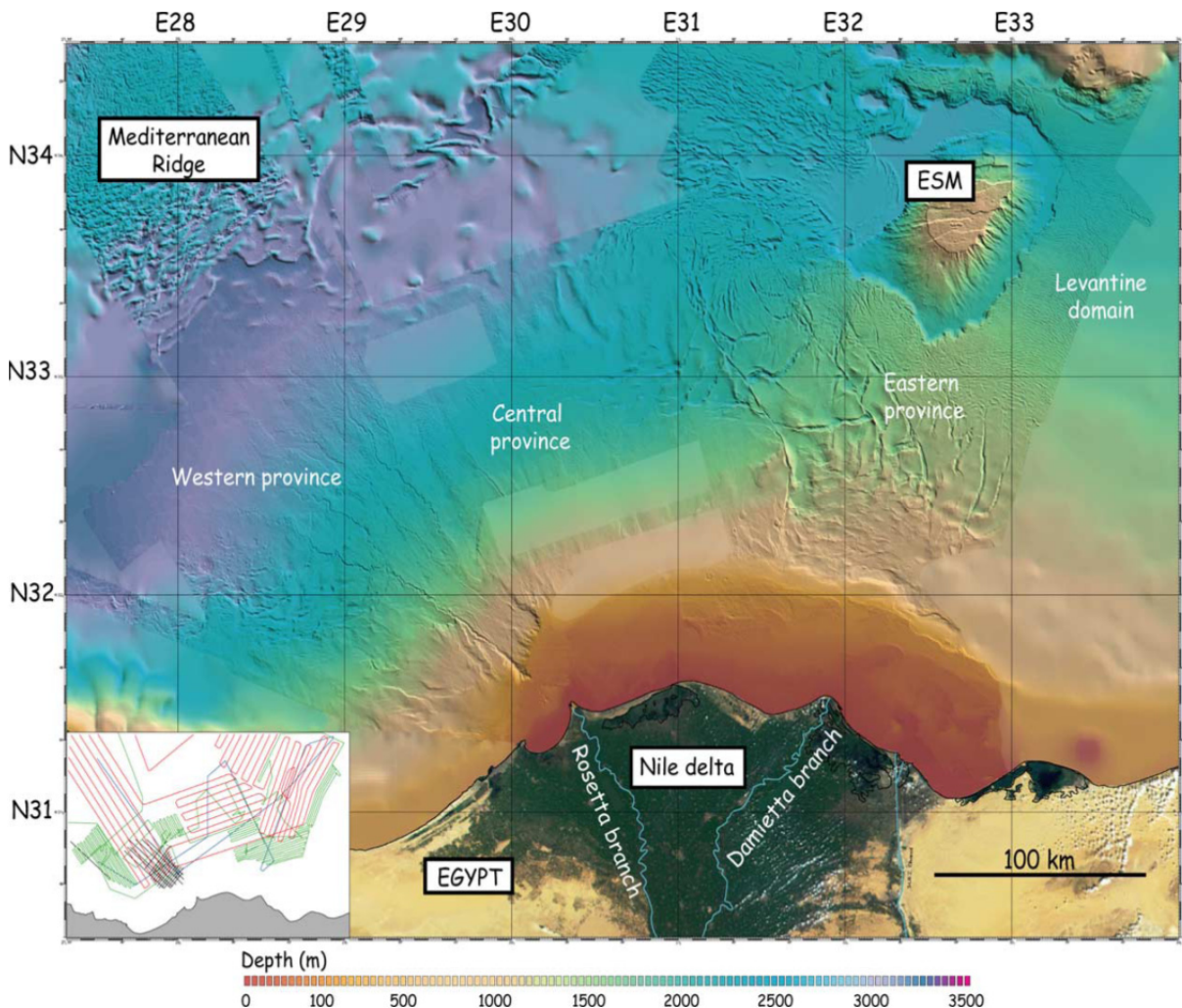
Figure 3.4: *Shaded bathymetric map of the Nile deep-sea fan (Loncke et al., 2006).*

The Nile deep sea fan can be divided laterally into the following three different parts (***Figure 3.5***) based on the distribution of modern sediment processes (Loncke et al., 2006): A) the eastern part which belongs to the area of main focus for this study and where since 2008 there was not information about this part (Folkman and Yossi, 2008) with the Damietta distributary which is dominated by a single long channel relative to smaller discontinuous channels embedded in mass transport deposits. This part of the Nile fan forms the continental shelf and slope of the northern Israel (Buchbinder et al., 1993). B) An intermediate part, constituted of mass transport deposits embedded with segments of discontinuous seabed channels and C) The western part which is supplied with sediments derived from Rosetta (Bellaiche et al., 2002), the western active branch of the delta, transferred through the canyon on the self-edge and deposited on the seabed of the basin as a network of dense turbidite channel complexes.
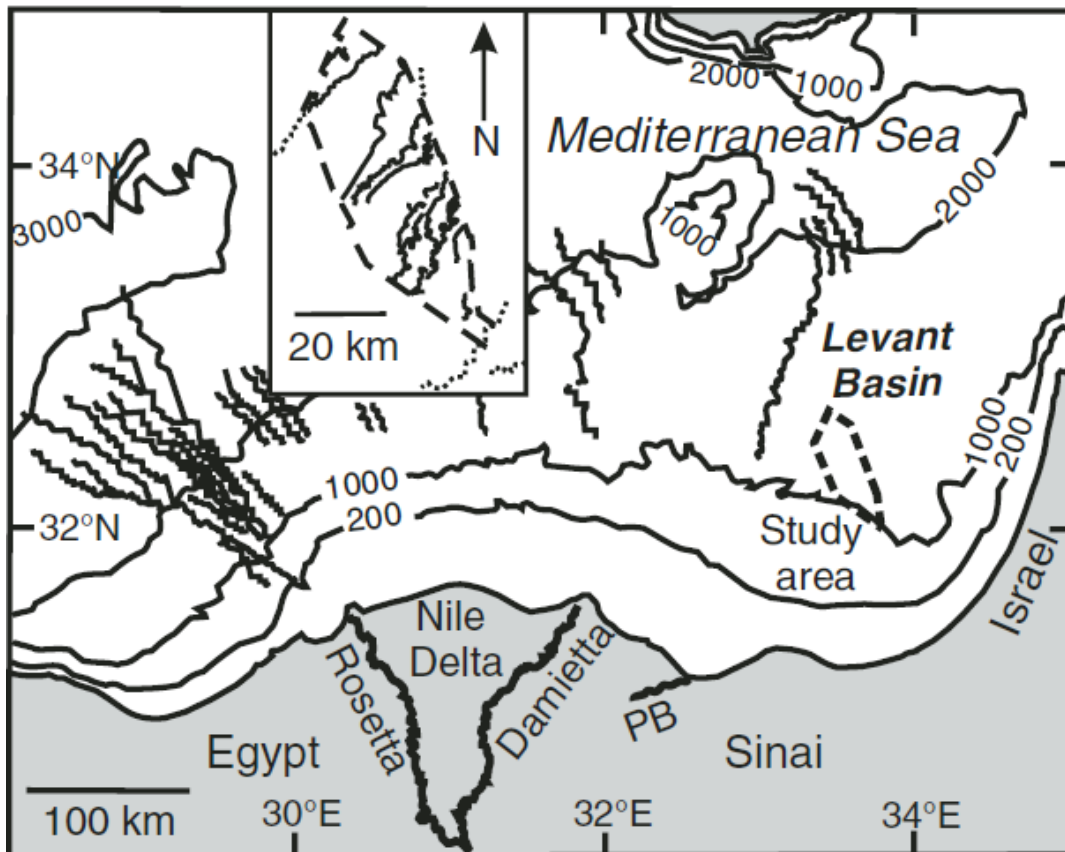
Figure 3.5*: The seabed turbidite channels at the three segments of the Nile's deep sea fan (Bellaiche et al., 2002) and inset with seabed channels from the study area (Folkman and Mart, 2008).*

3.5 Submarine channels of the study area

The study area can be characterized from channel complexes in the Plio-Quaternary unit, from the top of the Messinian evaporites until the present day seabed that have been affected from the thin-skinned deformation of the surrounding topography that is consisted of folding and strike slip faulting (Folkman and Mart 2008).

The channel path is affected from the structurally modified slope of the Levantine basin because of the fold and thrust belt setting created by compressional deformation resulted from the collapse of the Nile cone on the ductile Messinian strata (Clark and Cartwright, 2009).

On the top of the Messinian evaporites can be observed a system of subparallel sinuous channels (***Figure 3.6***) developed with NW-trending on a pre-Nile slope setting and they are segmented by polygonal pattern of densely spaced strike-slip faults (Folkman and Mart 2008). The fact that the direction of the channels is different compared with the overlying ones indicates a southeast source from the Levant platform from where the sediments where transferred through a pre-Nile NW-trending slope and finally they were deposited in the study area (Bertoni, 2006; Mart and Ryan, 2007).

23
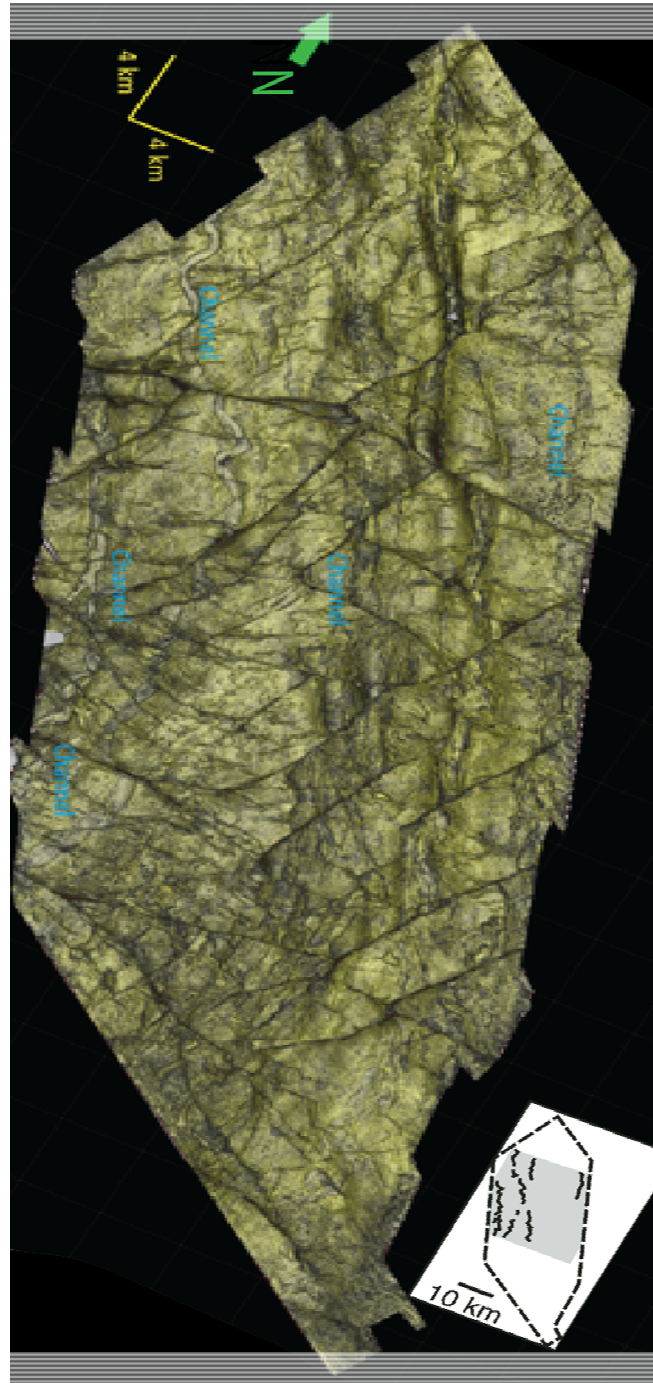
Figure 3.6: The sinuous channels on the Top of the Messinian strata (modified from Folkman, 2008).

The sub-seabed channels of the Plio-Pleistocene Unit above the Messinian evaporites and the seabed channels on the top of the Unit at the present day seabed are characterized from a network of NE-trending channels (Folkman and Mart, 2008). Until now (***Figure 3.7***), from the total amount of sixteen channels in the study area, eight have been mapped in that unit (***Figure 3.8***), from which six channels have been described qualitatively and quantitatively by Clark I.R. and Cartwright J.A. 2009, 2011. This has been achieved based on a detailed database of channel-structure interactions based in four end members: confinement, diversion, deflection and blocking (Clark and Cartwright, 2009, 2011).

Figure 3.7: *Map illustrating all the channels and folds of the Pleistocene sequence of the dataset.*

Figure 3.8: The mapped channels and folds of the study area.

3.6 The Messinian Evaporites

The seismic character of the evaporites *(Figure 3.9)* consists on the top from horizon M with high amplitude positive seismic reflection because of the seismic velocity contrast between the evaporites and the overlying Plio-Pleistocene marine clastic sediments and at the base it is constituted from horizon N with negative acoustic impedance contrast between the evaporates and the underlying deep marine sediments (Bertoni and Cartwright, 2007). In the evaporitic body can be observed four internal reflections that are different distorted and folded and indicate syn-depositional deformation. These reflections divide the evaporites into 5 transparent layers which suggest deposition during temporal sea level rises that resulted in a change of the evaporitic facies, possibly inter-bedded clastic sediments (Netzeband et al., 2006).
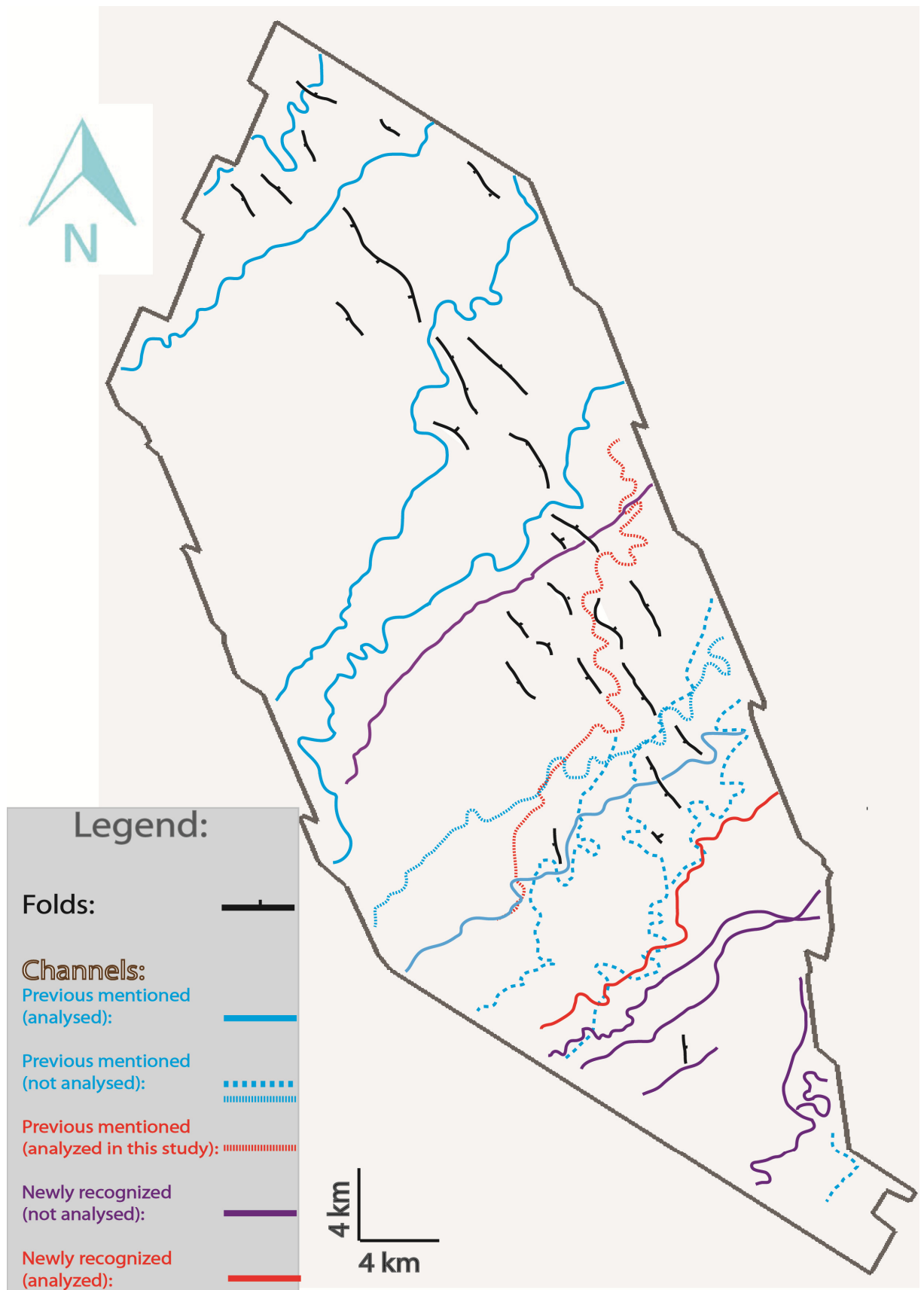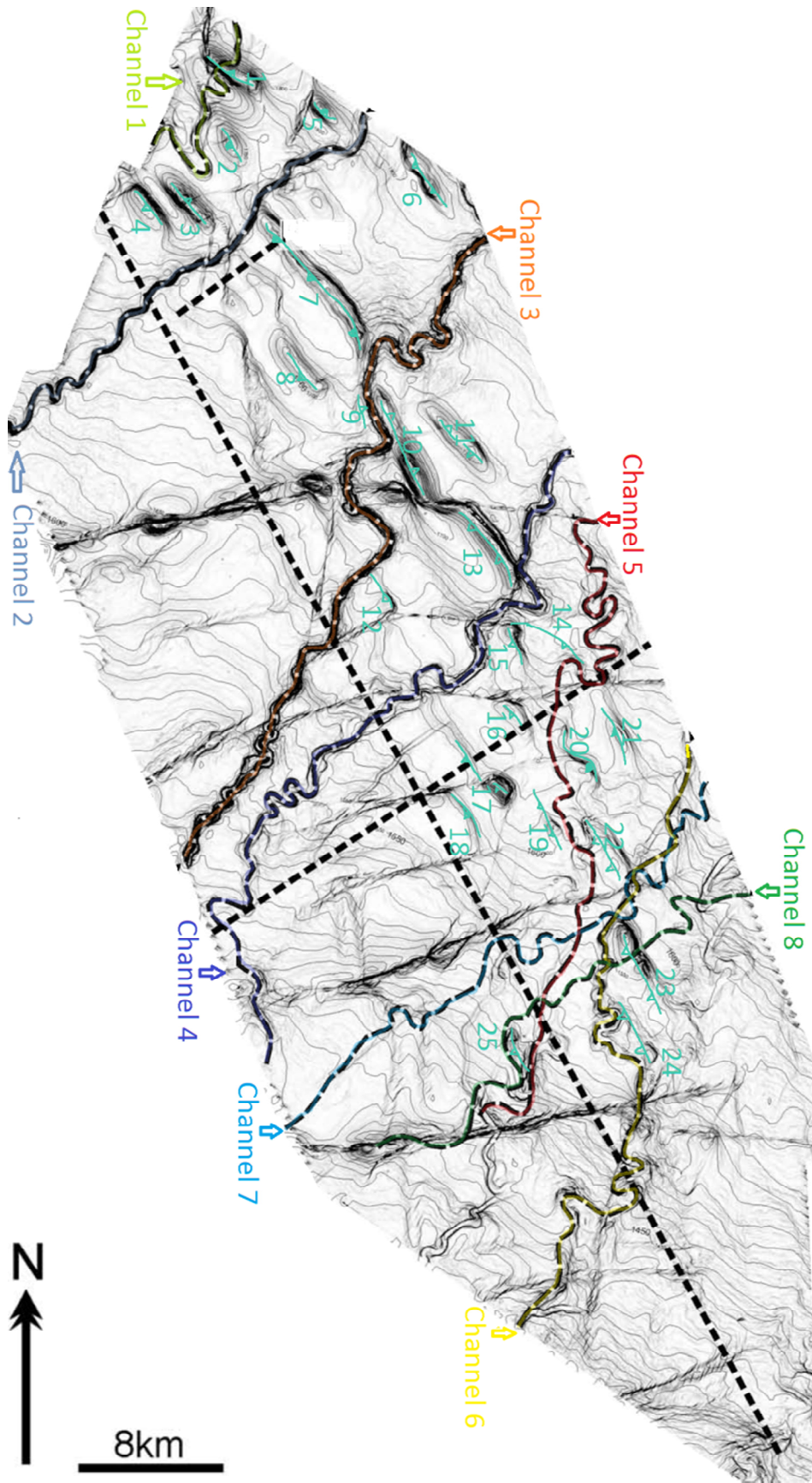
The unit of the Messinian Evaporites in the study area has an average thickness of 2 km and is bounded *(Figure 3.10 b)* to the top from Plio-Quaternary siliciclastic deposits (Ross and Uchupi, 1977) and is separated with them with an erosional unconformity traced throughout the whole Mediterranean sea (Almagor, 1984), the M-reflection. On the base the unit is separated by the Pre-Messinian Oligo-Miocene layers with the N-reflector (Ryan et al., 1970).
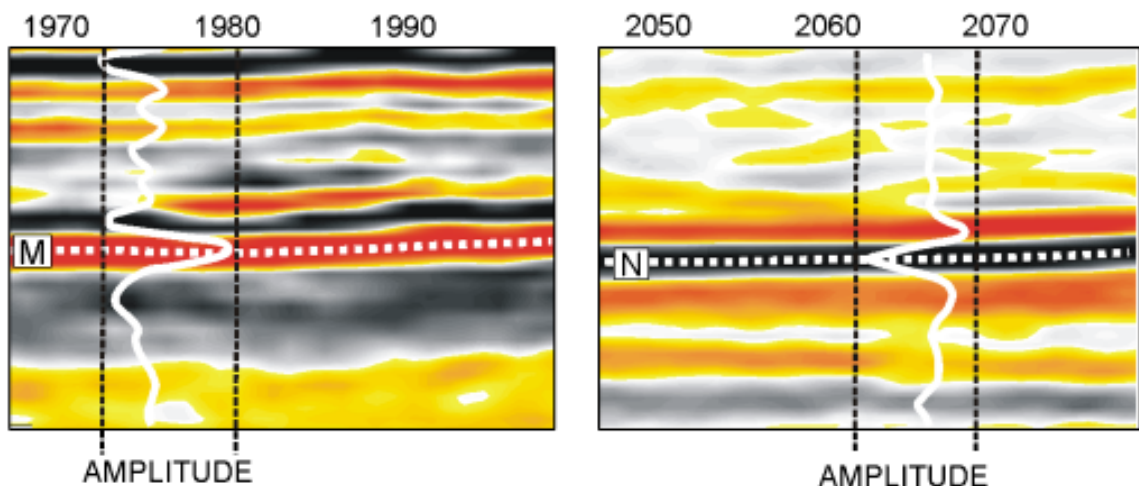
Figure 3.9: *Waveform response of a single wavelet of the Messinian top and* base (Bertoni and Cartwright, 2007).

The Messinian evaporitic layer of the Levantine Basin is characterized as comparatively young, single and massive and is considered to be consisted mainly of ductile halite with NNW-SSE flow direction (***Figure 3.10 a***) towards the Cyprus Arc (Netzeband et al., 2006). The sediment load that overlies the basinal Messinian strata varies along the basin margin (Huebscher, 2006) and the maximum thickness is 2 km in the basin and thins in a wedge-like manner towards the continental margin (Bertoni and Cartwright 2007). The Messinian paleo-slope and shelf are covered by a thin layer of the Messinian strata (Druckmann et al., 1995) and the marginal evaporitic part is mainly consisted of gypsum, anhydrate, or carbonates and intercalated shales.
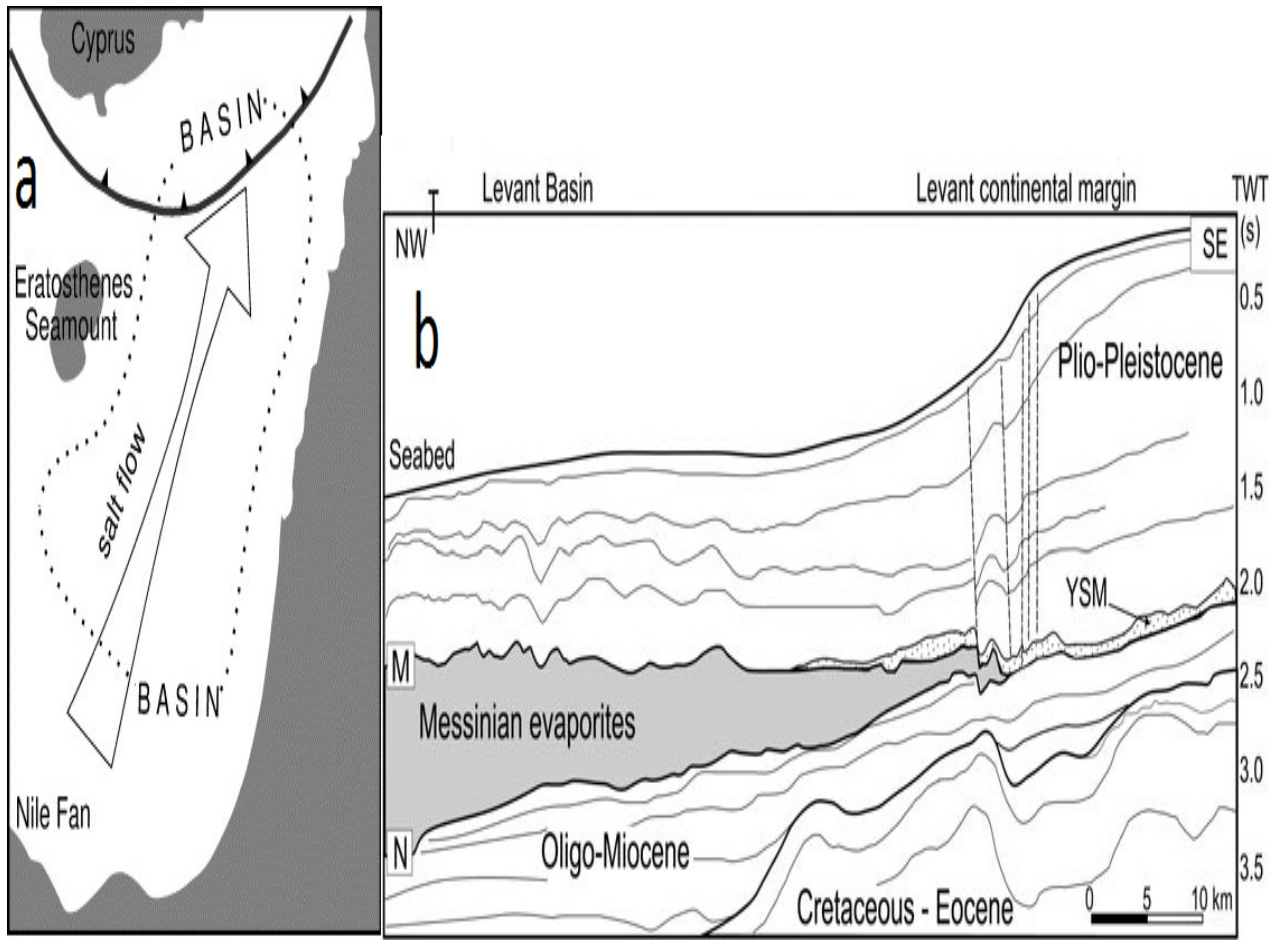
Figure 3.10: a) Messinian salt flow (Netzeband et al., 2006), b) Seismic stratigraphy of the Levant Basin and continental margin (Bertoni and Cartwright, 2007).

3.7 Plio-Pleistocene Unit

That Unit is composed with Pliocene-Holocene sediments which are mainly consisted of Nile derived deposits that constitute the distal part of the Nile's deep marine fan the thickness of which decreases northwards to the deep marine basin from 1100 to 500 m (Folkman and Mart 2008). The Unit have been subdivided in three different Units by Clark and Cartwright, 2009 *(Figure 3.6)* based on the differences of the dominant seismic facies.
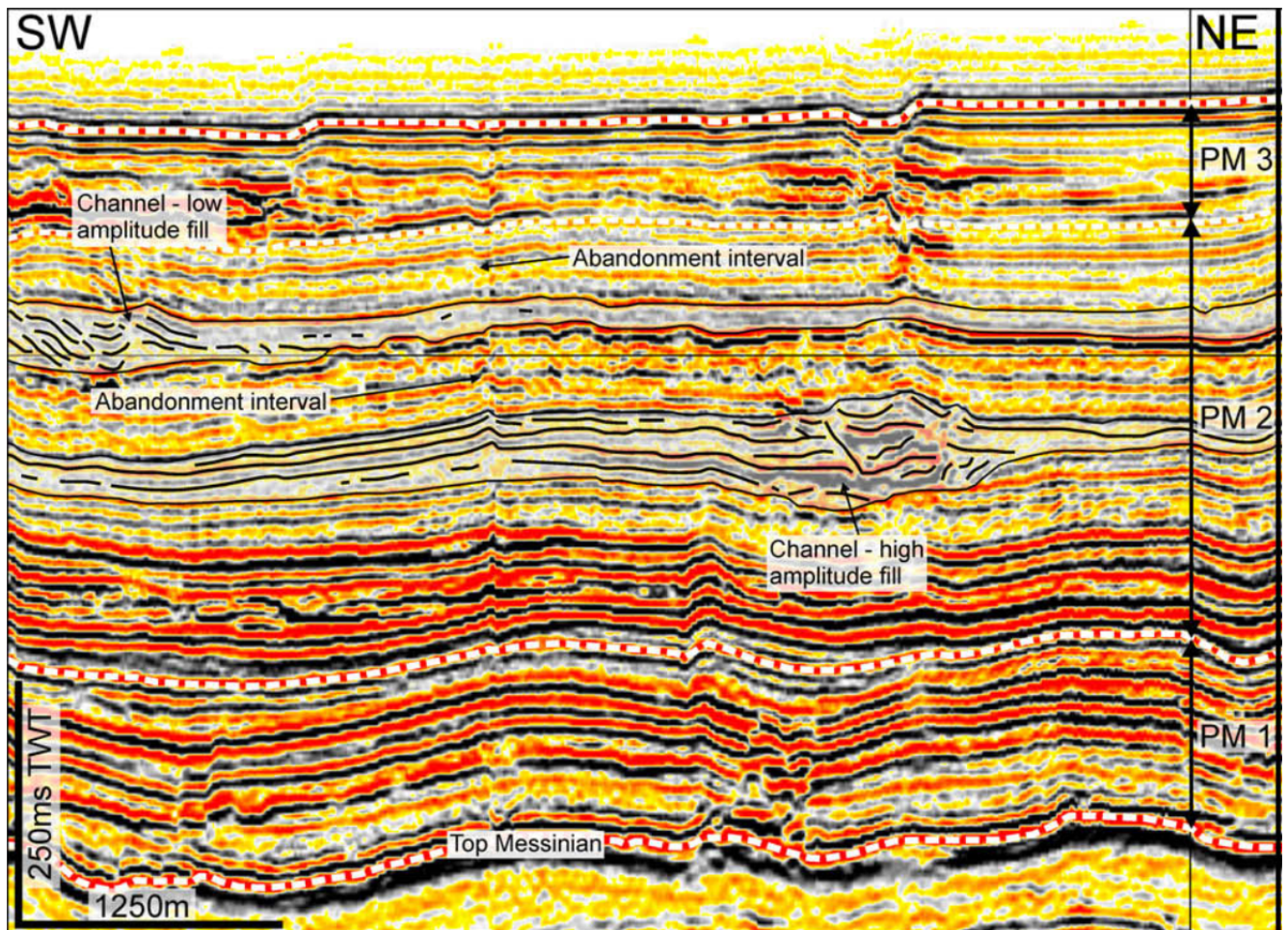
Figure 3.6: *The subdivision of the Pleistocene-Holocene Unit into three subunits (Clark and Cartwright, 2009).*

Post Messinian Unit 1

The Unit 1 which is the lower of the three units that have been mentioned at the literature, is separated from the Messinian evaporites with an erosional unconformity (Almagor, 1984) and its seismic character is mainly constituted of uniformly layered with overall high seismic amplitude (Folkman and Mart 2008), locally continuous and parallel reflections with poor continuity through the whole survey area (Clark and Cartwright, 2009).

The seismic facies of the unit indicate deep marine basin floor setting indicating the basinal stage of the evolution of the Nile deep sea fan during the early to middle Pliocene and constituted of terminal turbidite sheets rich in sand without significant channel complexes (Folkman and Mart 2008), although channels up to 500 m wide can be observed (Clark and Cartwright, 2009). The sedimentation in that Unit pre dates salt related deformation and provides evidence of post-Messinian faulting (Clark and Cartwright, 2009).

Post Messinian Unit 2

In the Unit 2 the seismic character that can be observed is composed of low to medium amplitude with localized packages of lower amplitude, the reflection continuity described as mainly continuous with areas of chaotic reflections that pass laterally into the more continuous units (Clark and Cartwright, 2009).

The low amplitude reflections in combination with chaotic reflections indicate mud rich mass transport deposits (Loncke et al., 2002; Frey-Martinez et al., 2005) while the low amplitude reflections in combination with thin seismic layers are indicators of rich in mud deposition of Hemipelagic sedimentation through the water column (Loncke et al., 2002). In that Unit are included larger (2 km width) than Unit 1 channel levee systems with wedge shaped levees that thinning progressively far from the channel axis. Possible periods of channel abandonment are indicated in that Unit from parallel reflections of constant thickness that separate the channels (Clark and Cartwright, 2009).

Expanded into the hanging wall and footwall synclines thrust related folds are interpreted as syn-kinematic intervals with the largest and most continuous structures to have been initiated earlier. Episodic growth of the thrust folds after the onset of deformation is indicated in the Unit by the separation of the growth packages by intervals of parallel reflections of constant thickness (Clark and Cartwright, 2009).

The sedimentary architecture of the lower part of that Unit compared to its upper part indicates interaction between two slope environment processes, mass transport and periodic turbiditic activity with Hemipelagic sedimentation respectively (Folkman and Mart 2008). This subdivision of the Units suggests two stages in the evolution of Nile deep sea fan from the middle Pliocene to the Late Pliocene with a basin stage and a slope environment stage respectively (Folkman and Mart 2008).

Post Messinian Unit 3

In the Unit 3 the seismic character that can be observed is mainly composed of continuous reflections of medium to high amplitude indicative of multiple embedded turbidite slope channel complexes that contain localized sand bodies (Folkman and Mart 2008) with the younger ones to be illustrated on the present day seafloor (Clark and Cartwright, 2009).

That Unit is strongly affected from Post-Messinian deformation which is indicated from the high amount of thickening and growth into the hanging wall and footwall synclines that are associated with thrust related faults (Clark and Cartwright, 2009). This Unit is assumed to have higher structural growth relative to the deposition rate in comparison with the Unit 2 because of the higher amount of growth into the fold limbs. The channels of the Unit are described as aggradational and not erosional because of the confinement of the channel axis between the levees instead of incision into the underlying sequences. The orientation in combination with the location of the channels suggests that they are derived from the Damietta branch of the Nile (Clark and Cartwright, 2009).

4. Dataset and Methodology

4.1 Dataset

The dataset used for the current study is a 3D seismic data volume acquired during the Gal_C survey in 2000 by BG and its joint venture partners and covers an area of 1.400 square kilometers. The data set was migrated with a single pass 3D post-stack time migration with an initial in-line acquisition trace interval of 6.25m and a cross-line spacing of 25m with a 1 ms sampling interval in order to generate after the final processing a 12.5m by 12.5m grid with 6400 bin cells per square kilometers after processing (Frey-Martinez et al., 2005). The seismic data are processed to near zero phase and is displayed using SEG normal polarity, with an increase in the acoustic impedance being represented by a positive amplitude (red) excursion on seismic trace of the sections.

The dominant frequency of the seismic data varies by decreasing with depth with the Plio-Quaternary sedimentary section overlying the Messinian evaporites with a dominant frequency of 50 Hz and the estimated vertical and lateral resolution for this interval being 10 and 40 m, respectively (Frey-Martinez et al., 2005). This was determined using an average interval seismic velocity of 2000m/s within the first 2.5 s of Pliocene unit of the 3D datasets and was derived from velocity checkshot data measurements made from the GazaMarine-1 exploration well (Frey-Martinez et al., 2005). The Messinian evaporites are characterized by a lower dominant frequency of 30 Hz and seismic velocity 4000 m/s with the resulting vertical resolution to be 22.5-50m (Bertoni & Cartwright, 2006). Although the frequency and velocity within the Messinian is variable and this results in significant changes in vertical resolution within this unit (Bertoni and Cartwright, 2006).

4.2 Methodology

The workflow of the thesis is based on the use of two Geosoftwares, the Petrel (version-2012) and the Geoteric (version-2013) with the main part to be made by the use of Petrel.

Initially the data imported into the software, the seismic cube was realized and a variance cube was extracted for the initial overview of the different elements of the whole study area. Then the area was subdivided by cropping of the dataset into two parts, the northern and the southern part which is the mostly analyzed. The subdivision of the study area is based on the fact that the previous studies have already analyzed the northern part of the survey in details. In terms of depth, the volume initially was "scanned" from the top of the Messinian evaporites until the present day seafloor in order to have a complete view for the whole area covered by the data and afterwards the volume was cropped on the z-axis on the level of the Pleistocene-Holocene unit which belongs to the upper part of the dataset.

Four horizons were interpreted throughout the whole volume, the lower horizon-M which belongs to the top of the Messinian evaporites, the second one who was the syn-tectonic horizon who in terms of depth consists the base of the main study area, the intermediate horizon who subdivides the Pleistocene-Holocene unit into two parts and the present day seafloor which consists the top of the sequence of main focus.

Afterwards the southern part of the data was subdivided into five Units bounded by six interpreted horizons. The color of each Unit is the color of the base of the Unit. The subdivision of the seismic stratigraphy into the different seismic stratigraphic Units is based on the different seismic facies and the continuity of the seismic reflectors.

The interpreted horizons were tracked based on the lateral continuity, at the s-crossing which is the area between a through (negative acoustic impedance) and a peak (positive) acoustic impedance or the z-crossing which is the area between a peak and a trough. The interpretation of the horizons at a z-crossing or an s-crossing offers a better precision in comparison to the interpretation at a peak or a through. The density of the interpretation has initially an increment of 32 between the in-lines, with denser interpretation in more complex areas. During the interpretation of the horizons at the in-lines the cross lines were used for the confirmation of the correct interpretation.

After the manual interpretation of the horizons the paintbrush interpretation was used on a 2D window. During the paintbrush on the 2D window were activated the interpreted horizon and the variance cube in order to identify difficult areas. After the paintbrush elevation time (ms) surfaces were created which represent the topography of the horizon and were used for the extraction of attribute and time thickness maps (ms).

The time thickness or isochron maps represent the TWT thickness of each Unit and were created by the use of the base and the top surface that bounds the Unit. The isochron maps can be used for the identification of the main sedimentary depocenters because they represent the thickness variations of the Unit.

Two types of attribute maps were extracted in order to illustrate the geological expression of the geophysical data, amplitude and variance which can illustrate the depositional features and the structures respectively.

The attribute maps were extracted by the use of time (ms) windows of minimum 20 ms and maximum 80 ms which are the minimum (depositional lobes) and maximum (aggradational channels) thickness of the depositional elements respectively.

Another technique that allowed the more precise analysis of the features between two selected horizons was the iso-proportional slicing which allowed the creation of a chosen amount of iso-proportional horizons between the two selected horizons.

Attribute maps extraction and iso-proportional slicing took place as well with the software Geoteric with the following steps:

1) Frequency decomposition technique where initially the frequency spectrum is decomposed and three dominant frequencies from the decomposed spectrum are chosen based on selected frequency volumes, depending on the highlighting of the geological expression of the main sedimentary bodies that respond at a certain frequency.

2) The color blending technique which allows the blending of the three selected frequency volumes and results in a RGB color blend volume that reveals the interplay of the three different frequency volumes through the enhance information of the depositional features. The best color blending was chosen based on qualitative comparison and with random seismic lines crossing the depositional features of interesting.

From the attribute maps extracted from Petrel and maps extracted from the Geoteric the main depositional features of each Unit recognized and confirmed with seismic sections vertical to the flow axis of each feature.

Submarine channels qualitative observations

The qualitative submarine channel observations is considered about the interaction between the channel evolution and the deformed underlying structures and has been achieved based on a detailed database of channel-structure interactions based in four end members (*Figure 2.10-1*): confinement, diversion, deflection and blocking. The levee geometries were used as well in order to provide information about the temporal interaction between the channel development and the topographic deformation in four different ways (*Figure 2.10-2*).

Submarine channel quantitative measurements

From the submarine channels of each Unit the most representative were selected and described qualitative and quantitative by the following measurements:

1) Sinuosity (*Figure4.1*) measurements with increment of 1 km along the main channel distance axis which based on Clark and Cartwright (2009) can be applied in order to illustrate the sinuosity ranges, at channels with meander widths of the order of 500-

1000 m. The sinuosity is calculated by the ratio of the along channel distance between to points divided by the straight line distance between these two points.
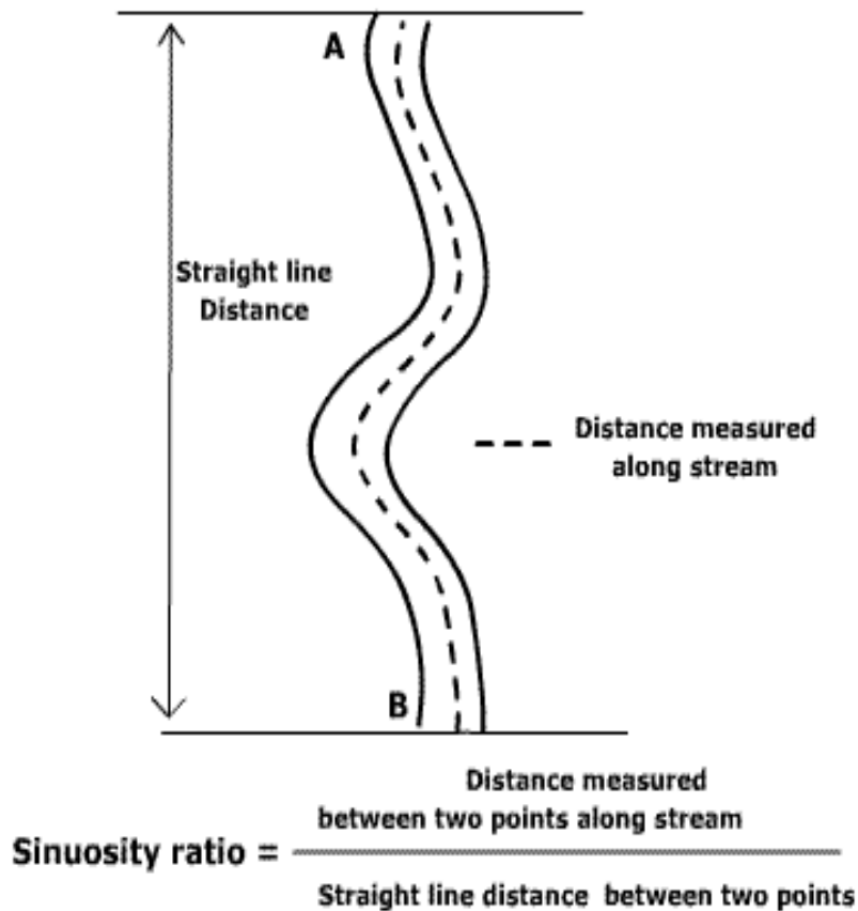
Figure (4.1): Sinuosity measurement.

1) Channel thalweg depth which represents the depth from the sea level to the channel floor.

2) Erosional depth which represents the depth from the sea level to the lowermost erosive surface of incision of the pre-channel sequence.

3) Centerline structure depth which is the depth from the sea level to the syn-tectonic horizon and allows the comparison of the underling deformation and the overlying channel erosional and thalweg depth.

The parameters that mentioned above have been measured *(Figure 4.2)* with an increment of 500 m along the channels sinuous length with the use of perpendicular seismic lines along the channel axis. The increment was chosen because of the channel morphology changes which were less than 1 km (Clark and Cartwright, 2009).

34

Figure (4.2): *Channel quantitative measurements (Clark and Cartwright, 2009,2011).*

The dimensions of the depositional features including crevasse splays, frontal splays and the structures including folds were measured based on the length of the of the long axis multiplied by the short axis of the area covered by the feature.

5. Results

5.1 Seismic Facies Description and Interpretation

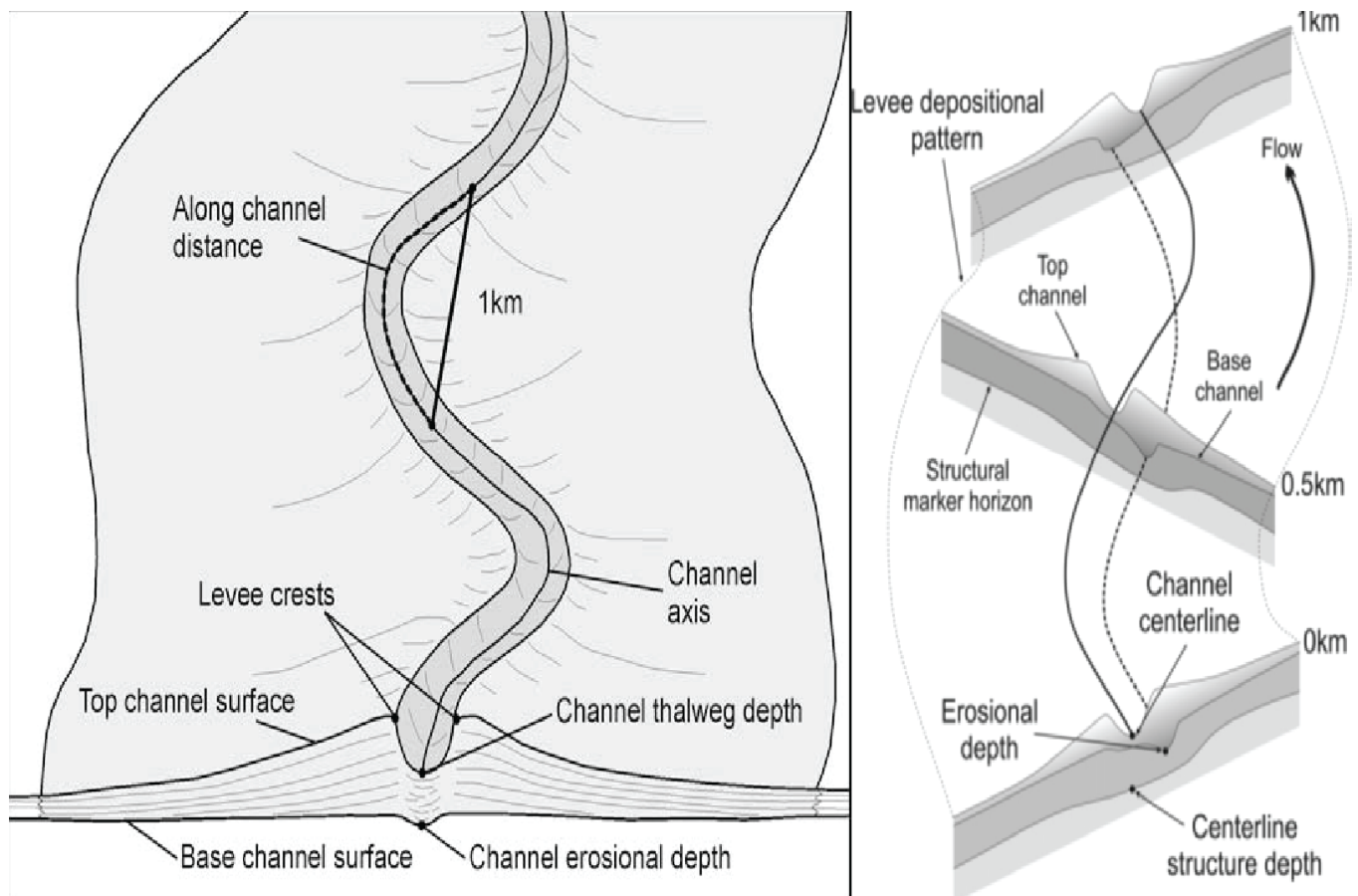In the following subchapter are described the main seismic facies (*Table 5.1)* that can be observed between the different Units in the study area of main focus. The five seismic facies which spatial and temporal distribution varies in the study area have been described based on their seismic character, internal and external geometry and in terms of depositional processes and sedimentary environment.

5.1.1 Seismic Facies 1

The seismic facies 1 *(Figure 5.1*) has seismic reflection parameters consists of discontinuous and high amplitude seismic reflections (HAR's) or medium amplitude reflectors, the reflection configuration is described as contorted and the external geometry as subhorizontal and in some case where incision occurs as U shaped.

The facies 1 can be interpreted as submarine channel fill deposits of meandering channels with sinuosity 1,9 and lateral accretion packages of 300 m wide and 70 ms TWT deep at the outer bends of the channel. Submarine channels with low sinuosity equals to 1,12 and erosional base with width 140 m are observed in areas of confinement as well. Based on the high amplitude pattern of the channels axis deposits the channel fill can be described as sand prone with thickness 20 ms TWT, features that have been described at other areas of deep water settings described from Posamentier and Kolla (2003) and Flood et al., 1997. The medium amplitude channel fill indicates muddy channel axis fill deposits. The responsible process for these deposits could be high energy flow of turbidity currents and gravity related deposits for the sandy prone channel fill and low energy turbidity currents for the muddy filled channel. In some cases is observed the combination of the two type of channel fill with erosional sandy base covered from muddy fill. The depositional environment indicates the submarine slope environment of the Levantine Basin.
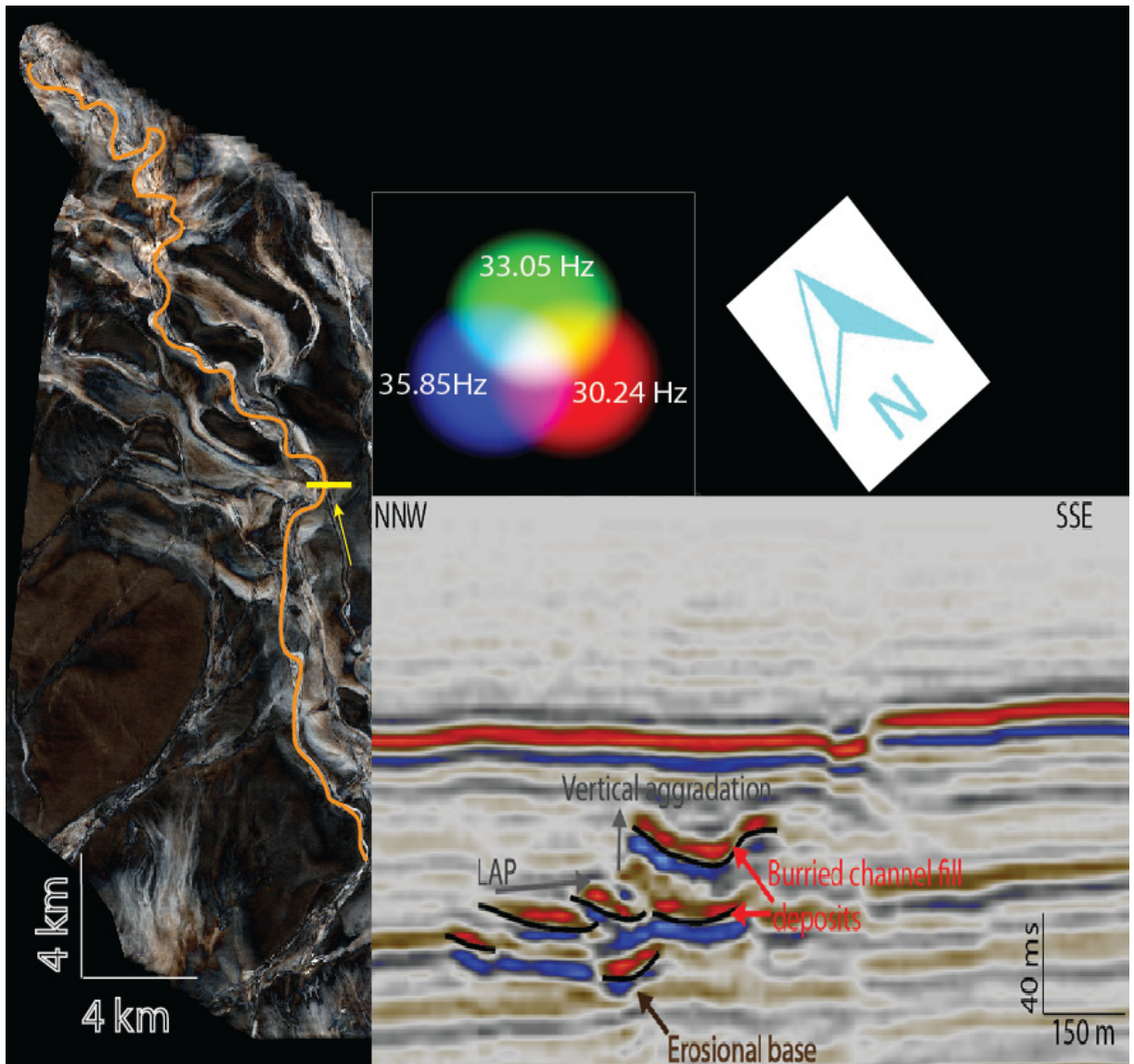
Figure 5.1: *Seismic section illustrating buried channel fill deposits and channelized lobe complex deposits from the channel 2 and 3 of the Unit 2 respectively.*

5.1.2 Seismic Facies 2

The seismic facies 2 (***Figure 5.2 a***) has seismic reflection parameters consist of continuous to discontinuous and low to medium amplitude seismic reflections, the reflection configuration is described in some cases as transparent and the external geometry at a cross section of the channel axis can be described as thinning out as transported away from the flanks of the channel. Onlap reflection terminations can be observed from the reflectors that start from the flanks of the submarine channel and end at the base of the levee deposits.

The facies 2 can be interpreted as channel overbank/levee deposits with width 2,5 km and height 80 ms TWT in unconfined areas with decrease at areas of confinement. The seismic character of these deposits indicates channel levee deposits at aggradational, non-high erosional deep water channels of other areas of deep water settings described from

Catterall et al., 2010. The responsible process for these types of deposits is the flow of the turbidity currents.

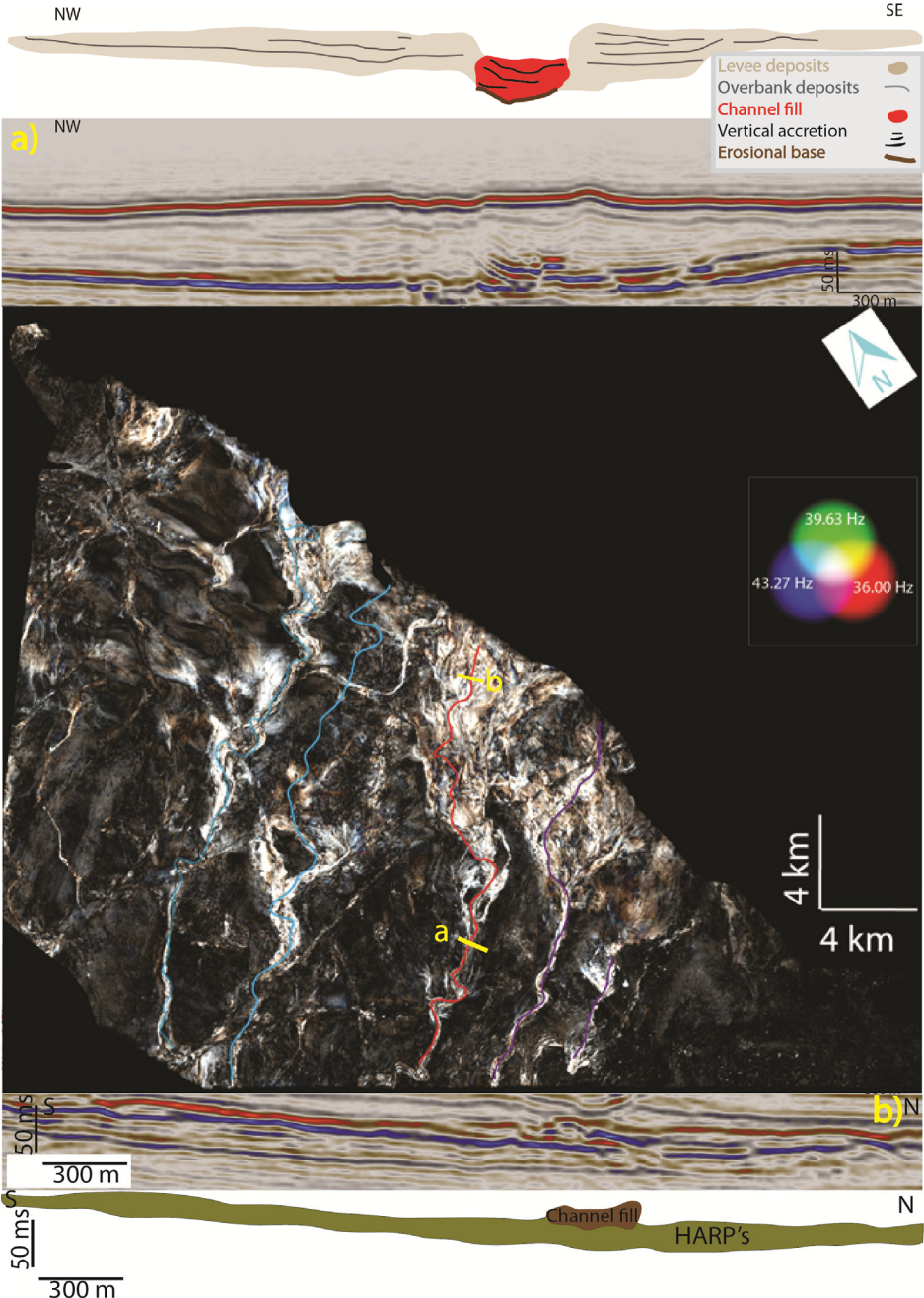*Figure 5.2*: *Attribute map of Unit 4 and seismic lines illustrating a) channel levee deposits (seismic facies 2) from the channel 7 and b) channelized lobe complex (seismic facies 4).*

5.1.3 Seismic Facies 3

The seismic facies 3 (*Figure 5.3*) has seismic reflection parameters that consist from discontinuous/discordant and low to medium amplitude seismic reflections, the reflection

configuration is described as transparent to chaotic/contorted and the external geometry as lens shaped with erosional base and irregular top.

The facies 3 can be interpreted as mass transport deposits MTD's based on the transparent, chaotic and low amplitude patterns which are indicators of debris flow deposits at other areas of deep water settings described from Posamentier and Kolla (2003). These deposits have an extend 18 km wide and they are 100 ms TWT high with basal grooves on their base and pressure ridges on the top with areas where channels excavate their top. The responsible process for these types of deposits are considered to be gravity flows while the environment can be described as relatively high energy slope setting. The internal architecture of the deposits is controlled by the gravity flows of MTC's that feeding the Facies 3 while the upper surface of the deposits was resulted from turbulent flows that created the channels.
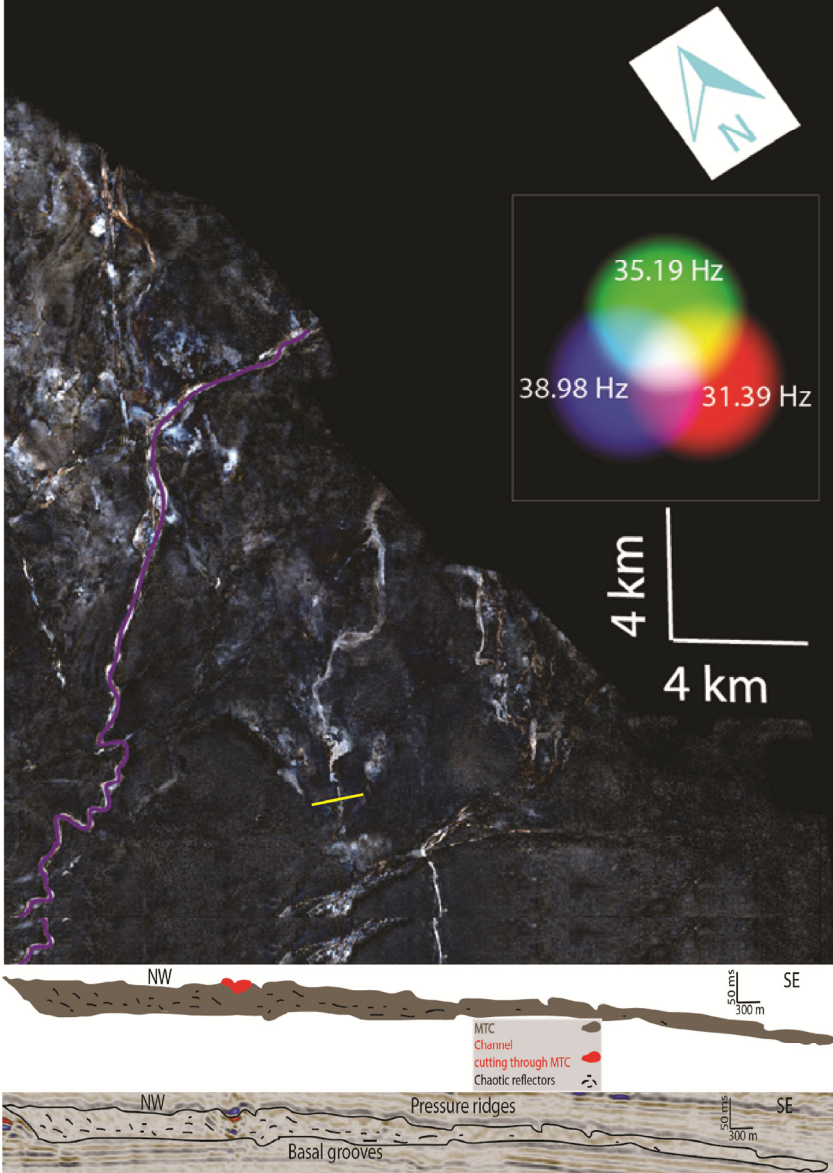

Figure5.3: *Attribute map of Unit 5 (Upper figure) and b) Seismic line illustrating mass transport deposits from the channel 10 of the Unit5.*

5.1.4 Seismic Facies 4

The seismic facies 4 (*Figure 5.2 b*) has seismic reflection parameters consist from continuous to slightly discontinuous and high amplitude seismic reflection packages (HARP's), the reflection configuration is described as relative flat and the external geometry is described as mounded in a cross-section view.

The facies can be interpreted as a channelized lobe complex with dimensions 1,2 km to 9 km wide, 3 km to 16 km length and thickness 20 ms (TWT) to 70 ms (TWT). Based on the continuous and slightly discontinuous high amplitude patterns which are indicators of sheet like units and distributary-channel complex deposits at other areas of deep water settings described from Posamentier and Kolla (2003). The responsible process for that type of deposits is the transition of the turbidity current flow from a confined to an unconfined area in combination with an increase in the slope gradient while the environment of these deposits is the basin floor of the Levantine Basin.

Smaller size deposits are characterized as crevasse splays resulted from the breaching of the outer bend levees. The proximal lobe area in the end of the feeding channel (Facies 1) is characterized by the presence of secondary channels while the distal lobe area is less complicated as it consists of the distributaries of the secondary channels. The lobe shape might be the result of the pre-existing topography which created the channelization of the sediment supply.

5.1.5 Seismic Facies 5

The seismic facies 5 (*Figure 5.4*) has seismic reflection parameters consists of continuous and medium to low amplitude seismic reflections, the reflection configuration is described as parallel to subparallel and the external geometry is described as sheet draped.

The facies 5 that in some cases seismically are illustrated as condensed section can be interpreted as pelagic/hemipelagic deposits based on the continuous and low amplitude patterns which are indicators of uniform low energy deep marine sedimentation processes in a basin floor setting. The facies could be interpreted as well as basin floor sheet shaped turbidite deposits.
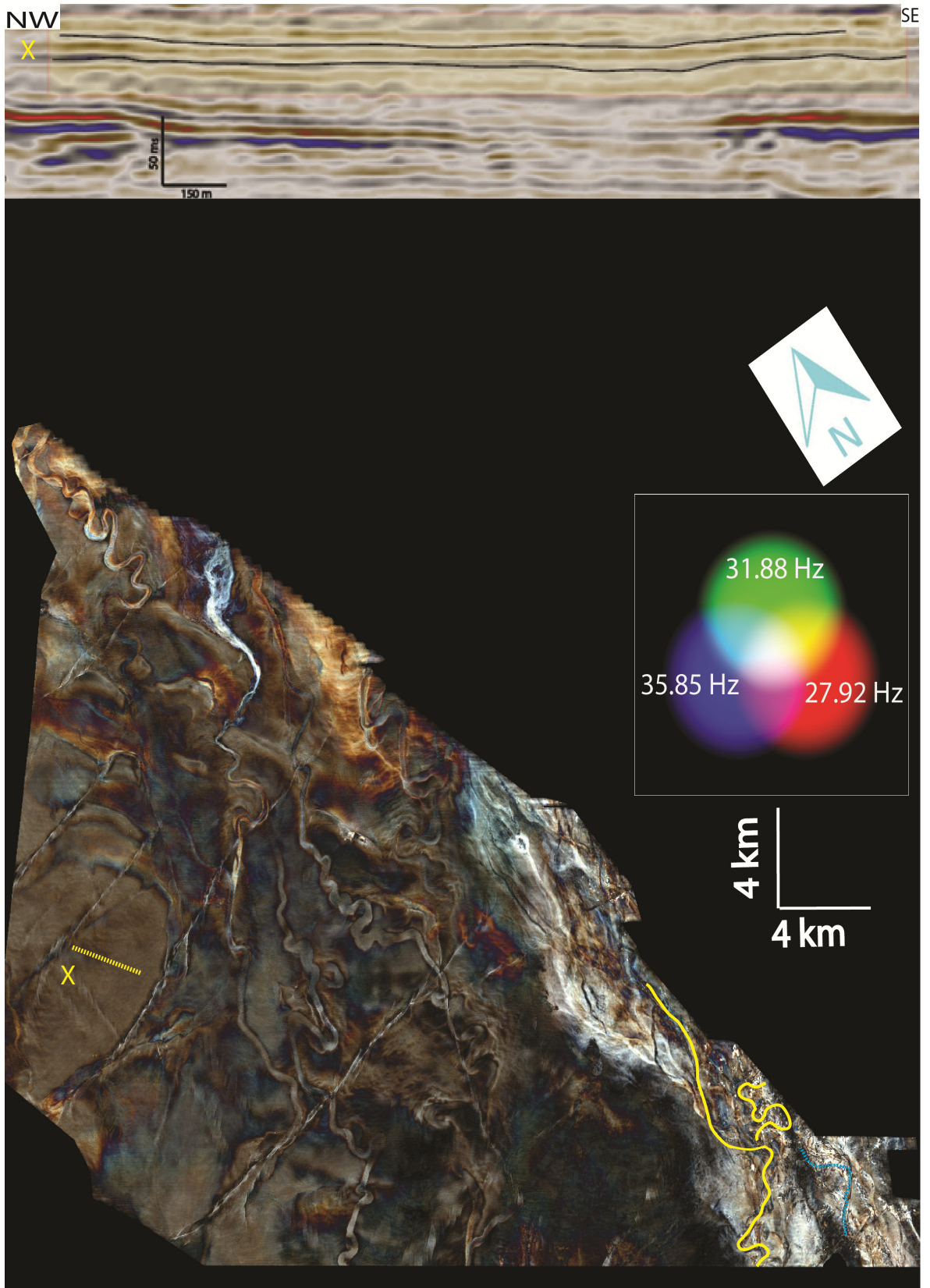
Figure 5.4: *Attribute map of Unit 1 (upper figure) and b) seismic line illustrating hemipelagic sedimentation or sheet like turbidite deposits from the channel 1 of the Unit 1.*

Seismic Facies	Seismic Character (reflection continuity and amplitude)	Internal Geometry	External Geometry	Process Interpretation	Environment Interpretation	Example Figure No.
Facies 1	Discontinuous contorted high or medium amplitude reflectors (HAR's)	Subparallel lateral accretion packages (LAP's)	Subhorizontal	High energy turbidity flow currents and gravity related deposits	Slope buried channel fill deposits feeding facies 4	4.1.1
Facies 2	Continuous/discontinuous low/medium amplitude reflectors and in some cases transparent, onlap on the HARP units	Parallel even	Wedge shaped at cross section geometry, thinning away from the flanks of the channel axis	Turbidity current overflow of channel levees	Channel levee/overbank deposits	4.1.2
Facies 3	Discontinuous/discordant, medium to low amplitude reflections	Contorte, transparent/chaotic	Lens shaped, erosional base, irregular top	Relatively high energy setting/gravity flow	Slope Mass Transport Deposits	4.1.3
Facies 4	Continuous to slightly discontinuous reflections of high amplitude (HARP's)	Relatively flat topped deposits in cross- section	Mound	Unconfined turbidity flows/transition from turbidity channel to lobe	Basin floor, channelized lobe complex (frontal or crevasse splay deposits)	4.1.1
Facies 5	Continuous, medium to low seismic amplitude	Parallel/ subparallel	Sheet drape	Hemipelagic sedimentation	Basin floor Hemipelagic deposits or turbititic deposits	4.1.5

Table 5.1: Description of the character of the main facies in the study area.

5.2 Unit Description

The analyzed sequence belongs to a previous characterized by Folkman and Mart (2008) slope stage and belongs to the upper Pleistocene-Holocene 500 m of the seismic dataset. Initially the Pleistocene-Holocene Unit was subdivided into 2 subunits for the whole area covered by the dataset (*Figure 5.5 a*) with base for the whole package to be the syn-tectonic horizon and the top to be the present day seafloor. Because of the detailed description of the northern most part of the dataset, the main area of focus belongs to the southern part of the area covered by the data where there are depositional elements that had not been identified before this study. This area has been subdivided into five different Units (*Figure 5.8*) based on the seismic facies and the continuity of the reflectors.

The Syn-Tectonic sequence for the whole range of the dataset was subdivided into two subsequent Units:

1) The lower Unit consists of the seismic Facies (1, 2, 3 and 4) and is bounded on the base from the (purple color) Base Syn-tectonic surface (*Figure 5.5 b*) and on the top from the (green color) Intermediate surface which is the surface that separates the Syn-tectonic sequence into two parts. The selection of the Base Syn-Tectonic surface was based on the weakly developed onlap on the fold-limbs and the tilting of the channel levees on the limbs of the folds indicated by the tilting of the reflectors towards the fold crest (*Figure 5.6*). The Base Syn-Tectonic surface was tracked along an s-crossing and is characterized from a fold zone (red color) with northwest-southeast trending, east-west strike slip (brown color) faults and southwest-northeast strike slip faults. The depth of the surface from the present day sea-level varies with the shallower parts of the surface to be at the south western part with depth -1525 ms TWT while the deepest areas are at the eastern part of the surface with depth -2000 ms TWT.

   The Intermediate surface (*Figure 5.5 c*) was tracked along a z-crossing and is characterized from the same fold zone with the Base Syn-Tectonic surface with northwest-southeast trending but with a reduced number of folds towards the southeast. East-west strike slip faults can still be observed but there are not southwest-northeast strike slip faults like the Base Syn-Tectonic surface. The depth of the surface from the present day sea-level varies with the shallower parts of the surface to be at the south western part with depth -1425 ms TWT with a progressive increase in depth towards the eastern part of the surface with depth -1425 ms TWT.

2) The Upper Unit consists of the seismic Facies (1, 2, 4 and 5) and is bounded on the base from the Intermediate surface and on the top from the (blue color) Seafloor surface *(Figure 5.5 d)* which is the surface of the top of the Syn-tectonic sequence. The Seafloor surface was tracked along a peak reflector because of the high continuity of the seafloor reflector and is characterized from a fold zone (red color) with northwest-southeast trending and east-west strike slip faults. The depth of the surface from the present day sea-level varies with the shallower parts of the surface to be at the south western part with depth -1300 ms TWT while the deepest areas are at the eastern part of the surface with depth -1800 ms TWT.

The thickness map (*Figure 5.7*) of the Syn-tectonic sequence is characterized from a decrease in thickness towards the northwest with the fold crests to be areas of the minimum thickness (yellow-red color) values because of the pinching out of the two bounded surfaces (Base and Top Syn-tectonic) sequence. The thickest part of the sequence is observed at the south eastern area of the thickness map with thickness 500 ms TWT. On the map can be identified the presence of east-west strike slip faults and segments from the seabed channels of the study area.
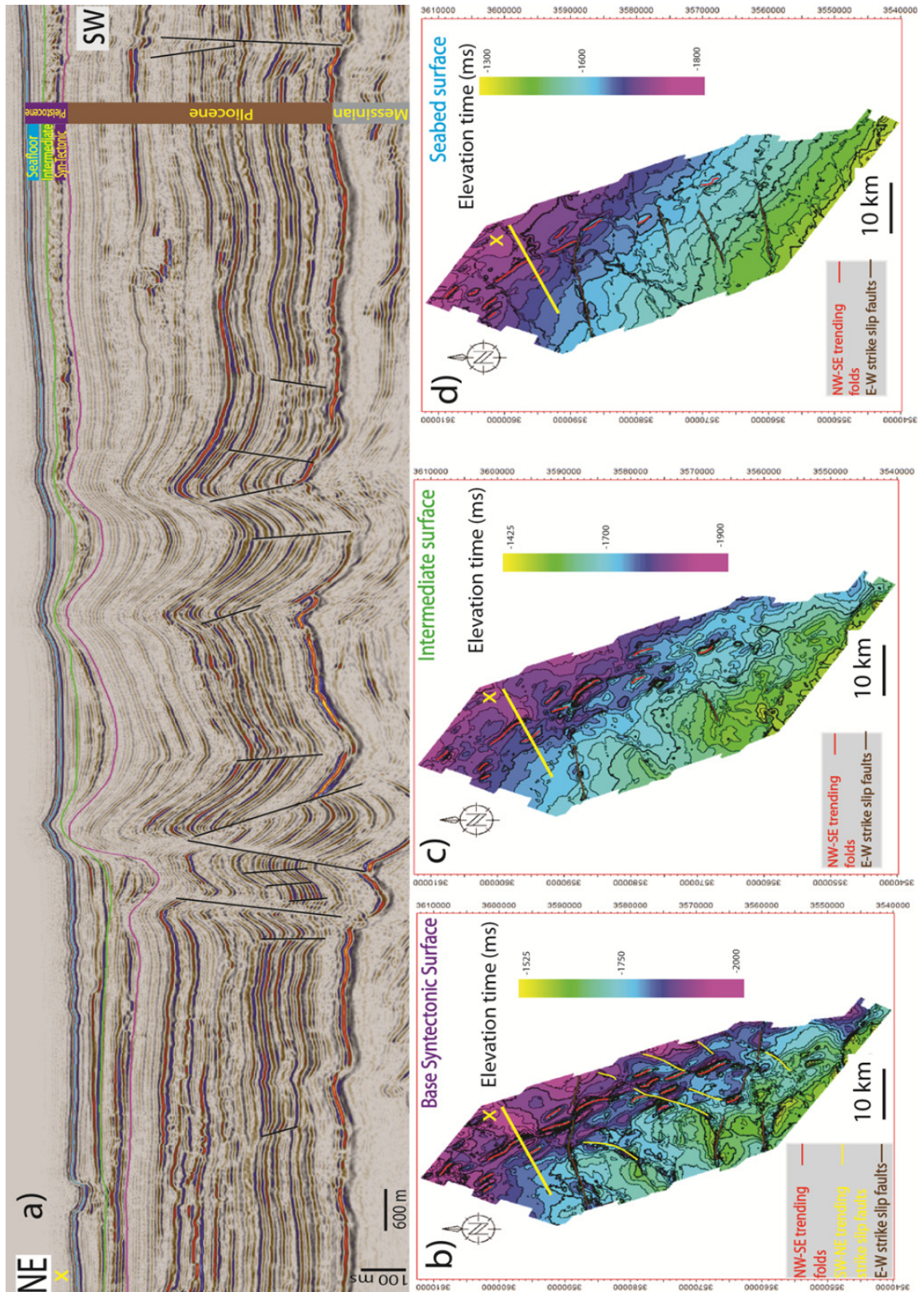
Figure 5.5: *a) Seismic line illustrating the top of the Messinian sequence and the Post Messinian layers of the study area and the upper Pleistocene part subdivided into two Units b) surface of the base Syn-Tectonic horizon, c) surface of the Intermediate horizon and c)surface of the Top Syntectonic horizon-present day seafloor.*

45

Figure 5.6: The Base Syn-Tectonic surface indicated by the tilted of the levee channels in combination of weakly onlap on the fold limbs.

Figure 5.7: *Time thickness map TWT of the Syn-Tectonic sequence.*

Figure 5.8: *The subdivision of the Syn-tectonic sequence of the southern part of the study area into 5 Units.*

5.2.1 Unit 5

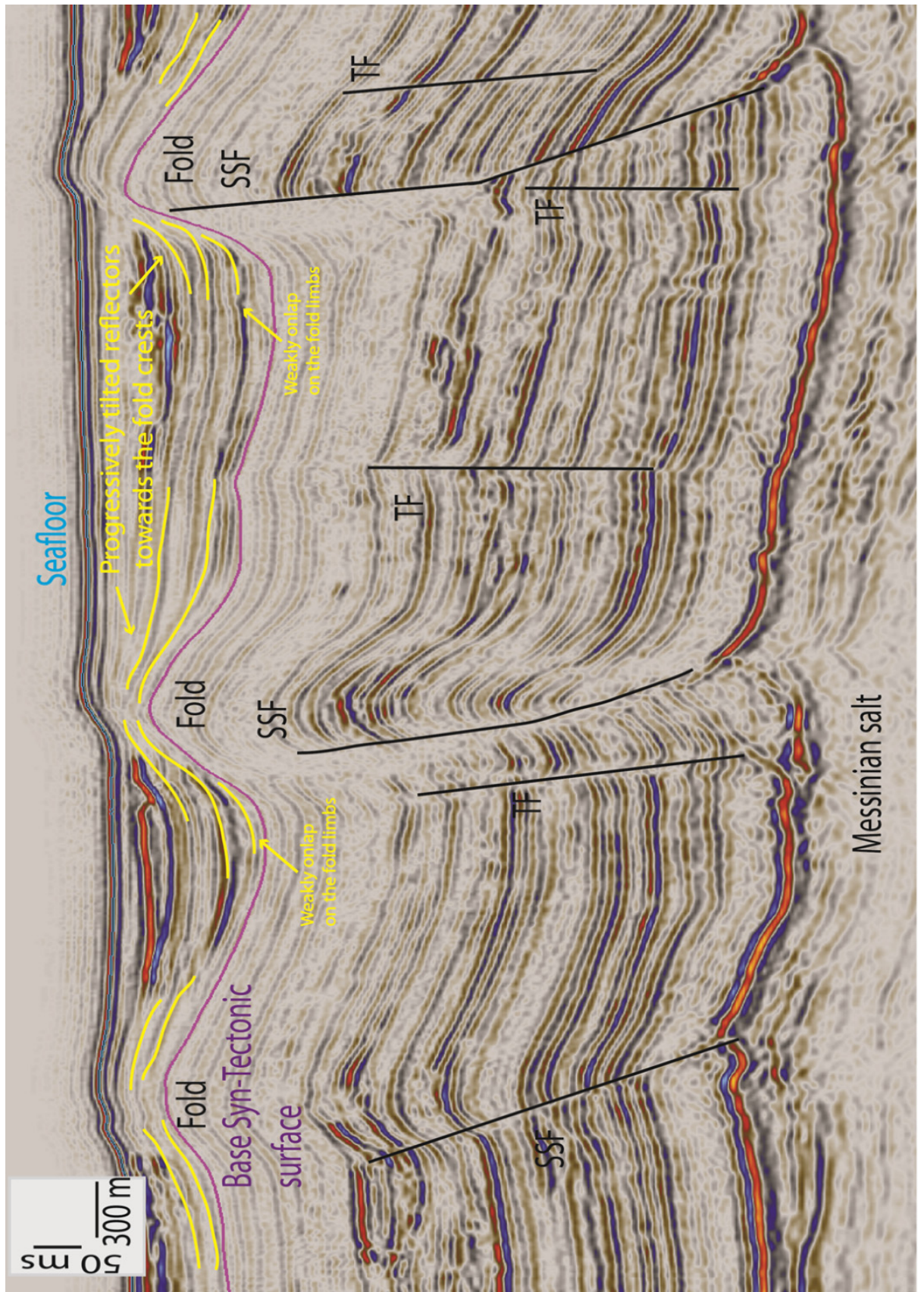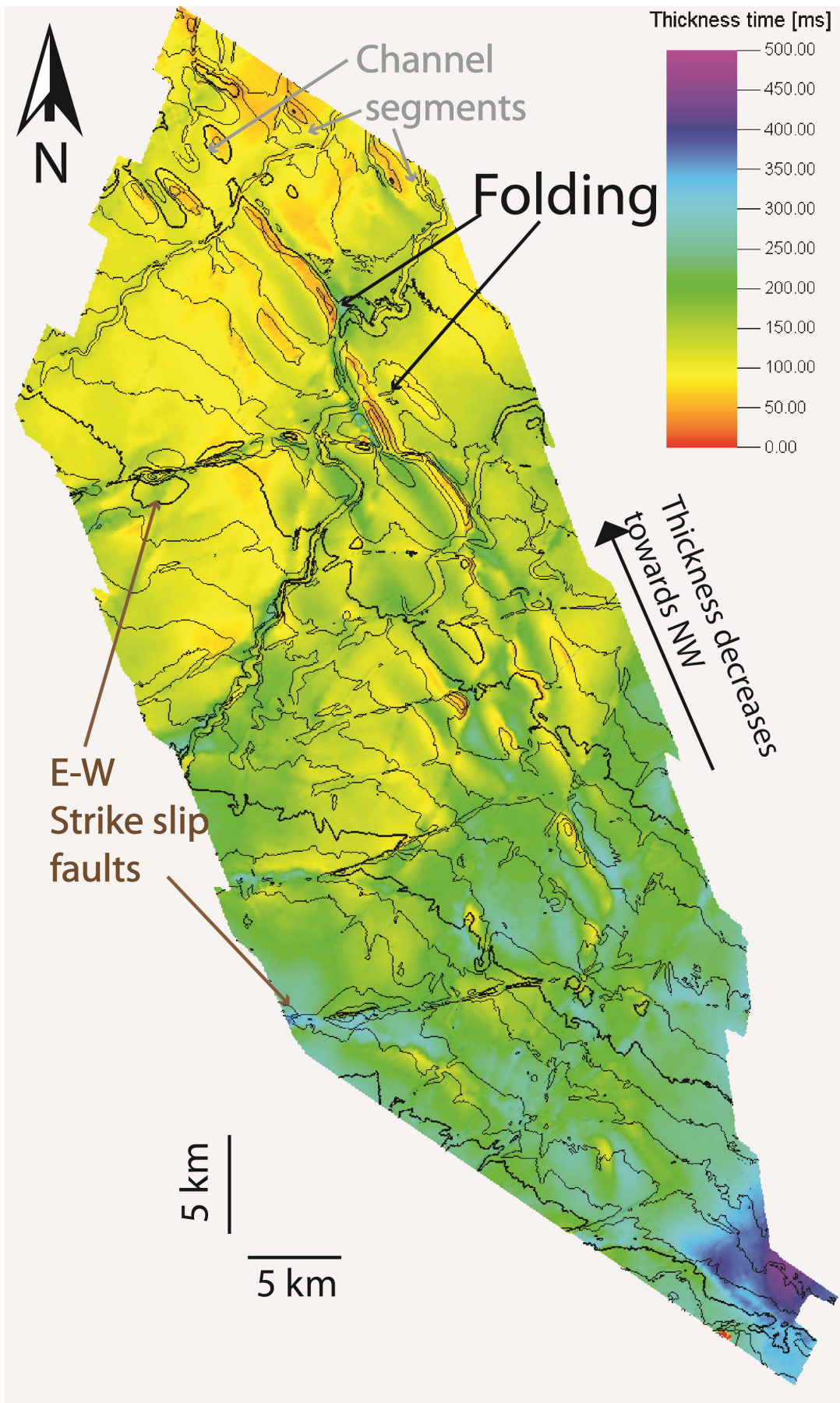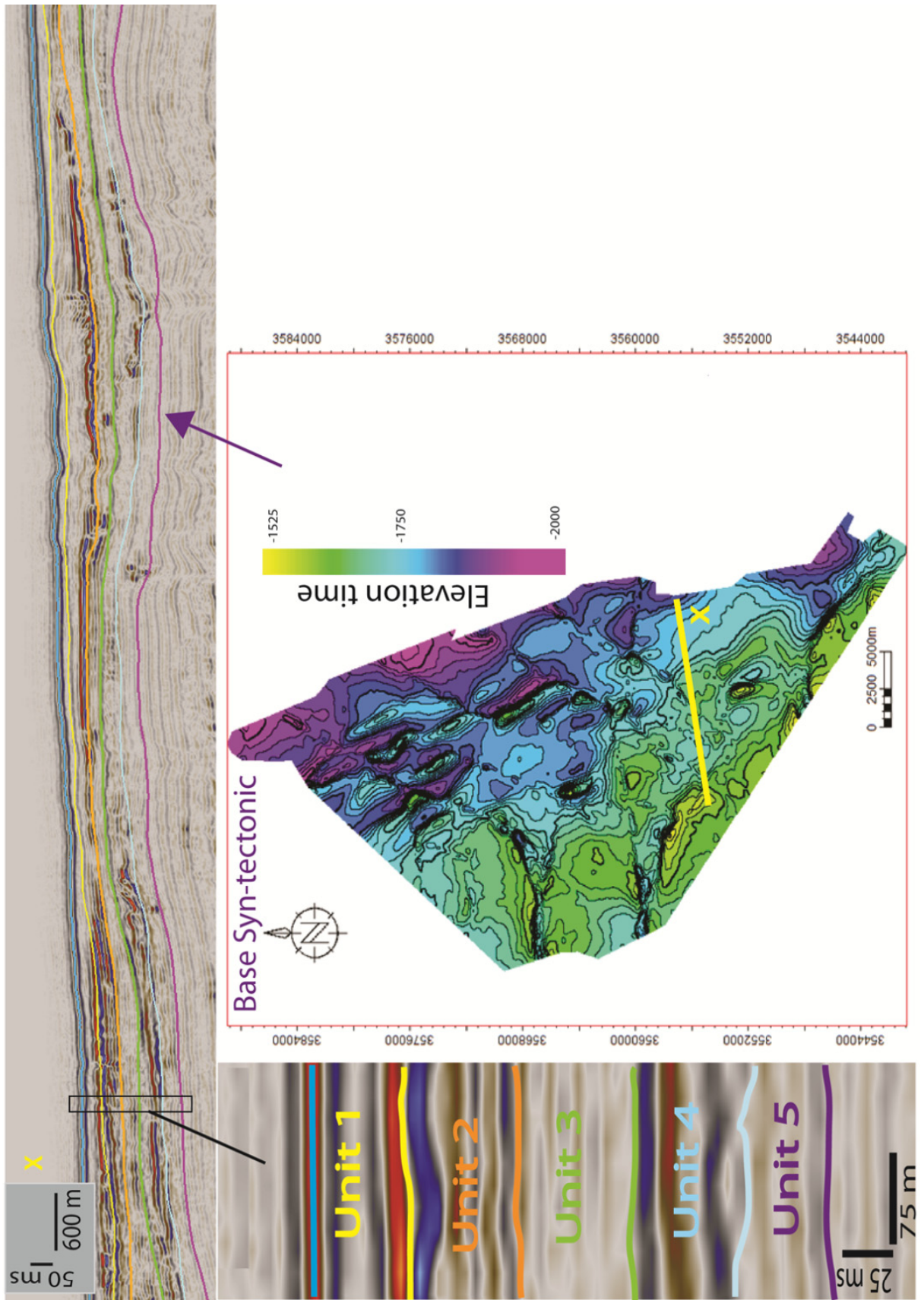The Unit 5 (purple color) is the lower Unit of the Syn-Tectonic sequence and is bounded on the top by the surface 5 (light blue color) and on the base by the (purple color) surface 6 (Base Syn-tectonic surface) *(Figure 5.9)* which is the base of the Syn-Tectonic sequence.

The Base Syn-Tectonic surface has been tracked along an s-crossing and is characterized from an increase in depth with the maximum values (-1920 ms, TWT) observed at the eastern part of the surface and at the fore limb synclines while the minimum values observed at the southwestern parts (-1520 ms TWT) of the surface. The thickness map of the Unit 5 (*Figure 5.10)* illustrates an overall thinning of the surface towards the northeast with the minimum values observed at the fold crests where the two surfaces pinch out and the maximum values at areas of forelimb synclines and in areas along the channel flow where the channel axis is meander.

In the Unit 5 can be observed channels (*Figure 5.11)* located to the southern part of the Unit and consist of the main channel which has been described as (purple color) channel-10 for the area and four channel segments (blue dashed color). The main channel has a northeast flow direction with average sinuosity 1,29 which is higher at the southwest part of the channel and decreases towards the northeast. The length of the channel is 22,31 km. The four of the channel segments are located 7 km southern from the main channel, are spaced 2-4 km, have sinuous lengths 3-9 km and have a northeast flow direction with an exemption for the southern channel segment which flow direction is towards the east.

In terms of seismic facies, Unit 5 consists of four of the Seismic Facies (1, 2, 3 and 5), with the most dominant being Facies 3 at the south part which is incised from the channel 9 of the overlying Unit 4 and has thickness 70 ms and 15 km width with the reflecting MTC's indicated from chaotic and low amplitude to transparent seismic character. The seismic Facies 1 is observed along at the main channel flow of the Unit 5 with discontinuous, contorted, and medium amplitude subparallel reflectors indicative of buried channel fill of depth 60 ms TWT and width 250 m. The seismic Facies 2 *(Figure 5.11 c)* can be observed from continuous/discontinuous, low to medium amplitude, parallel even reflectors indicative channel levee deposits across the channel flow axis with lateral extend 700 m at each side of the channel and height 30 ms TWT. The seismic Facies 5 reflects hemipelagic deposits that occur at the largest part of the area.

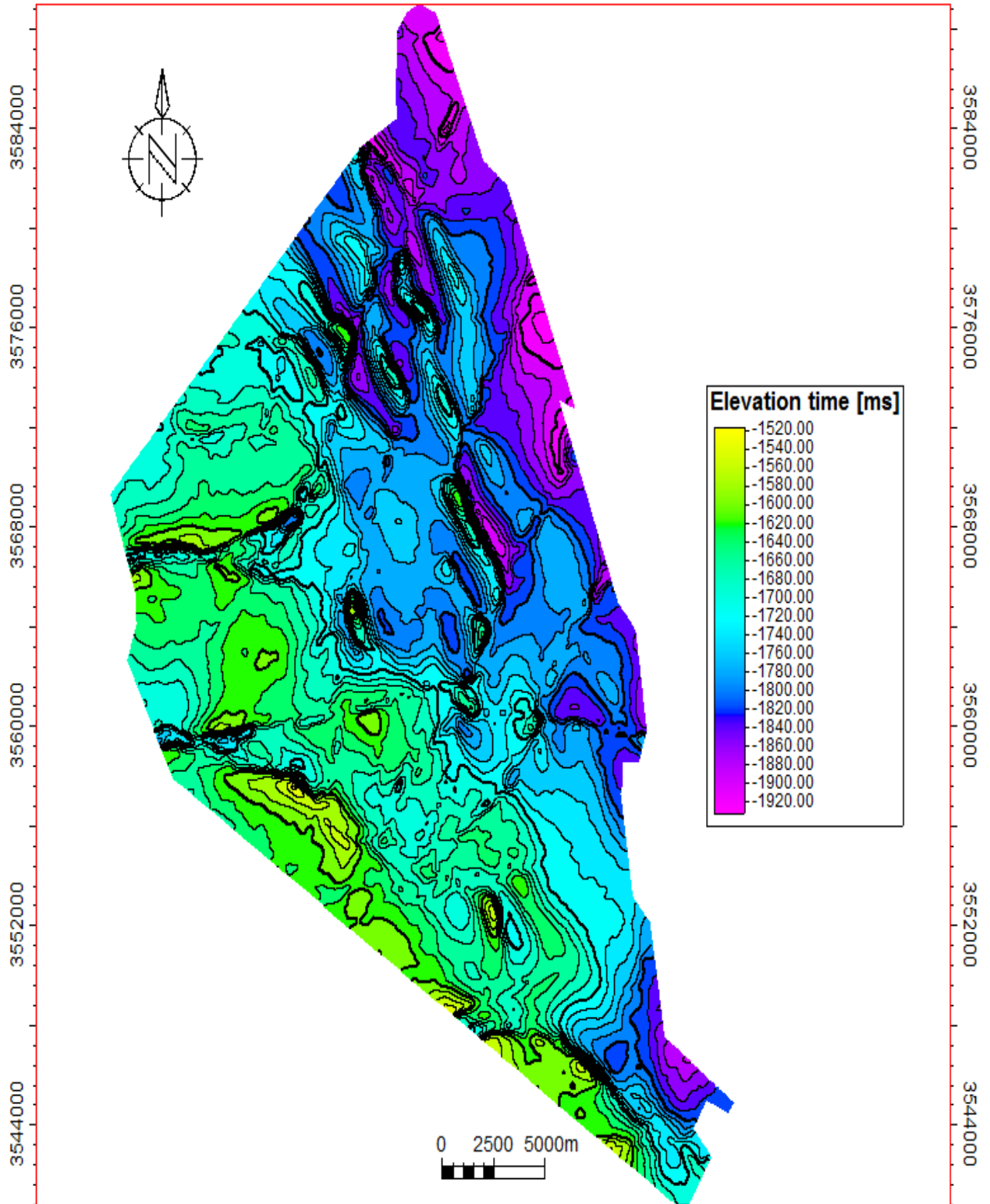**Figure 5.9:** *Elevation time map TWT representing the base of the Unit 5- surface 6 of the study area (Base Syntectonic Unit).*
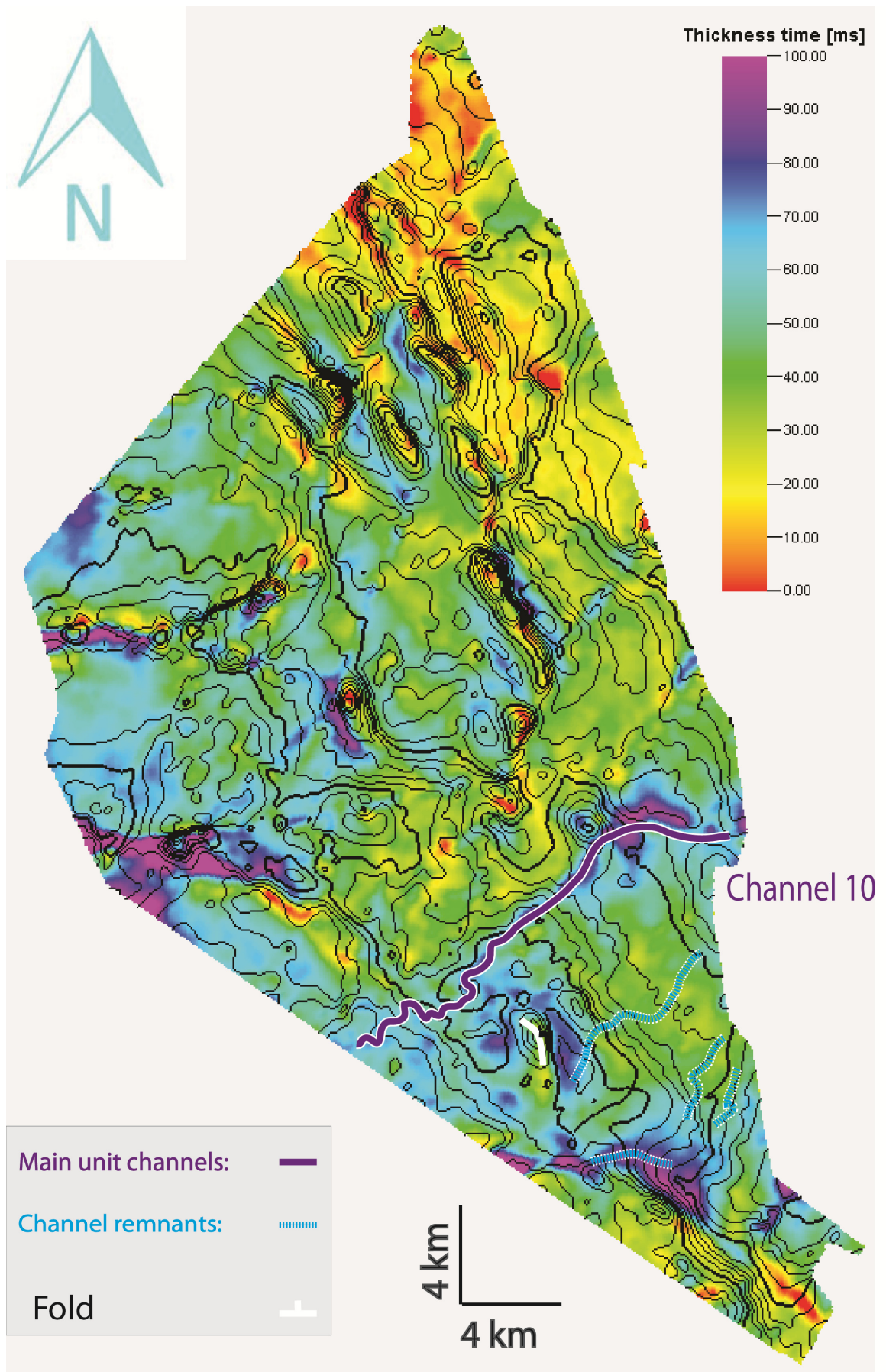
Figure 5.10: TWT thickness time (ms) surface of Unit 5.
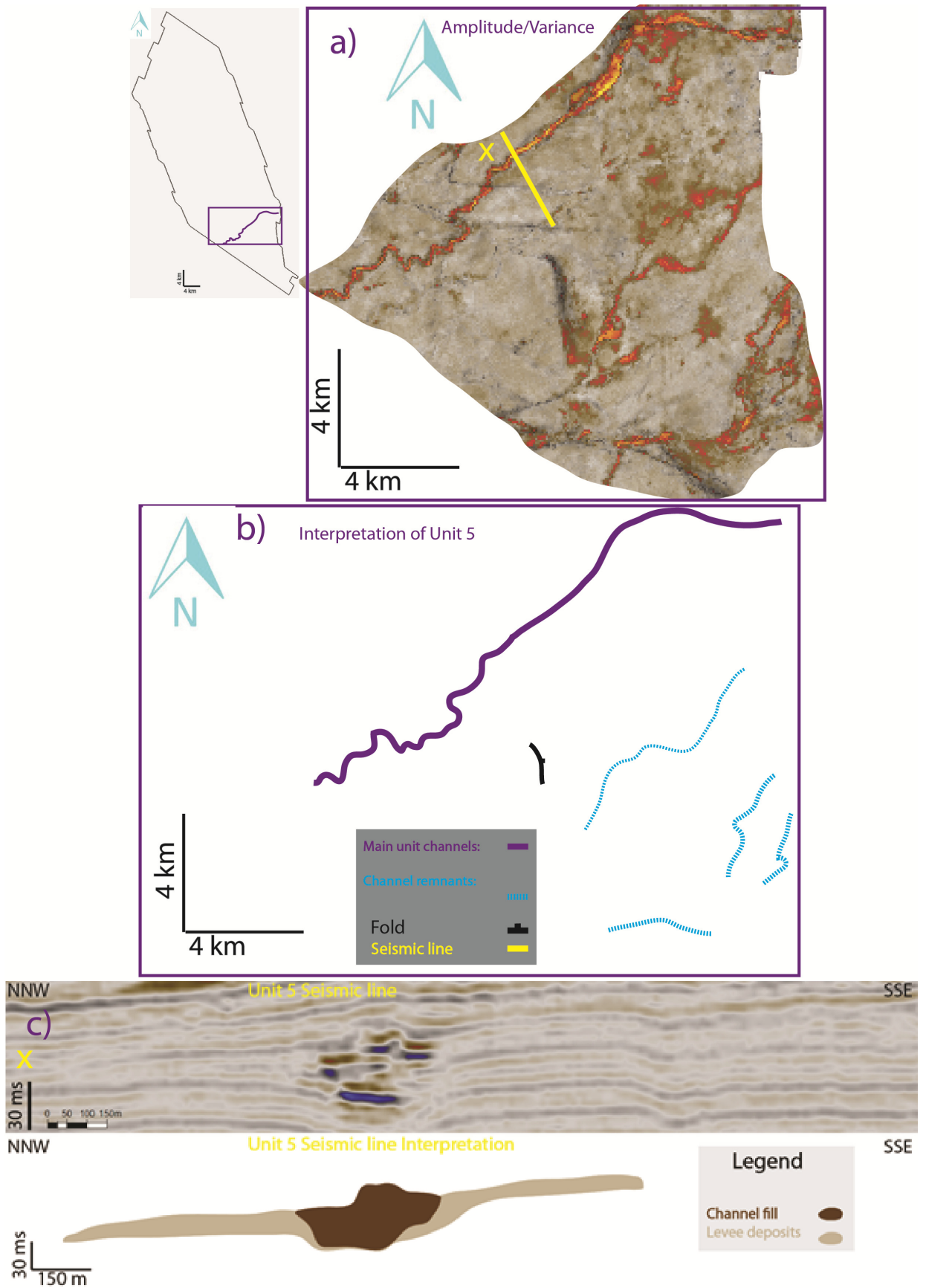
***Figure* 5.11:** *a) Amplitude attribute map combined with variance, illustrating the main depositional elements of Unit 5 and b) their interpretation in plain view, c) seismic line illustrating channel fill surrounding by levees.*

5.2.2 Unit 4

The Unit 4 (light blue color) is located above the Unit 5 and is bounded on the top by the surface 4 and at the base by the light blue color surface 5 (***Figure 5.12***).

The surface 5 has been tracked along an s-crossing and is characterized from an increase in depth with the maximum values (-1900 ms, TWT) observed at the northeastern part of the surface while the minimum values observed at the southwestern parts (-1520 ms TWT) of the surface. The thickness map of the Unit 4 (***Figure 5.13)*** illustrates the thinnest areas (10 ms) to be mostly located around the fold crests while the thickest values (100 ms TWT) are observed at the southern part of the area where there are mass transport deposits, at the middle and north-east part of the Unit at areas along channel meandering and unconfined areas where the channel transits to depositional lobe occurs respectively.

In the Unit 4 can be observed 5 channels (blue color) (***Figure 5.14)*** located in the middle part of the Unit with distance between each of them 2-8 km. The northern channel is the channel number 5 which has an erosional base with length 39,52 km and sinuosity 1,49. The channel 5 is affected with confinement and diversion from the folds 4,5 and 6 located at the downstream part of the channel flow. Along the channel flow are observed the following 4 crevasse splays at the channel bends: crevasse splay 1 is the first upstream with dimensions 1,6 km^2, the crevasse splay 2 with dimensions 1,9 km^2, the crevasse splay 3 with dimensions 1,2 km^2 and the crevasse splay 4 with dimensions 2,3 km^2. The average thickness of the crevasse splays is 20 ms (TWT). The downstream part of the channel is characterized by confinement and diversion from the pre-existing folds upon entering the fold belt while after the exit from the fold belt it changes flow direction 30 degrees towards the north and unconfinement resulting in the deposition of the frontal splay 1 (***Figure 5.15 a)*** with extension 20,5 km^2 and thickness 80 ms (TWT) .

Southern of the channel 5 in distance 2 km is located the channel 6 with length 27,45 km and sinuosity 1,45. At the upstream part the channel 6 is characterized from developed levee deposits that decrease in size towards the downstream part of the flow. The channel 6 has a northeast flow direction which is diverted from the pre-dated of the channel fold 3 and it crosses the post-dating fold 4 and it is diverted at the downstream part of the flow from the fold 5. At the northern outer bend of the channel 2 km south west from the fold 3 there is the crevasse splay 5 of the Unit which covers an area 4,8 km^2 and has thickness 25 ms (TWT) while after the diversion at the fold 3 the frontal splay 3 is deposited at an area of 38 km^2 with thickness 75 ms (TWT). After the channel exits the fold belt (***Figure 5.15 b***) it deposits the frontal splay 2 with extend 14 km^2 and thickness 30 ms (TWT). Two distributary channels are observed to the southern part of the frontal splay deposits.

Seven kilometres southeast of the channel 6 is located the channel 7 with length 32,48 km, sinuosity 1,49 and flow direction northeast. At 12 km from the upstream part of the channel flow there is the crevasse splay 6 extending 1,9 km^2 and has a thickness 25 ms (TWT). At 5 km downstream from the point of the crevasse splay deposition the channel

passes to the transition zone from channel to frontal splay (***Figure 5.14 c)*** with the deposition of the lobe 4 extending 31,5 km^2 and 60 ms thick (TWT) and two distributary channels.

The channel 8 is located 3 km southern from the channel 7 and has length 16,94 km, sinuosity 1,22 and north east flow direction. At distance 7 km after the from the upstream part of the channel is located the frontal splay 5 (***Figure 5.15 c***) with extend 29,3 km^2 and thickness 55 ms (TWT) and one distributary channel.

The southern channel of the Unit 4 is located 2,5 km southern of the channel 8 is the channel 9 with length 7,21 km, sinuosity 1,12 and northeast flow direction. The channel is diverted from the fold 1 deposits the crevasse splay 7 with extend 1,1 km^2 and thickness 25 ms (TWT).At the downstream part the channel deposits the frontal splay 6 (***Figure 5.15 d***) with extend 9.75 km^2 thickness 50 ms (TWT), and one distributary channel.

In terms of seismic facies, Unit 4 consists of all the Seismic Facies (1, 2, 3, 4 and 5), with the mass transport deposits to be the most dominant at the southeastern part of the Unit indicated from chaotic and low amplitude to transparent seismic character. The Facies 4 of the Unit 4 are the prominent facies of the eastern part of the Unit 4 can be observed at the downstream part of the channels flow from continuous to slightly discontinuous, high amplitude (HARP), relative flat reflections indicative of channelized lobe complex deposits. The seismic Facies 1 is observed along at the main channel flow of the Unit 4 with discontinuous, contorted, HAR subparallel reflectors of depth 50 ms TWT and width 190 m. The seismic Facies 2 can be observed from continuous/discontinuous, low to medium amplitude, parallel even reflectors indicative channel levee deposits across the channel flow axis with lateral extend 1 km at each side of the channel and height 45 ms TWT. The seismic Facies 5 is observed at the northern part of the Unit and reflects hemipelagic or turbidite deposits that observed as continuous, parallel reflectors of low amplitude.
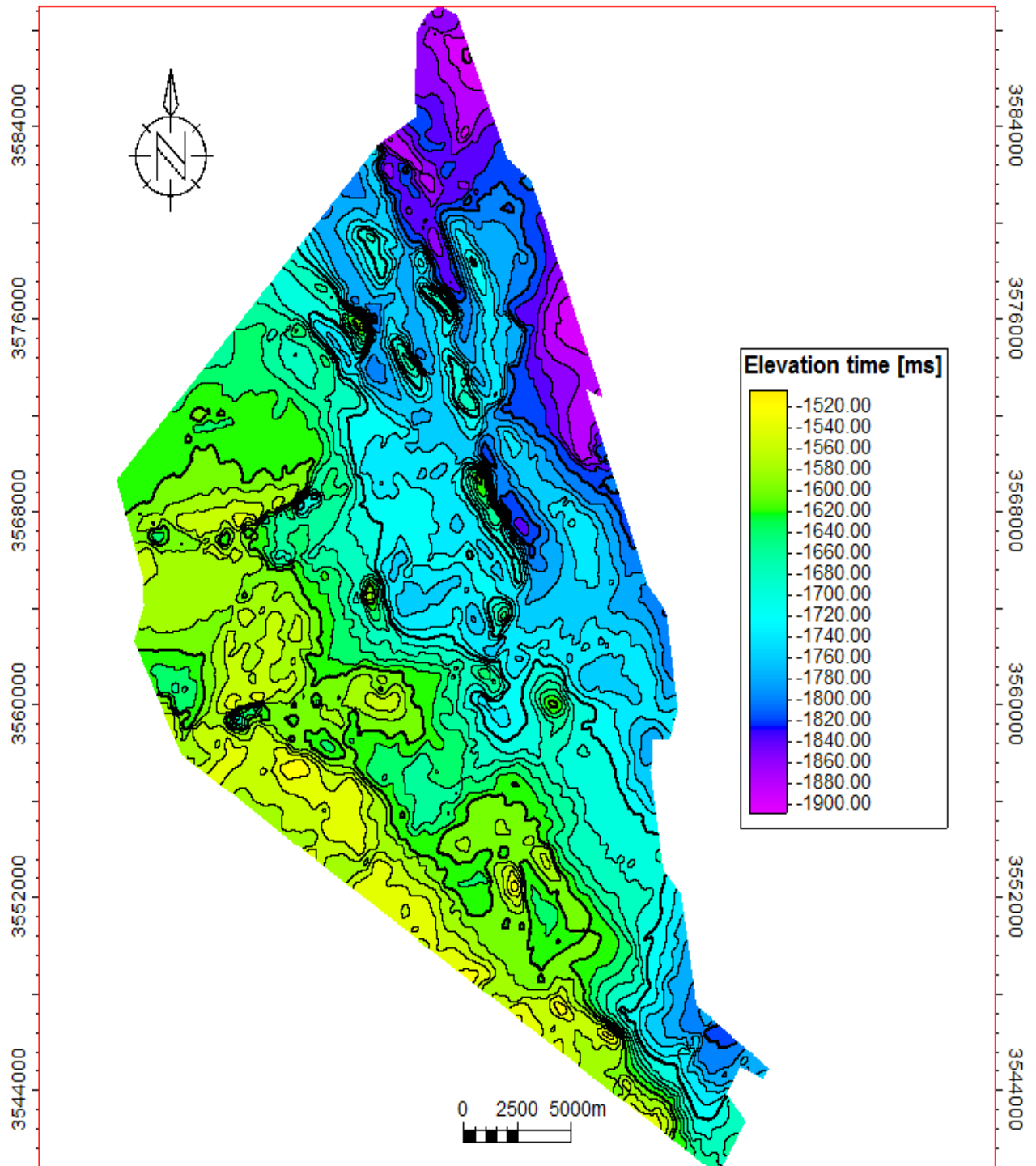
Figure 5.12: *Elevation time map TWT representing the base of the Unit 4- surface 5 of the study area.*
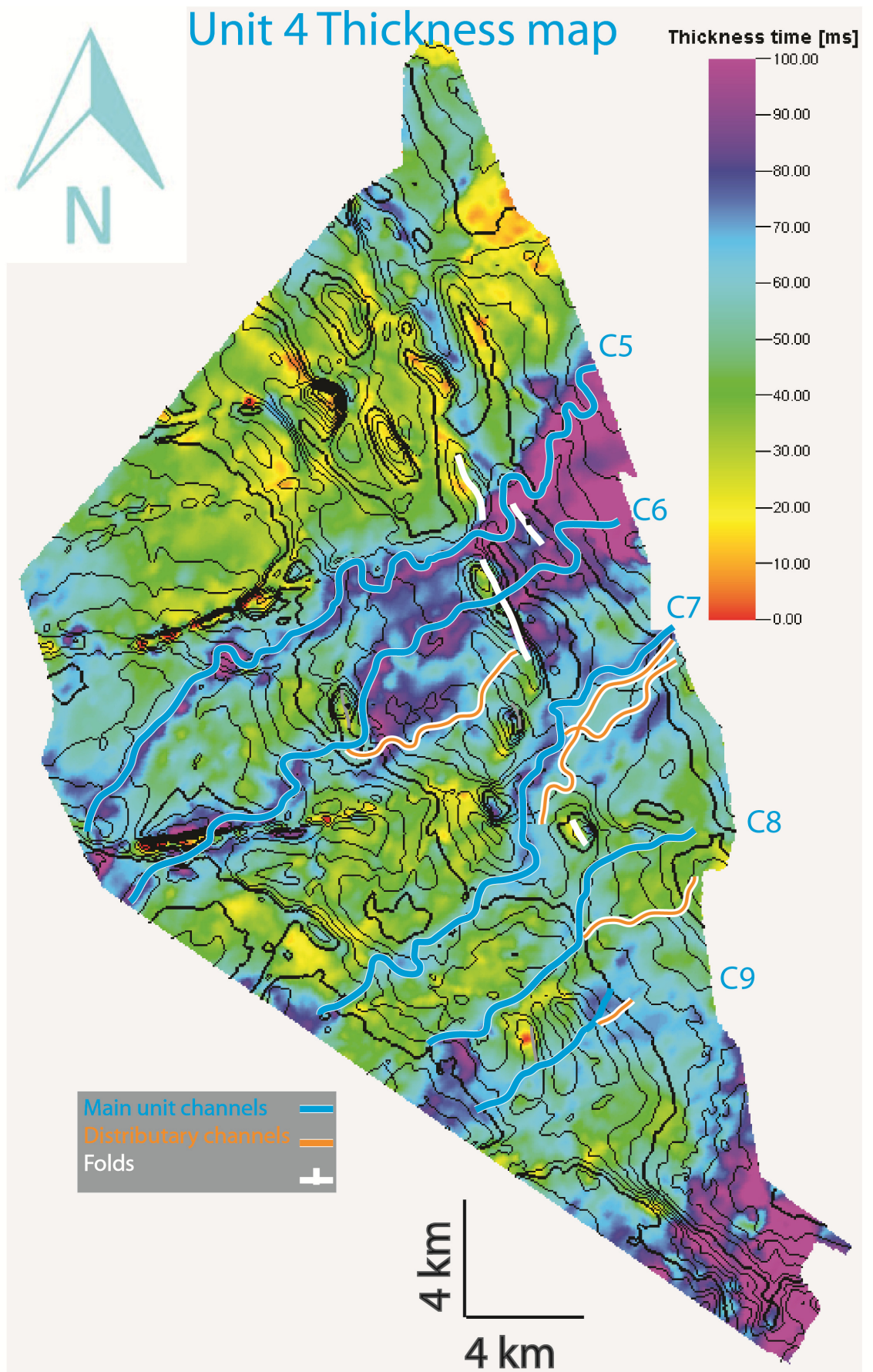
Figure 5.13: *TWT thickness time (ms) surface of Unit 4.*

Main sedimentary elements of Unit 4
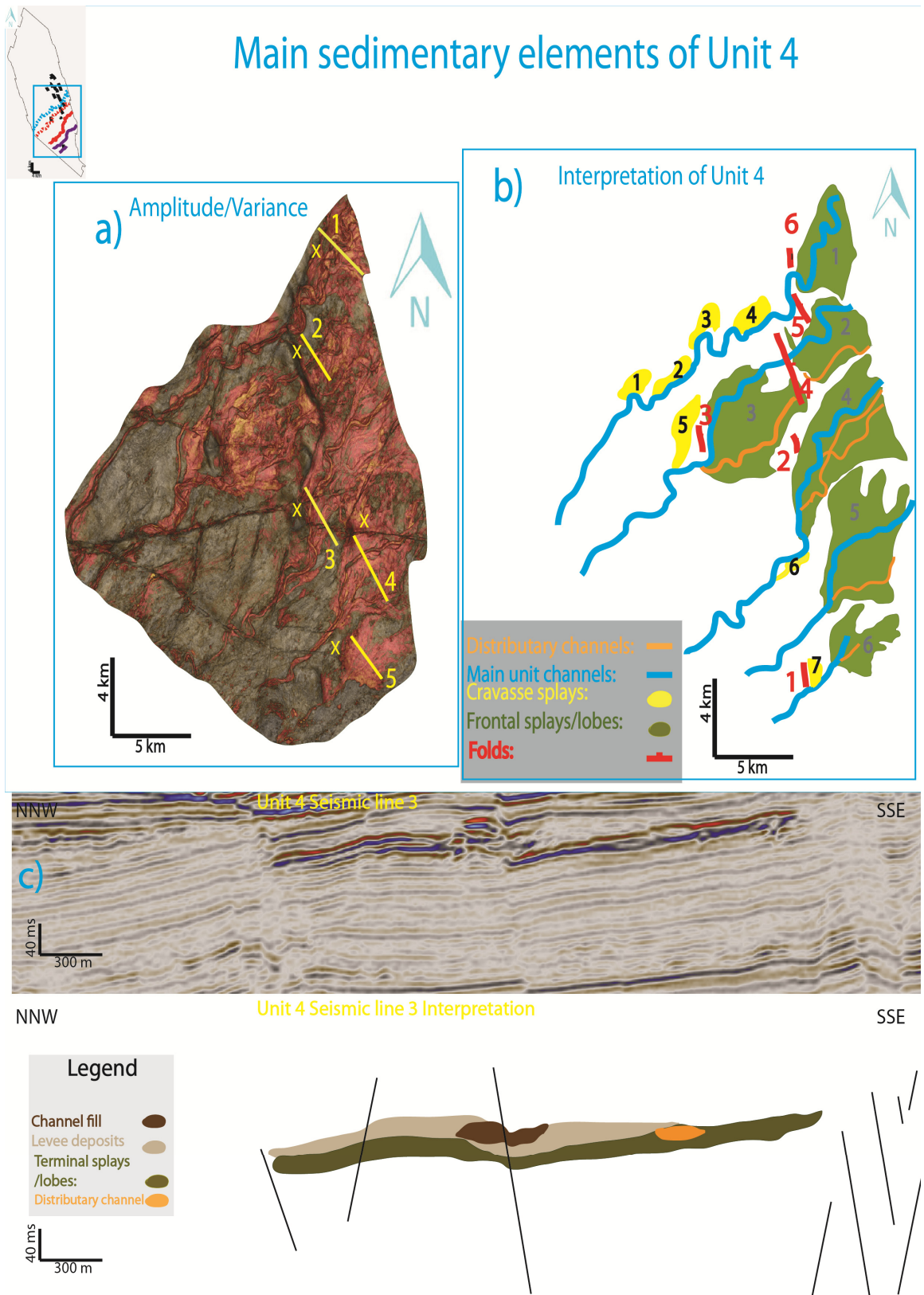
Figure 5.14: *a) Amplitude attribute map combined with variance, illustrating the main channels of Unit 4 and b) their interpretation in plain view, c) seismic line illustrating channel fill surrounding by levees deposits that overlie the frontal splay 4.*
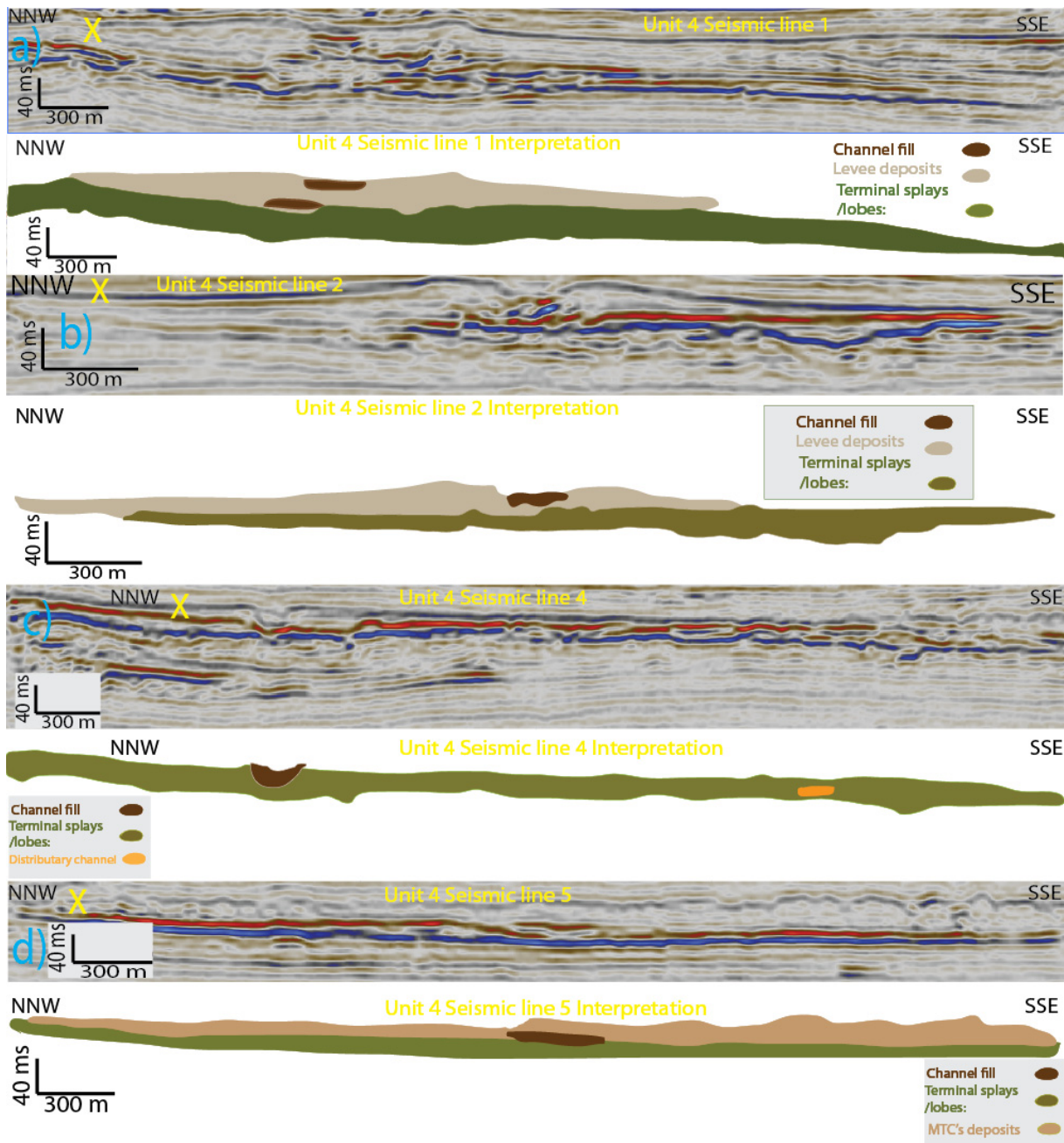
Figure 5.15: *Seismic sections with their interpretation from the down slope deposits of channel 5 a), 6 b), 8 c) and 9 d).*

The most representative channel of the Unit 4 that has not been described before is the channel 7 which is characterized from the seismic Facies (1, 2 and 4). At the first 5 km the channel is characterized from high sinuosity 1,85 resulted from unconfinement in combination with the small gradient of the underlying topography which abruptly decreases towards north-east for 8 km with subsequent increase of incision. At 15 km the sinuosity increases to 1,39 as the axis flow is transferred in area of topographic low created by faulting and is accompanied by aggradation of the channel deposits. At 23 km the channel axis decreases the sinuosity because of confinement created from the bounding pop-up structures (***Plot 5.1***) developed from strike-slip movement in a zone of local transpression. The exit of the channel from the confined area results in the transition from channel to frontal splay. On

the same time when the channel exits the area of confinement it increases abruptly the sinuosity because of diversion from the fold 2 and it becomes aggradational (***Figure 5.16 A***). After diversion the channel's sinuosity is characterized from a small decrease and the channel becomes aggradational (***Figure 5.16 B***).
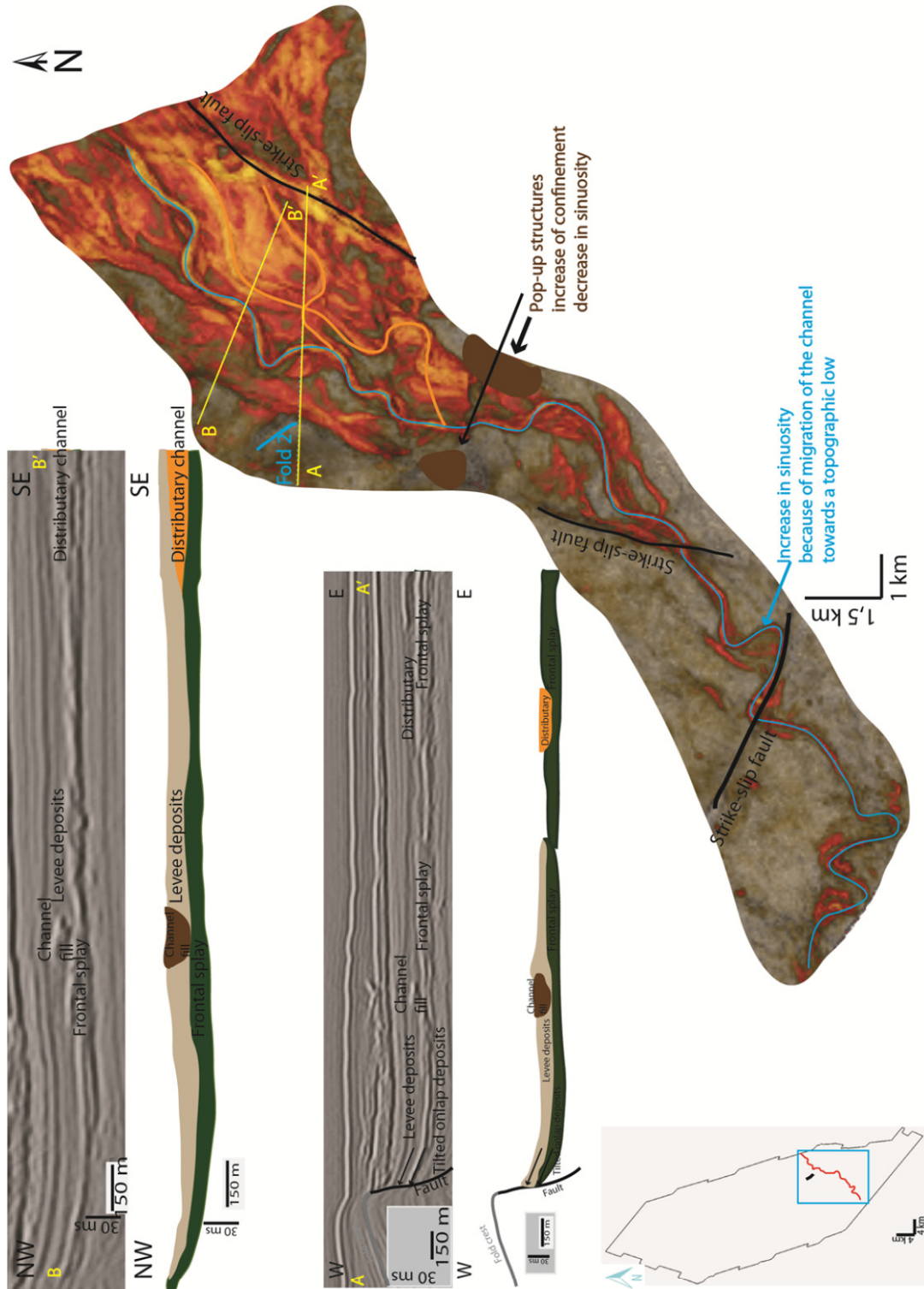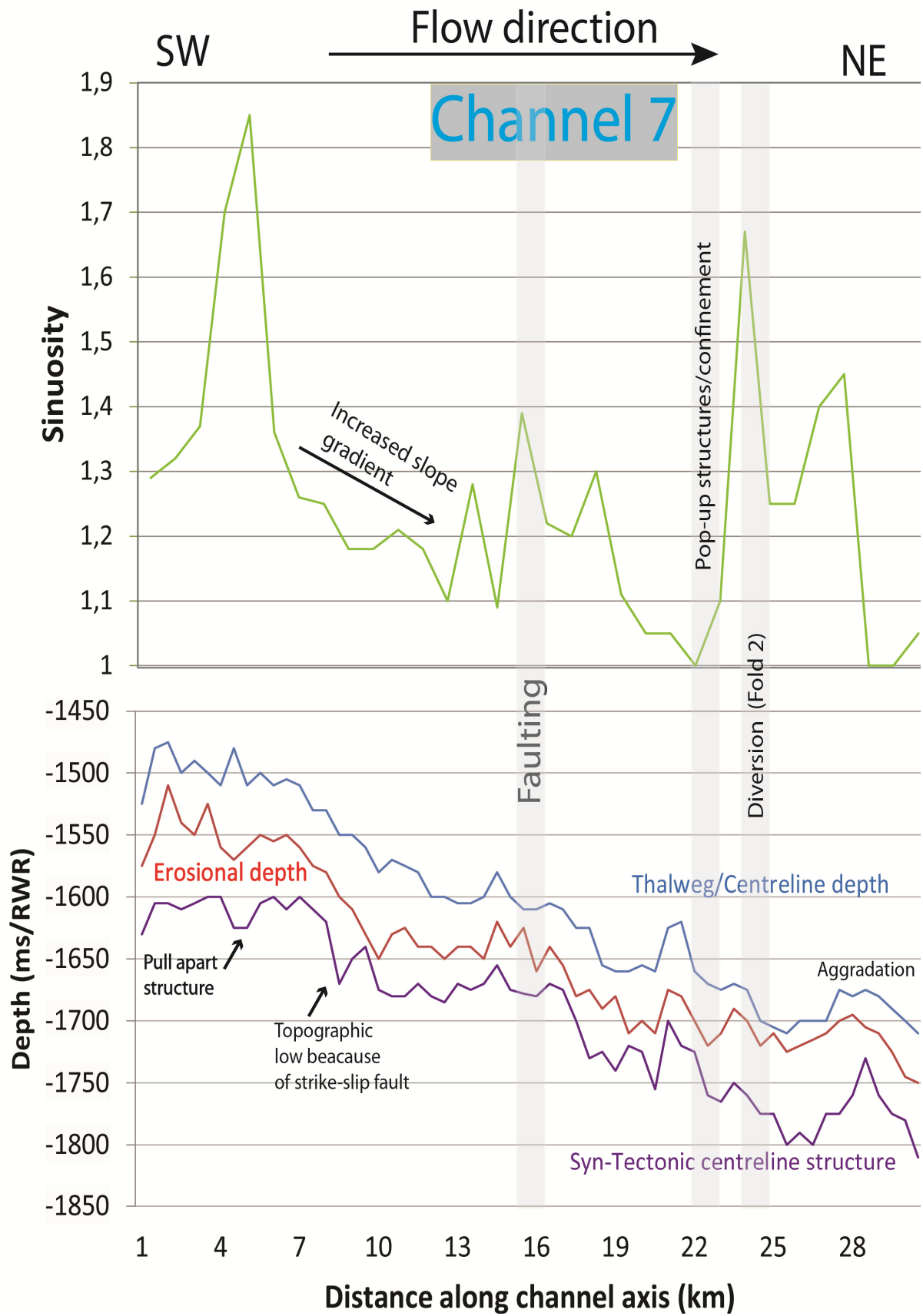

Figure 5.16: *Plan view of channel 7 with the transition zone from confinement because of surrounding structures (pop-up structures) to unconfinement and A) diversion from fold 2 accompanied from increase in sinuosity and B) channel aggradation.*

Plot5.1: Quantitative measurements of channel 7.

5.2.3 Unit 3

The Unit 3 (green color) that is located above the Unit 4 is bounded on the top by the (orange color) surface 3 and by the (green color) surface 4 (Intermediate surface) on the bottom *(Figure 5.17)* which is characterized from a progressive deepening towards the northeast. The thickness map of the Unit 3 (*Figure 5.18)* illustrates an overall thinning towards the northwest and an accommodation area is observed at the south east part of the area.

The main depositional elements of the Unit 3 (*Figure 5.19)* consist of the main channel which has been described as channel-4 (green color) and one frontal splay. The main channel has an east-northeast flow direction with average sinuosity 1,17 and the sinuous length of the channel is 27,78 km. The channel development pre-dates of the strike slip faulting in the area, fact that is observed from the offset of the channel while it post-dates the fold 14 which cause to the diversion of the channel. After the channel 4 exits the fold belt it becomes unconfined and deposits a frontal splay with extension 53.21 km^2 and thickness 50 ms (TWT).

In terms of seismic facies the Unit 3 consists of four of the mentioned Facies with the most dominant through the whole area to be the Facies 5 which consists of hemipelagic or turbidite deposition with continuous, low amplitude and subparallel reflectors. The Facies 1 can be observed at the northern part of the Unit 3 with discontinuous, contorted, high amplitude (HAR), subparallel reflectors indicative of buried channel fill. The Facies 4 of the Unit can be observed at the downstream part of the channel flow and consists of (*Figure 5.19 c*) continuous to slightly discontinuous, high amplitude (HARP), relative flat reflections indicative of channelized lobe complex deposits.

Figure 5.17: *Elevation time map TWT representing the base of the Unit 3- surface 4 of the study area (Intermediate surface).*
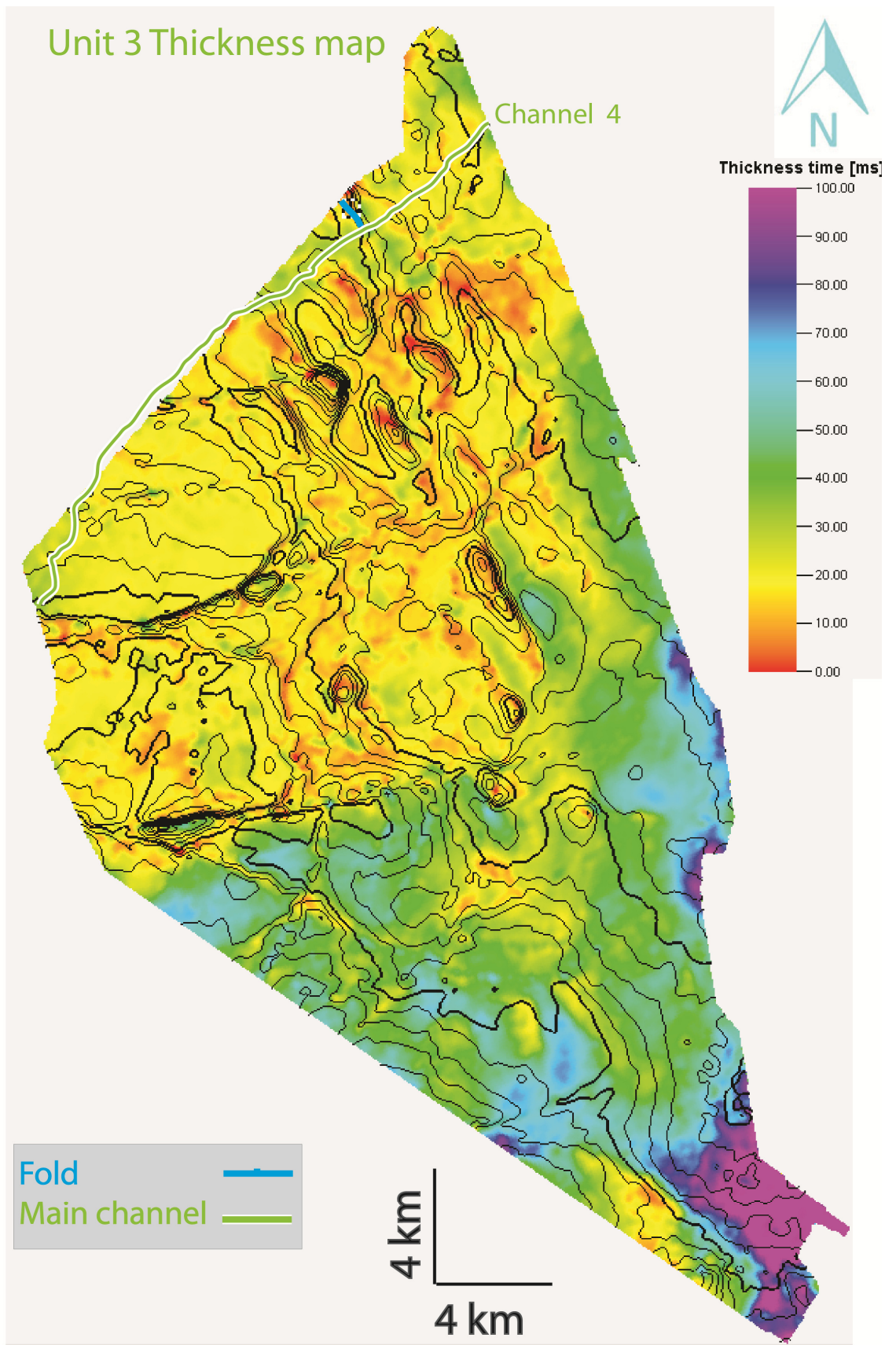
Figure 5.18: *TWT thickness time (ms) surface of Unit 3.*
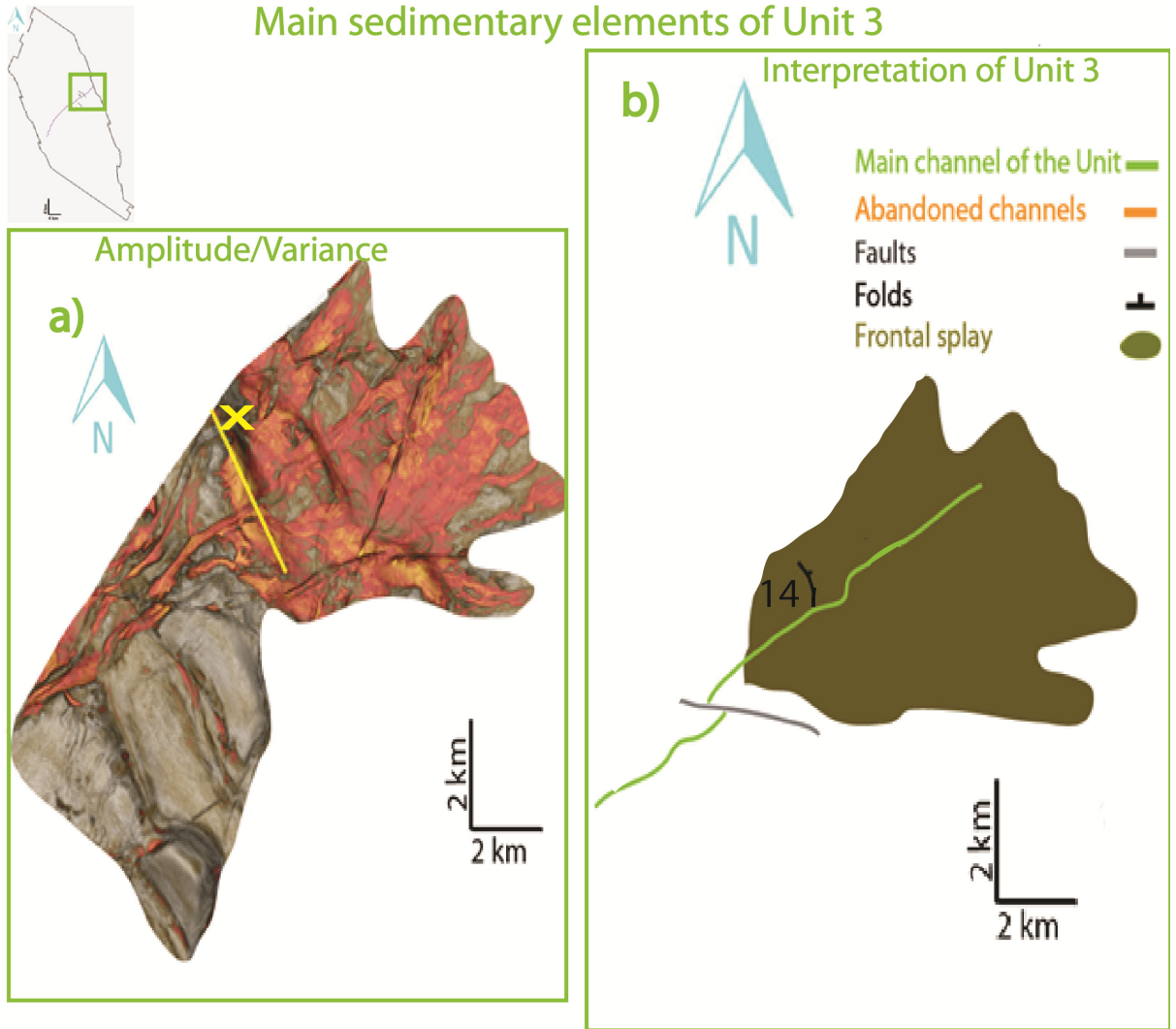
Figure 5.19: *a) Amplitude attribute map combined with variance, illustrating the main depositional elements of Unit 3 and b) their interpretation in plain view, c) seismic line illustrating channel fill that feeds the frontal splay.*

5.2.4 Unit 2

The Unit 2 (orange color) that is above the Unit 3 is bounded on the top by the surface 2 (yellow color) and by the (orange color) surface 3 (*Figure 5.20*) on the base. Both of the bounded surfaces are characterized from a progressive deepening towards the north east. The thickness map of the Unit 2 (*Figure 5.21)* illustrates the thinnest part of the Unit to be northwest while the thicker areas which act as depocentres are mostly observed at areas along the channels flow.

The main depositional elements of the Unit 2 (*Figure 5.22)* consist of two main channels (dashed orange color) which have been described as channel-2 and channel-3 for the area of analysis, three avulsion channels (orange color) , 2 abandoned channels (red color), 9 crevasse splays yellow color) and 3 frontal splays (dark green color). From the two main channels the northern channel-2 has a northeast flow direction with average sinuosity 1,63 which is high at the northern part of the channel and decreases towards the south. The length of the channel is 43,54 km and the channel fill has an average thickness 50 ms (TWT). The second main channel-3 of the Unit 2 is located southern of the main channel-2 and has an overall sinuous length 34,13 km and average sinuosity 1,44. Southern of each main channel can be observed one 1 abandoned channel indicated by red color number as abandoned channel-1 and abandoned channel-2.

The main channel-2 consists of two avulsion nodes (purple color) and three avulsion channels. The avulsion node upstream of the flow is observed before the channel emerges enters the fold belt (black color) and consists the pathway for the flow of the avulsion channel-1 with length 8,8 km which is characterized from 5 crevasse splays, crevasse splay -1 with dimensions 3,72 km^2, crevasse splay-2 with dimensions 2,98 km^2, crevasse splay-3 with dimensions 4,24 km^2, crevasse splay-4 with dimensions 1,75 km^2 and crevasse splay-5 *(Figure 5.22 c)* with dimensions 9,7 km^2. The second avulsion node can be observed when the channel-3 has enter the fold belt and has result to two avulsion channels, the avulsion channel-2 with length 1,76 km that is characterized from the crevasse splay-7 with dimensions 4,92 km^2 and the avulsion channel-3 with length 2,3 km that is characterized from the crevasse splay-8 with dimensions 4,46 km^2. After the channel-2 has exit the fold belt two crevasse splays can be observed at the channels bends, the crevasse splay-6 and the crevasse splay-9 with dimensions 5,5 km^2 and 5,3 km^2 respectively. From the three frontal splays the two of them that can be observed at the southwest part of the Unit 2 have not been measured because of their unknown source channel which is not covered by the dataset. The third frontal splay at the eastern part of the Unit 2 was fed from the abandoned channel-2 and it has dimensions 31,67 km^2.

In terms of seismic facies the Unit 2 consists of three of the mentioned Facies with the most dominant through the whole area to be the Facies 1 and 2 can be observed in the middle part of the Unit 2 across the channel flow path with discontinuous, contorted, high amplitude (HAR), subparallel reflectors indicative of buried channel fill and continuous/discontinuous, low to medium amplitude, parallel even reflectors indicative channel levee deposits

respectively. The Facies 4 of the Unit 2 can be observed at the eastern part of the Unit 2 downstream part of the abandoned channel-1 flow and is consisted from continuous to slightly discontinuous, high amplitude (HARP), relative flat reflections indicative of channelized lobe complex deposits (***Figure 5.22 d***).
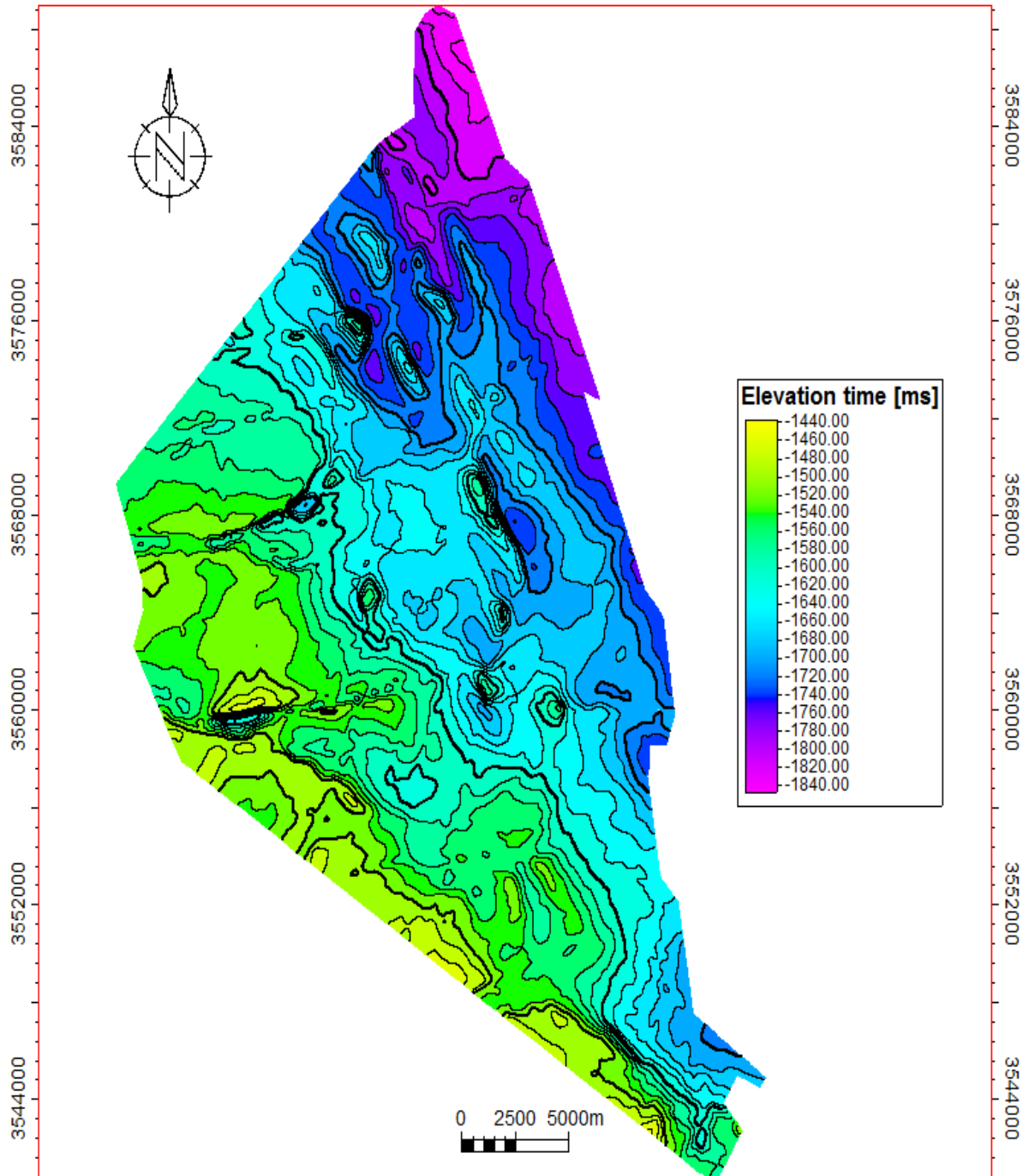

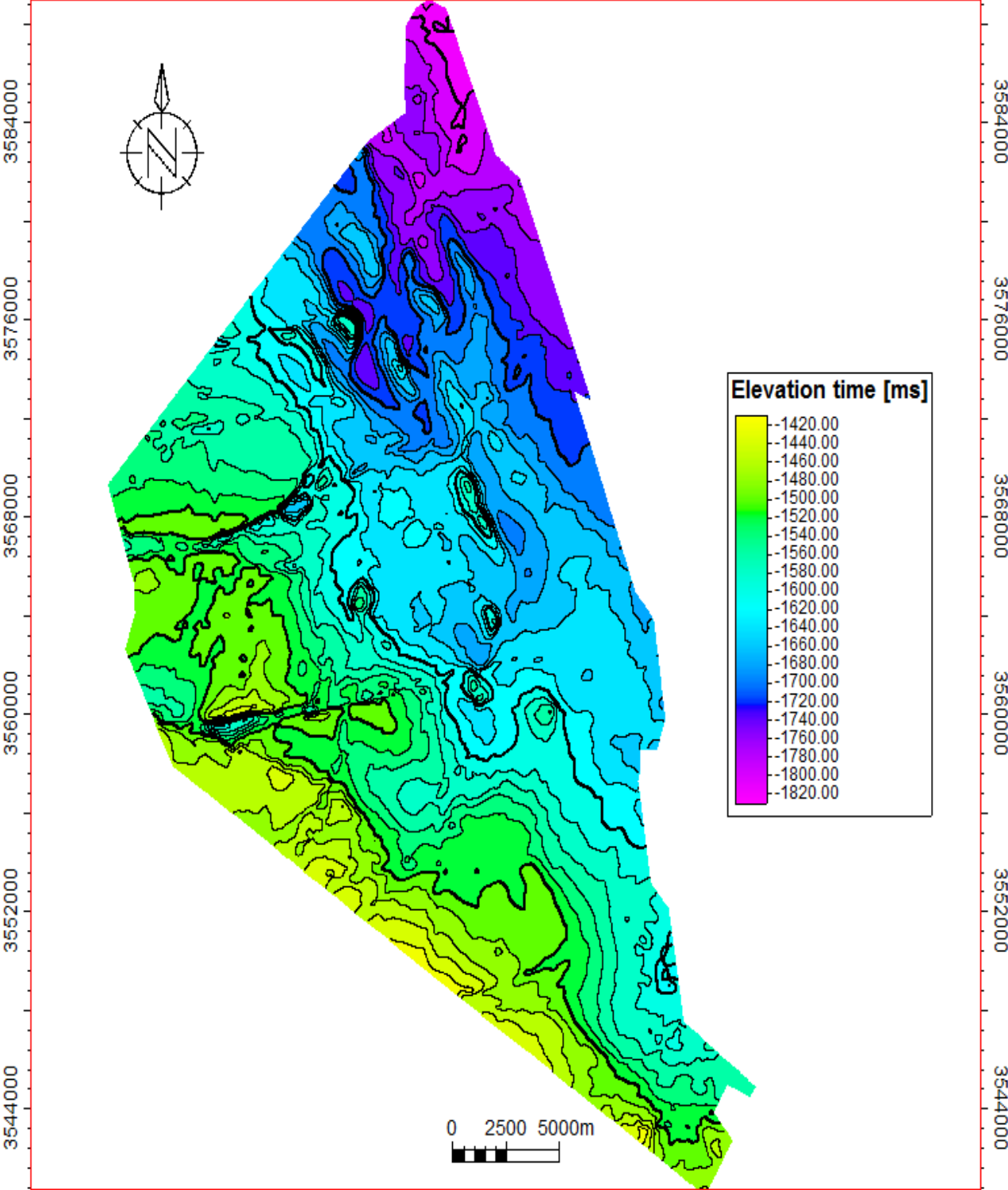***Figure 5.20:*** *Elevation time map TWT representing the base of the Unit 2- surface 3 of the study area.*
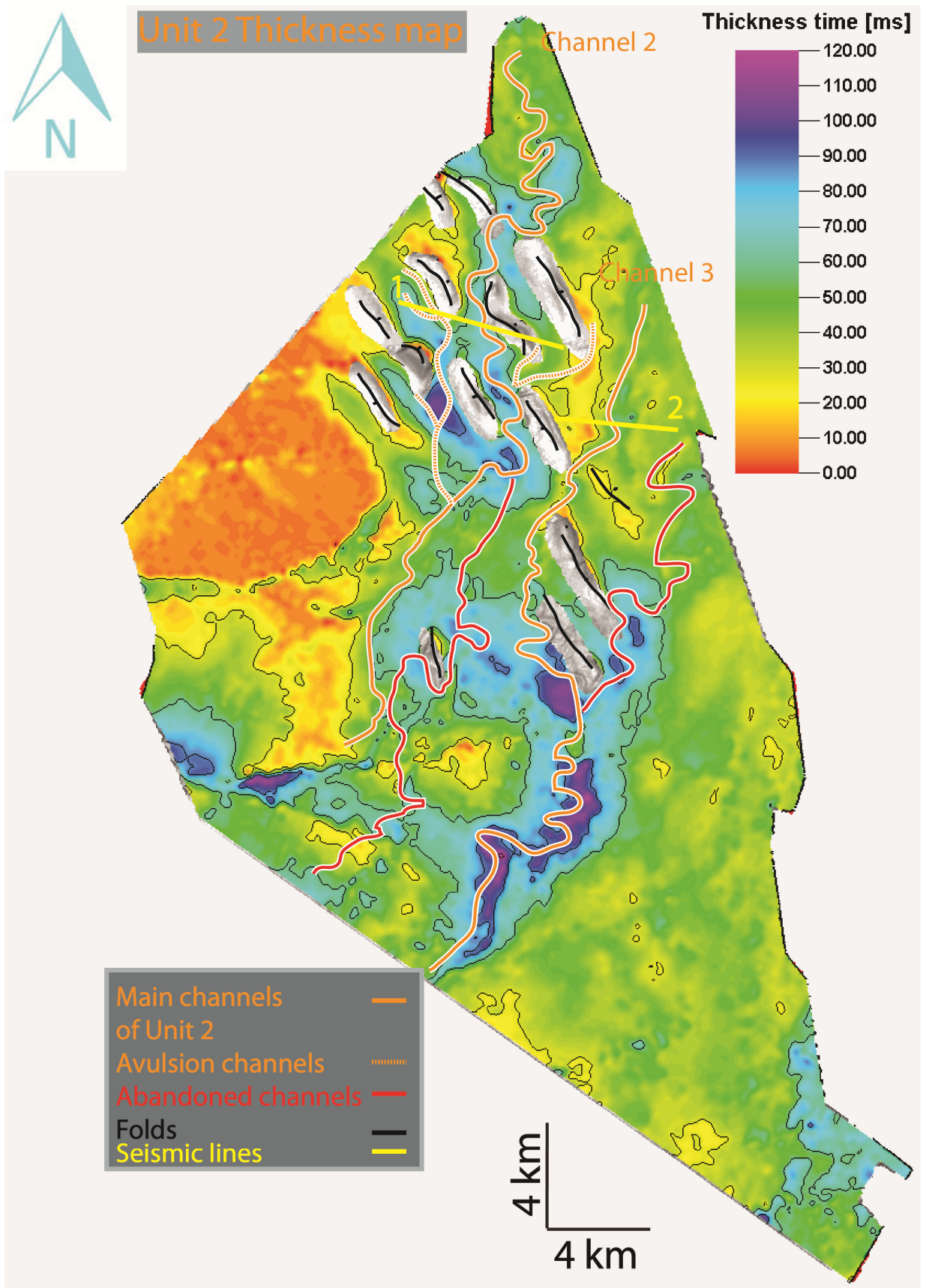
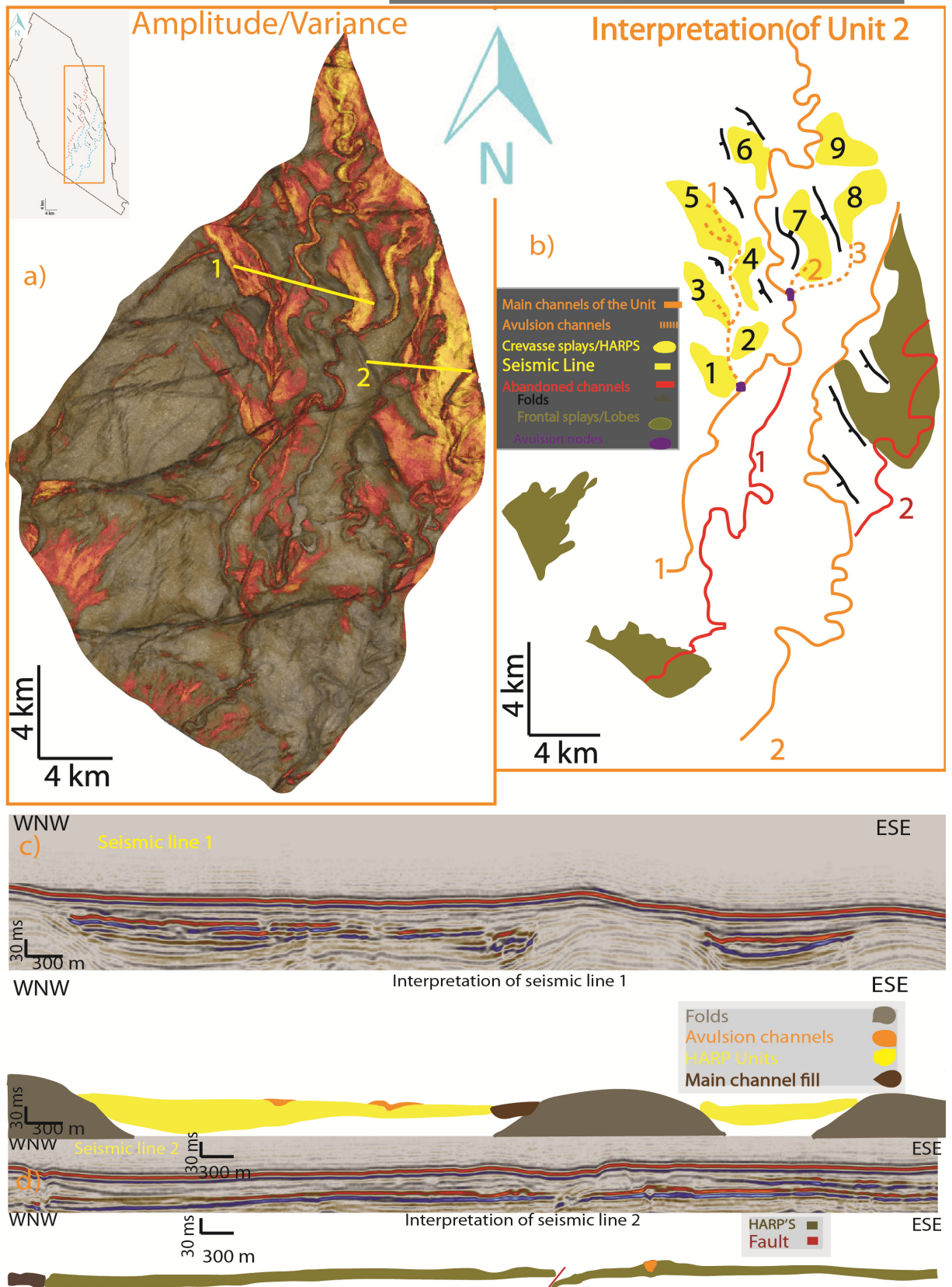***Figure 5.21:*** *TWT thickness time (ms) surface of Unit 2.*

Figure 5.22: a) Amplitude attribute map combined with variance, illustrating the main depositional elements of Unit 2 and b) their interpretation in plain view. Seismic lines c) illustrating the main depositional elements of the channel 2 and d) 3.

The most representative channel of the Unit 2 that has not been described before is the channel- 2 which is characterized from the seismic Facies (1, 2 and 4). At the first 17 km the channel is characterized from an average low sinuosity 1,3. Along that distance the channel is characterized from well-defined levees and erosional base while it progressively becomes aggradational down flow. After the channel crosses the first E-W strike slip fault it is characterized from change in flow direction towards the south-east and an increase in sinuosity because of lateral migration towards the bathymetric low resulted from a pull-apart structure created by the strike slip fault in a zone of transtension (***Figure 5.23***). After the lateral migration the channel is diverted from the E-W strike slip fault towards the north and enters the fold belt.

In the fold belt the channel initially is deflected towards the north-west (***Figure 5.23 a***) from the coeval growing fold 6 and migrates laterally towards the pre-dating fold 9 where the channel is diverted (***Figure 5.23 b***) again north-east towards the fold crest of fold 6. After the channel is diverted from the fold 9 it migrates laterally back to the fold 6 where it is deflected again north-west (***Figure 5.2.3 c***) towards the fold 9. After the channel is deflected and exits the fold 6 it is observed an avulsion point along the outer bend of the northern side of the channel which results to decrease of vertical aggradation of the channel. Afterwards the channel reach the fold 9 it is going to be diverted again north-east towards the pre-dating fold 8 where it is diverted north-west towards the coeval growing fold 13. The fold 13 (***Figure 5.23 d***) deflects the channel flow axis which cause lateral migration of the channel north-east towards the fold 8. After the channel migrates laterally towards the fold 8 it is diverted towards the north-west where at 2 km from the point of diversion from fold 8, a topographic low results in the lateral south-east migration of the channel towards the coeval growing fold 7 where the channel is deflected towards the north. After the deflection from the fold 7, the channel has exit the fold belt with subsequent loss of confinement, it flows towards the north and is characterized from increase in sinuosity and subsequent aggradation.
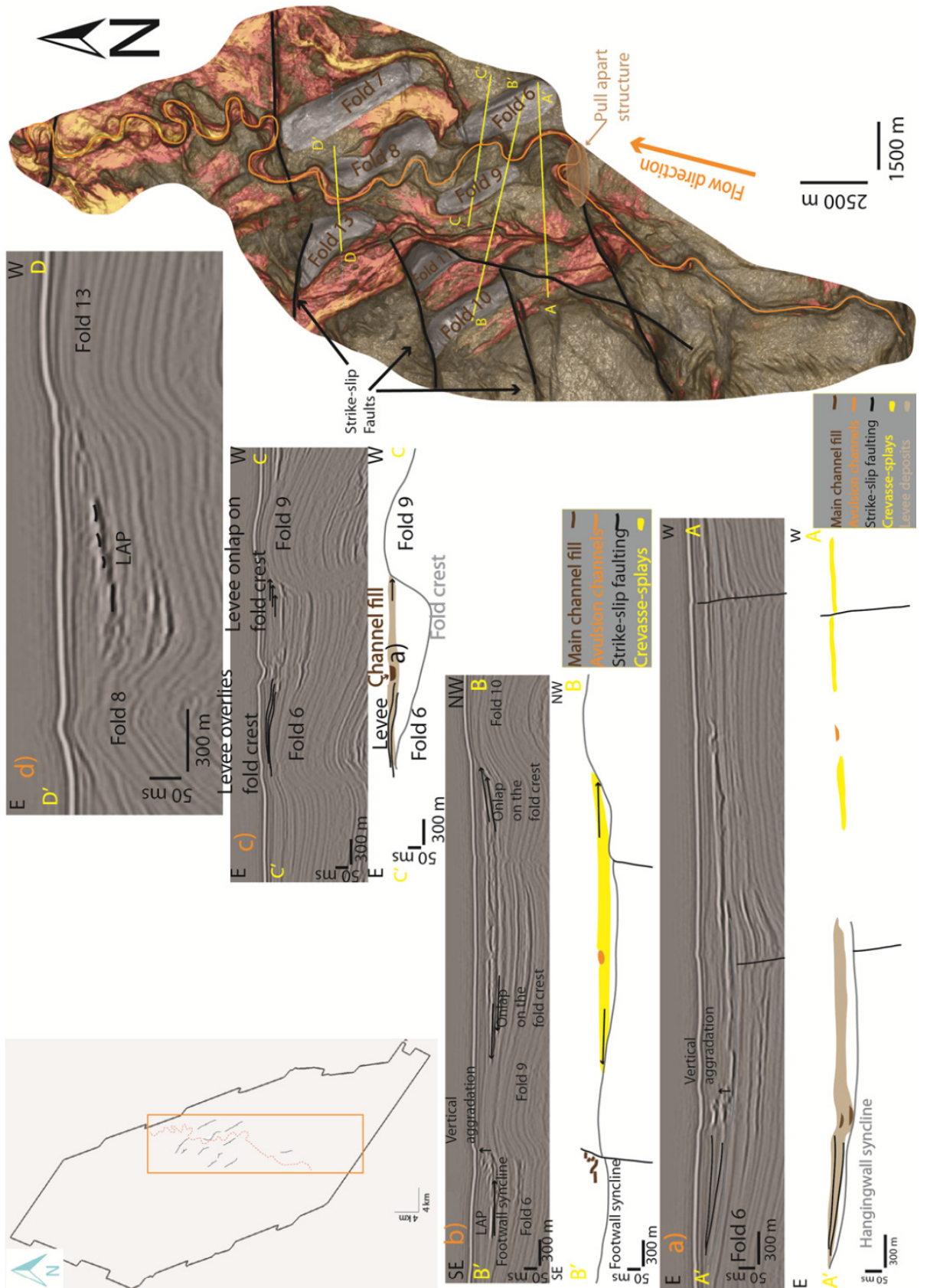
a) **Figure 5.23:** *Plan view of channel 2 and seismic profiles with a) channel deflection from fold 6, b) channel diversion from fold 9 and confinement of crevasse splay deposits from folds 6 and 9, c) channel deflection from fold 6 and d) channel diversion from fold 13.*
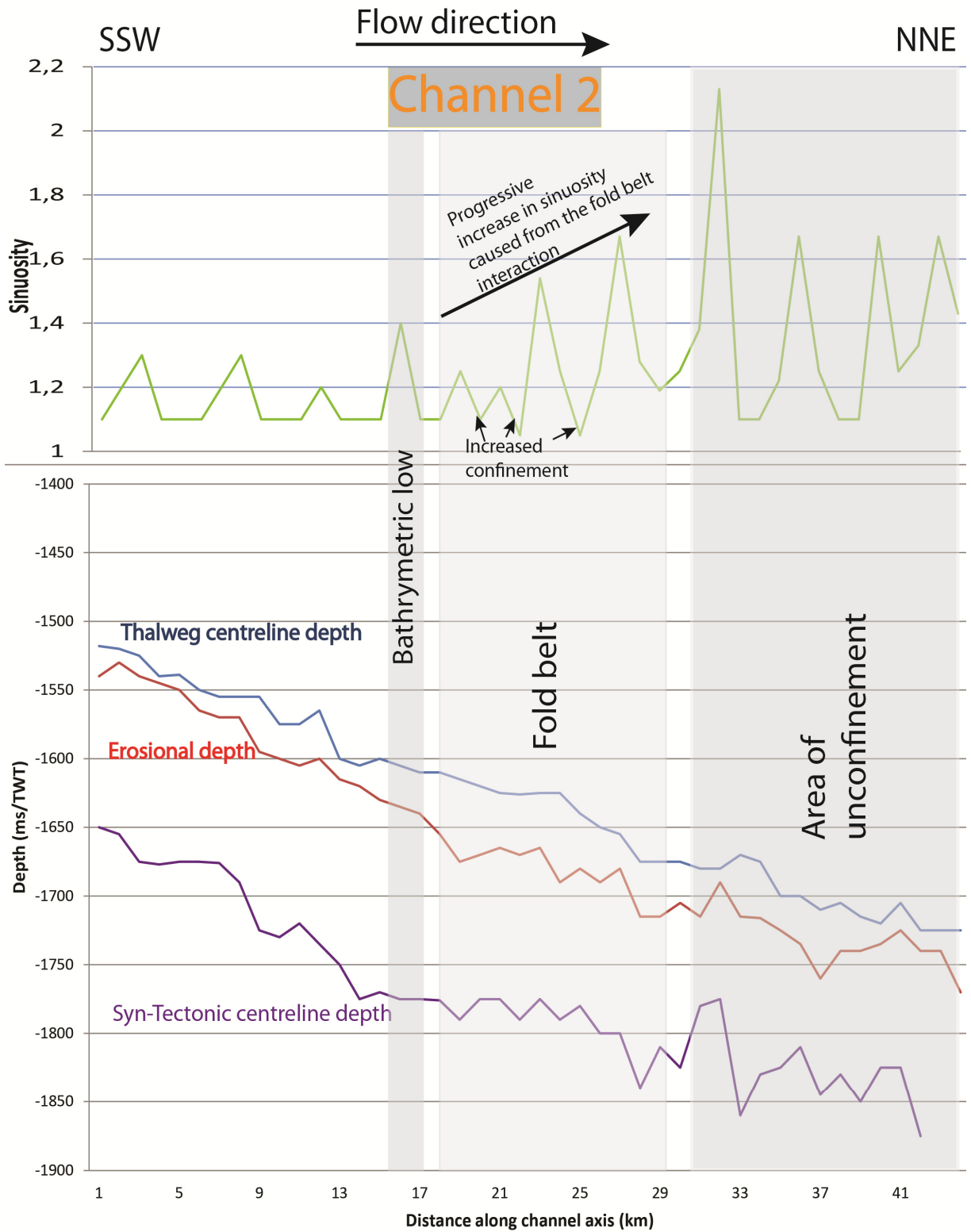
Plot5.24: *Quantitative measurements of channel 2.*

71

5.2.5 Unit 1

The Unit 1 (yellow color) is the uppermost Unit and is bounded on the top from the seafloor surface 1 (blue color) (***Figure 5.24***) which marks the top of the seismic study package and on the base by the (yellow color) surface 2 (***Figure 5.25***). Both of the bounded surfaces are characterized from a progressive deepening towards the north east. The thickness map of the Unit 1 (***Figure 5.26)*** illustrates an overall thinning towards the north and an accommodation area is observed at the south east part of the area.

The main depositional elements of the Unit 1 (***Figure 5.27)*** are consisted from the main channel which has been described as channel-1for the area of analysis, four distributary channels and three frontal splays. The main channel is 16,5 km long and has a northward flow direction with average sinuosity 1,17 which is high at the southern part of the channel and decreases towards the north. In the south eastern part of the Unit 1 it can be observed an abandoned channel (red color) and a channel remnant (blue dashed color).

The dimensions between the three frontal splays vary from east to west with the eastern Frontal splay 1 to be the smaller with an extent of $5,6km^2$ and thickness 45 ms (TWT) and is fed by the southern distributary channel of the system which length is 5,6 km. The intermediate Frontal splay 2 is the biggest in size with extent 19,1 km^2 and thickness 65 ms (TWT) and is fed from the longer distributary channel with length of 8,2 km. The western Frontal splay has an intermediate size of 11,6 km^2 and thickness 50 ms (TWT) and is fed from a distributary channel of total length 7,1 km.

In terms of seismic facies, Unit 1 consists of four Seismic Facies (1,2,4 and 5), with the most dominant being Seismic Facies 5 reflecting hemipelagic that occurs across the whole area. The Facies 1 and 2 can be observed at the south eastern part of the Unit 1 with discontinuous, contorted, high amplitude (HAR), subparallel reflectors indicative of buried channel fill and continuous/discontinuous, low to medium amplitude, parallel even reflectors indicative channel levee deposits respectively. The Facies 4 of the Unit can be observed at the downstream part of the channel flow and is consists from continuous to slightly discontinuous, high amplitude (HARP), relative flat reflections indicative of channelized lobe complex deposits.
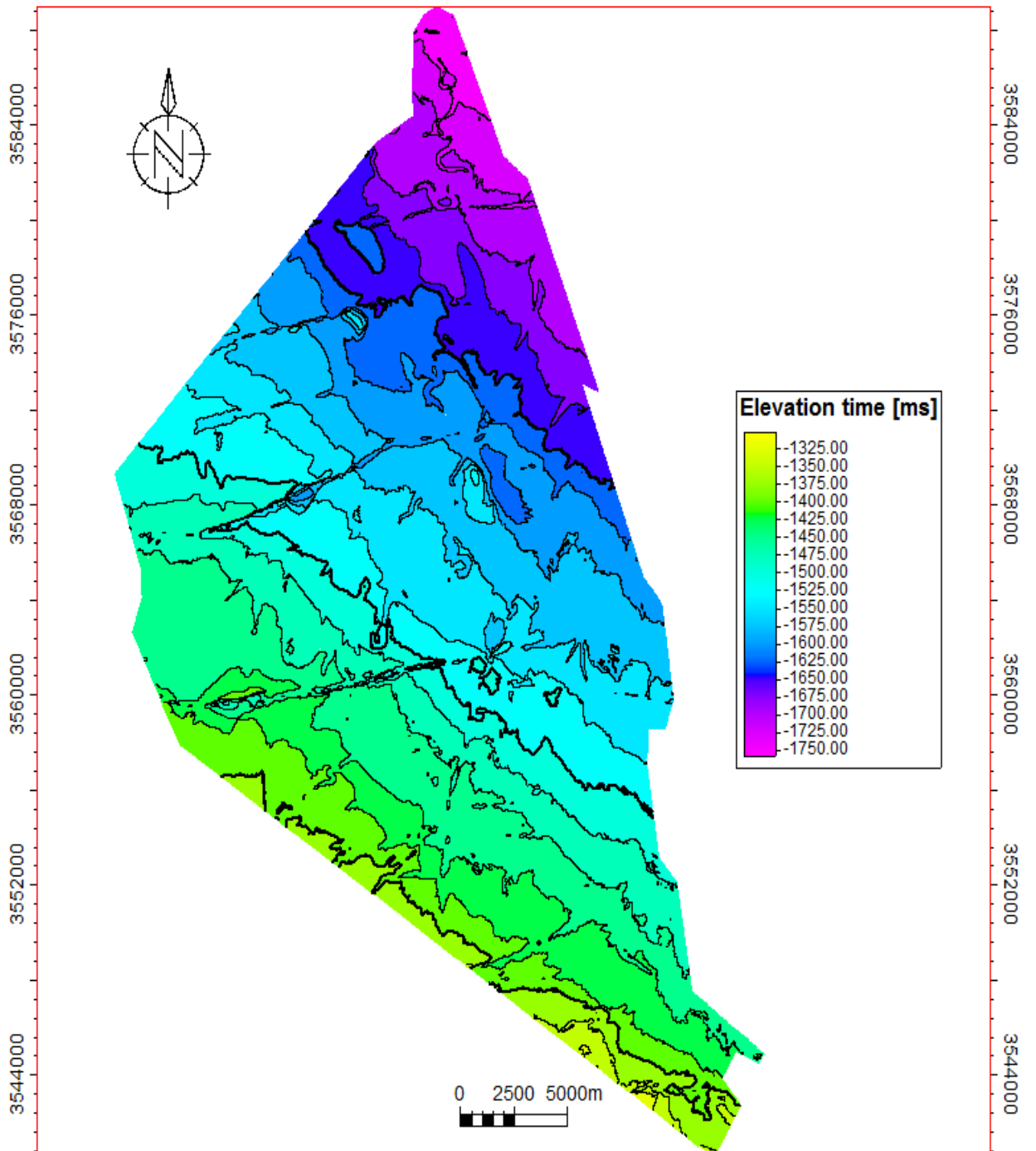
Figure 5.24: *Elevation time map TWT representing the top of the Unit 1- surface 1 of the study area (Seafloor).*
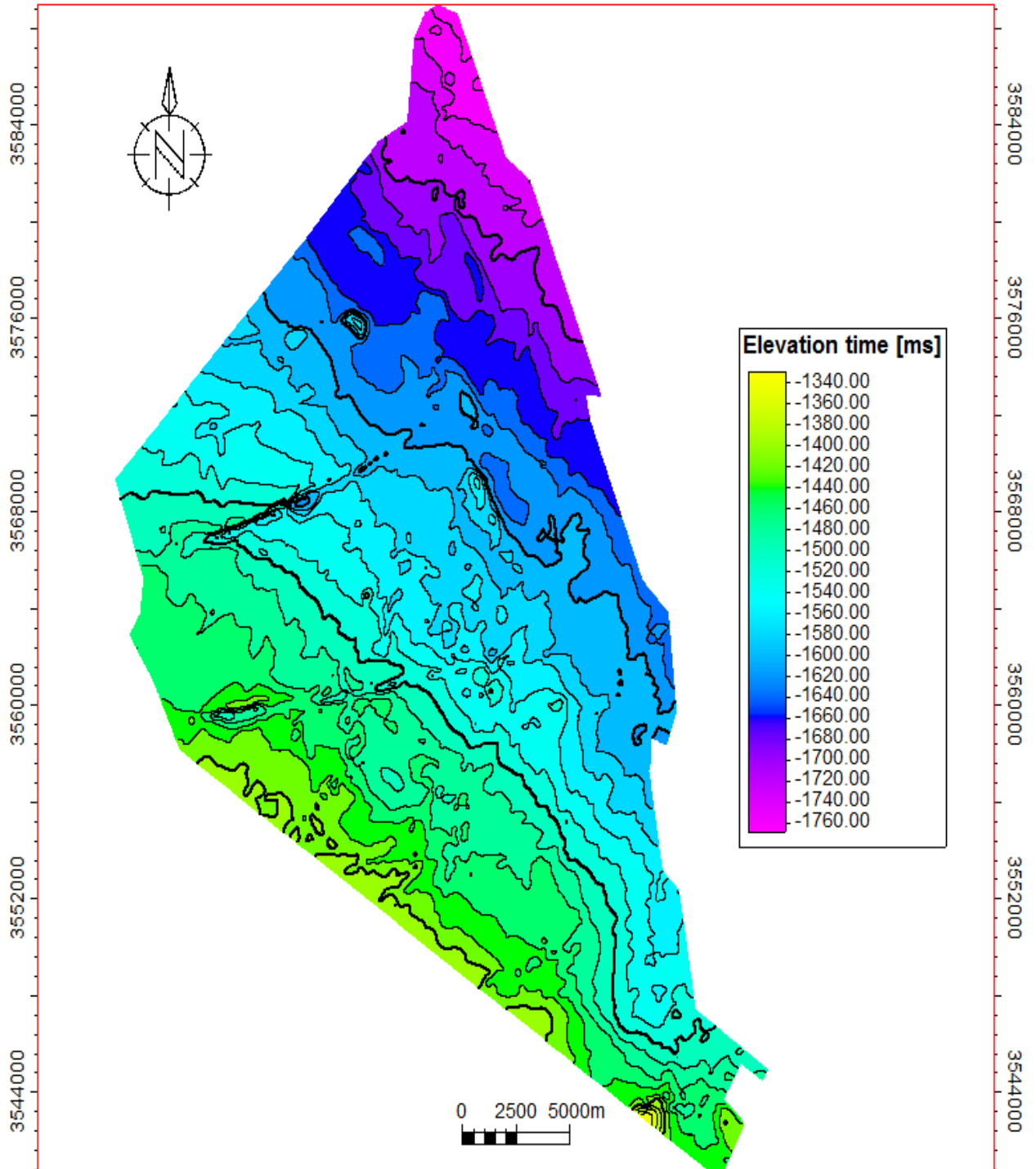
Figure 5.25: *Elevation time map TWT representing the base of the Unit 1- surface 2 of the study area.*
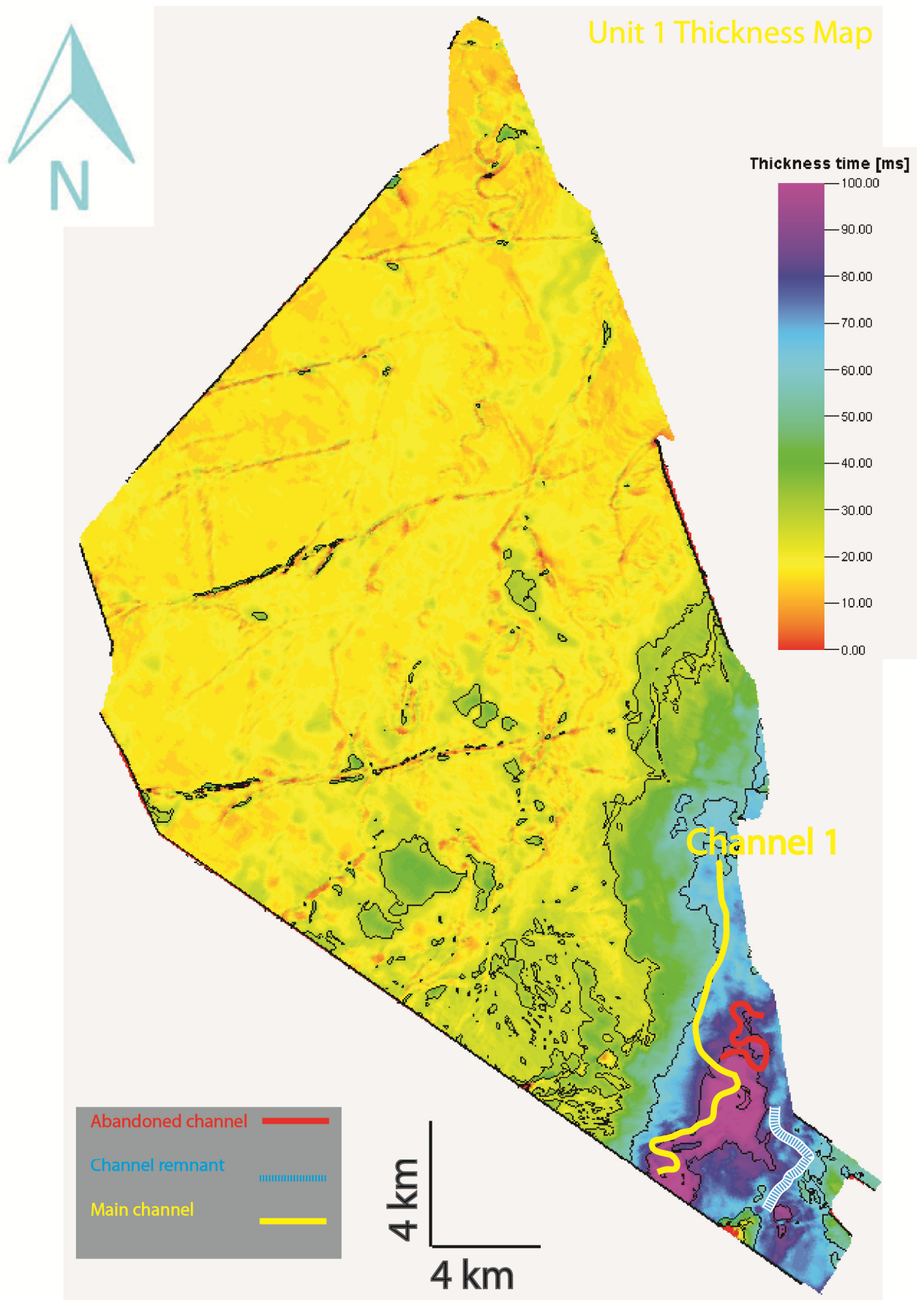
Figure 5.26: TWT thickness time (ms) surface of Unit 1.
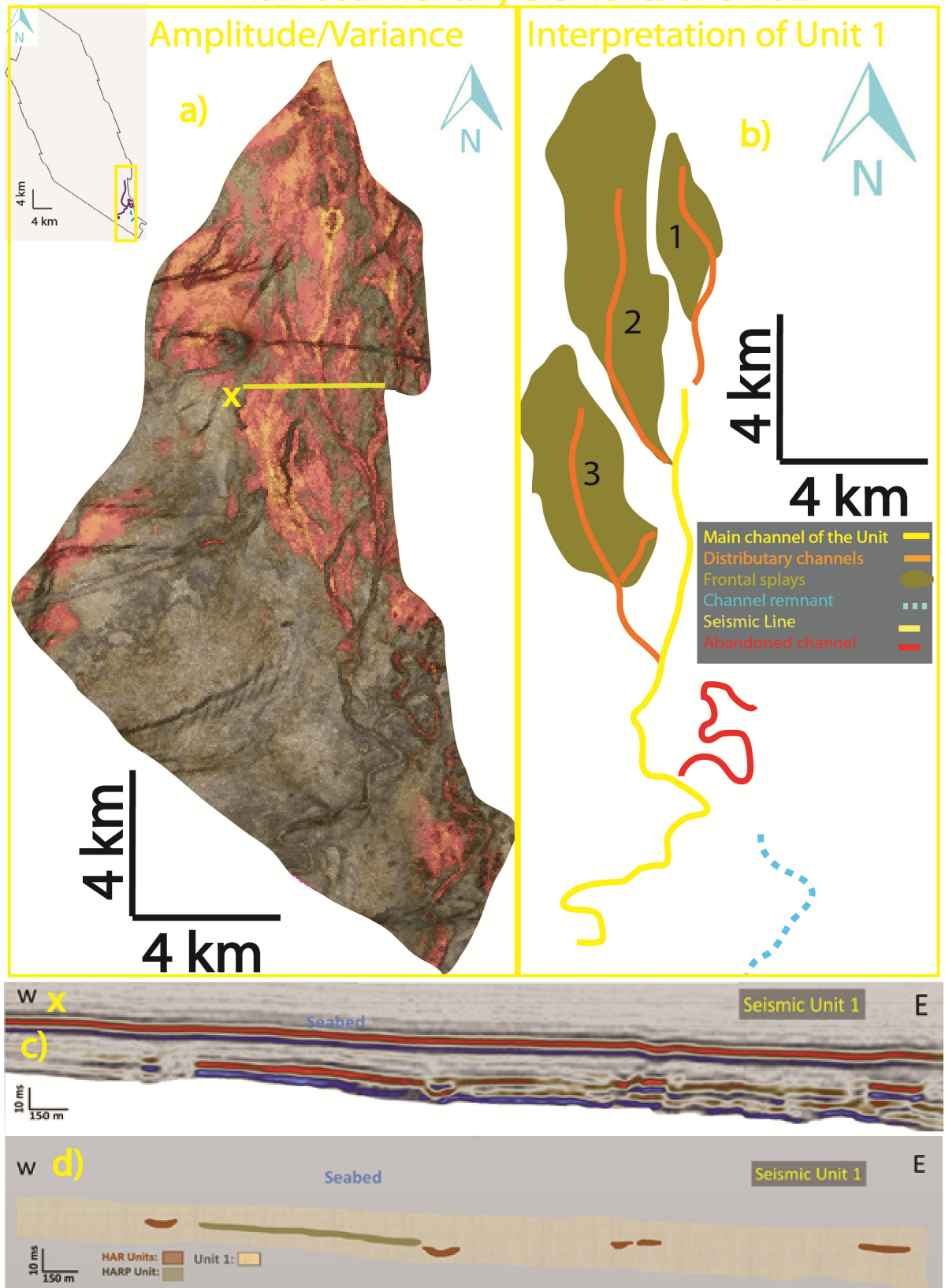
Figure 5.27: *a) Amplitude attribute map combined with variance, illustrating the main depositional elements of Unit 1 and b) their interpretation in plain view, c) seismic line and d) interpretation the main depositional elements of the Unit 1.*
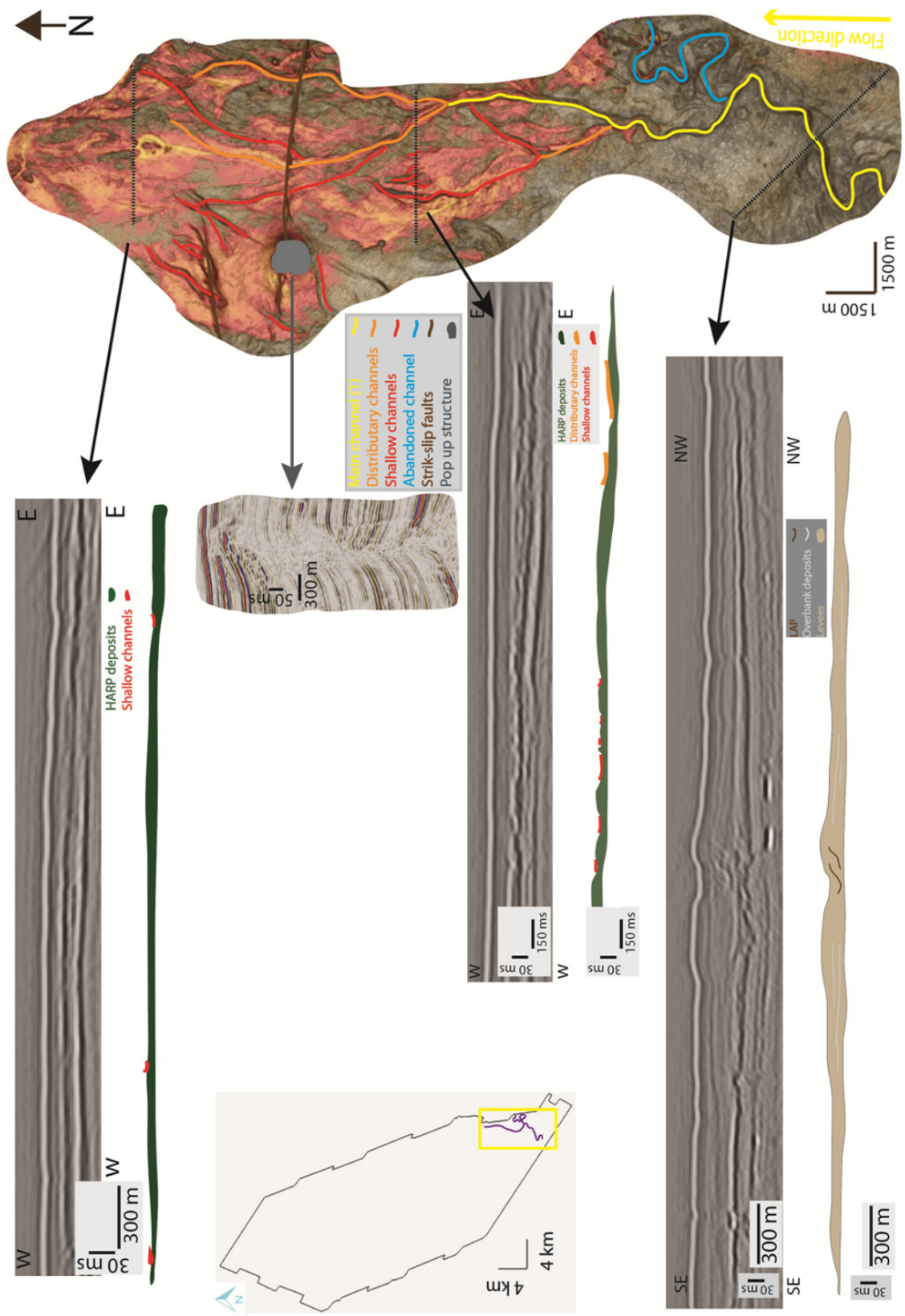
Figure 5.28: *Plan view of channel 1 that illustrates the transition of the flow from levee channel to frontal splay.*

Unit Number	Channel Number	Total length/km	Sinuous length/km	Sinuosity
1	1	14,32	16,45	1,17
2	2	38,51	43,54	1,63
	3	23,73	34,13	1,44
3	4	23,82	27,78	1,17
4	5	26,44	39,52	1,49
	6	18,86	27,45	1,45
	7	25,31	32,48	1,49
	8	15,04	16,94	1,22
	9	6,46	7,21	1,12
5	10	18,12	22,31	1,29

Figure 5.29: *Map with the summary of the main channels of the five Units (lower part) and table with their key characteristics (upper figure).*

78

6. Discussion

6.1 Synthesis of the main results

The examined Syn-tectonic Plio-Pleistocene sequence consists of five subsequent seismic Units that contain the most common depositional elements of deep water settings (*Figure 2.11*) described (e.g. Posamentier and Kolla, 2003).

The prominent sedimentary features observed in the study area consist of submarine channels that are mostly aggradational and from a general trend of an overall decrease in the rate of incision along strike from the southwest to the northeast across the study area where the flow becomes unconfined downslope and deposits frontal splays.

The structures within the study area affect the channel morphology in terms of channel location, orientation and sinuosity, with a decrease in sinuosity because of confinement and change in the channel flow towards topographic lows.

The depositional elements of the study that were fed from the submarine channels include two types of depositional lobes:

a) Small scale lobes which are represented seismically by 1 km long and 20 ms (TWT) thick high amplitude reflection packages. These are deposited because of the increase in the erosive power of flow along the channel axis, resulting in the channel levee breaching with the creation of crevasse channels which are the conduit for the deposition of the small-scale lobe crevasse splays. These deposits are observed along the flow of the channel-2 (Unit 2) and the channels of Unit 4.

b) Bigger scale lobes deposits that seismically are illustrated by extended high amplitude reflection packages. These occur at the transition point from submarine channel to frontal splay deposits at areas where the slope gradient becomes steeper and the flow unconfined. These deposits are observed at the down flow part of the channels of the Units 1, 3 and 4.
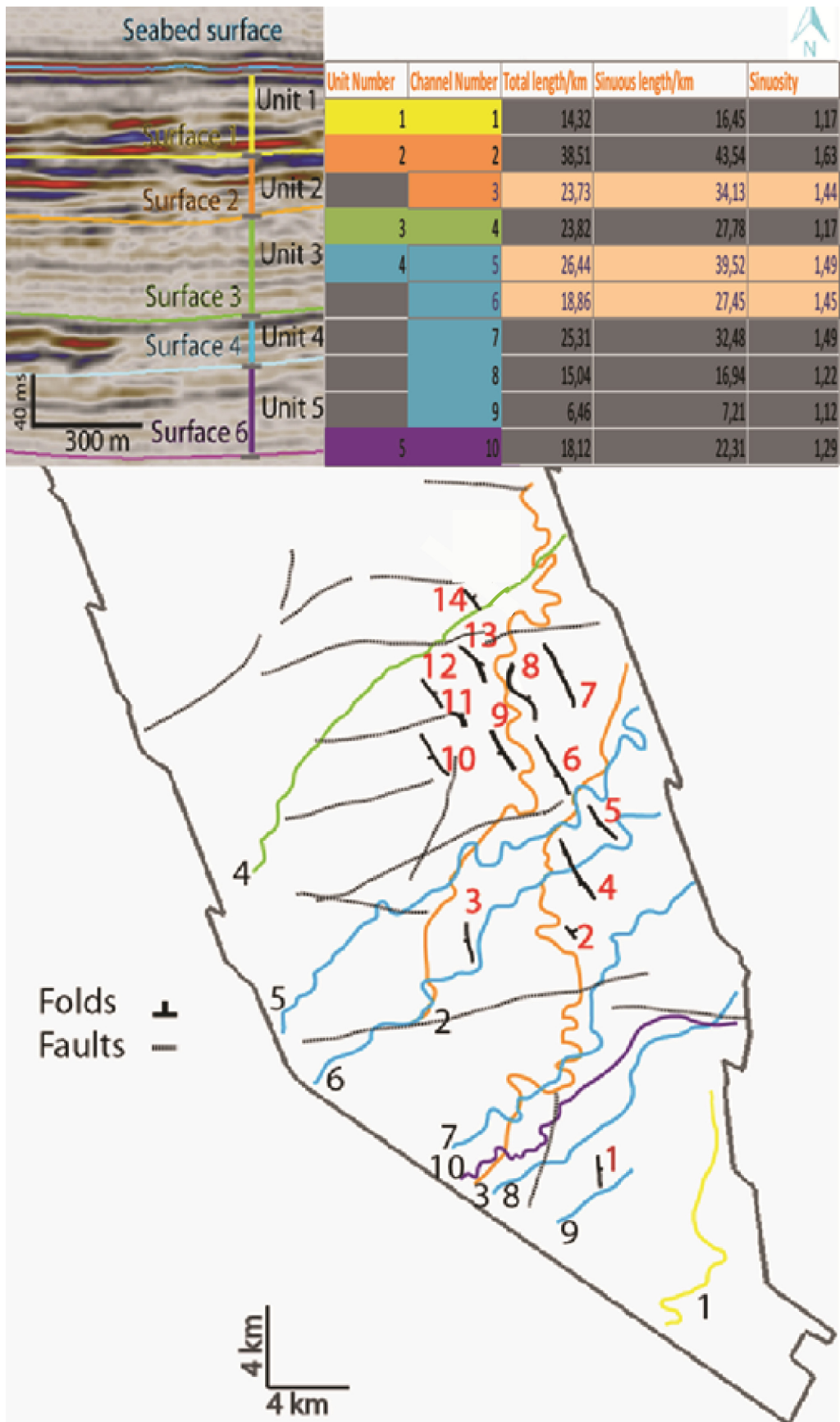
The other sedimentary features observed include mass transport deposits which are dominant in the southeastern part of the area and in some cases appeared to be incised by overlying

channels. Hemipelagic or sheet-like turbidite sedimentation is also observed, mostly in the upper layers of the seismic sequence and in the north-eastern part of the study area.

6.2 Topographic controls on submarine channels and lobes

The evolution of the channels in the study area is controlled locally by the underlying structures which have been created as the result of thin-skinned deformation consists of folds and strike slip faults. The northwest-southeast- trending folds have created a fold belt which is the main cause of channel-structure interaction in the area. These structures act as bathymetric obstacles and modify the evolution of the submarine channels temporally and spatially in a way that has been described in terms of four end members (e.g. Clark and Cartwright, 2009). These four end members are: diversion, deflection, blocking and confinement and represent the relationship between type of interaction depending on the time difference between the channel evolution and the underlying structural growth (Clark and Cartwright, 2009).

The channels in the study area have a flow direction towards the north-east and sinuosity that varies from low to very high. The channels at the upstream part of the flow are characterized by an erosive base (seismically channel fill cutting through the underlying strata) and well-defined levees (seismically low amplitude reflectors of wedge-shape that thinning progressively form the channel axis). Downstream the channel fill becomes aggradational (seismically HAR's stacking vertical each other) and in some cases crevasse splays (seismically small extension HAR's) occur at the outer channel bends (e.g. channel-2 (Unit 2) and the channel-5 (Unit 4)).

Where the channels cross the fold belt they have an increase in sinuosity because of the effects of diversion or deflection. The effect of confinement by the surrounding folds across a long distance with the channel-2 to be representative is observed through a set of diversions and deflections of the channel axis in the fold belt. Channel-2 (Unit 2) is characterized by a set of diversions and deflections along its flow path.

The restriction of lateral migration of the channel because of surrounding structures results in an overall decrease of the channel sinuosity depending on the quantity of confinement. However the sinuosity is still preserved in a moderate level because of the deflections and diversions while characterized from lateral migration seismically indicated by (LAP's), towards a newly forming topographic low such as the axis of a growth syncline. Channel shifting towards a topographic low is also observed in areas of small scale pull-apart

structures developed by strike slip faults. Another example of decrease in sinuosity because of confinement is observed in channel-7 (Unit 4), where the confinement is the result of small scale pop-up structures developed by strike-slip faults in zones of transpression.

Blocking is not be observed in the area of study, although the fold 4 (Unit 4) seems in a plan view to create an obstacle but from the seismic lines it is identified that the fold growth post-dates (folded levee package on the fold crest) the channel evolution.

After channels exit the fold belt zone they are unconfined and are characterized by an increase in sinuosity when the slope gradient decreases with the most well-defined example being channel-2 (Unit 2). The exit from the fold belt in combination with an increase in the slope gradient results in the transition from channel to frontal splay deposits (seismically large scale HARP's) with the most representative examples derived from the channels of the Unit 4 and more precisely the channel 7 which is also characterized from a decrease in sinuosity because of high degree of confinement from the surrounding structures consist of pop-up structures which represents the model illustrated in *Figure 6.1 A* in terms of sinuosity and the model illustrated in *Figure 6.2 A* in terms of transition from a confined to an unconfined zone. The channel 1 (Unit 1) illustrates the same transition but for this case the main driving force is the increase in slope gradient.

A model for channel-topography interaction based on the analysis of the data used in this study can be summarized as follows:

1. When the submarine channels cross a fold belt with the scale of confinement allowing a moderate degree of preserving in the sinuosity, they change direction towards a topographic low created by folds which results in the subsequent diversion or deflection (*Figure 6.1*). This model deviates from the model of Clark and Cartwright 2009 in terms of the distance between the pre-existing surrounding structures which is short and limits the ability of the channel to migrate laterally and form plan form geometry although aggradation in combination with no-active structure cause in a decrease in unconfinement.

2. When flows are confined in a fold belt over long distance the increase in confinement results in the decrease in sinuosity which is preserved in a moderate level because of the multiple and successive deflections and diversions from the surrounding structures (*Figure 6.1*).

3. When flows exit from a zone of confinement to an unconfined zone, they transit from channels to frontal splays when the slope gradient increase while if the gradient decreases are characterized from an abrupt increase in sinuosity (*Figure 6.2*).
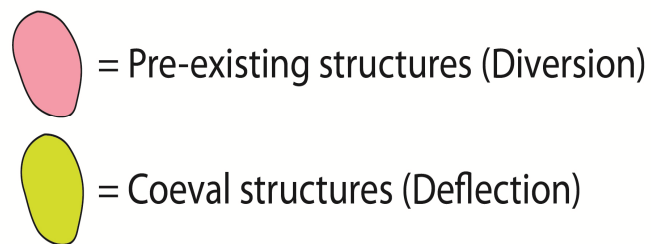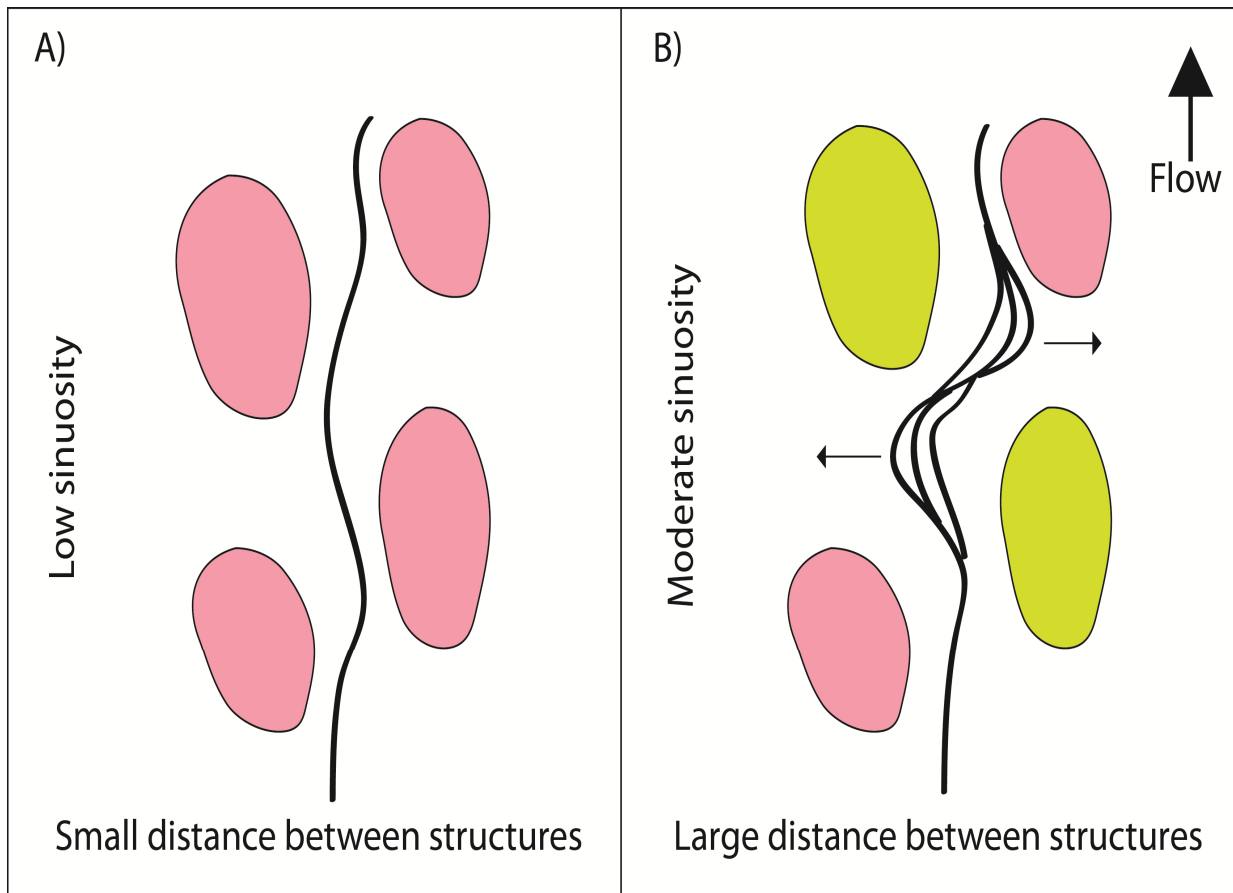
Figure 6.1: *A) confinement produced from pre-existed structures that deviate short distance that does not allows diversion of the flow and subsequent increase in sinuosity and B) confinement produced from pre-existed and coeval structures that deviate large distance and results in multiple diversions and deflections.*
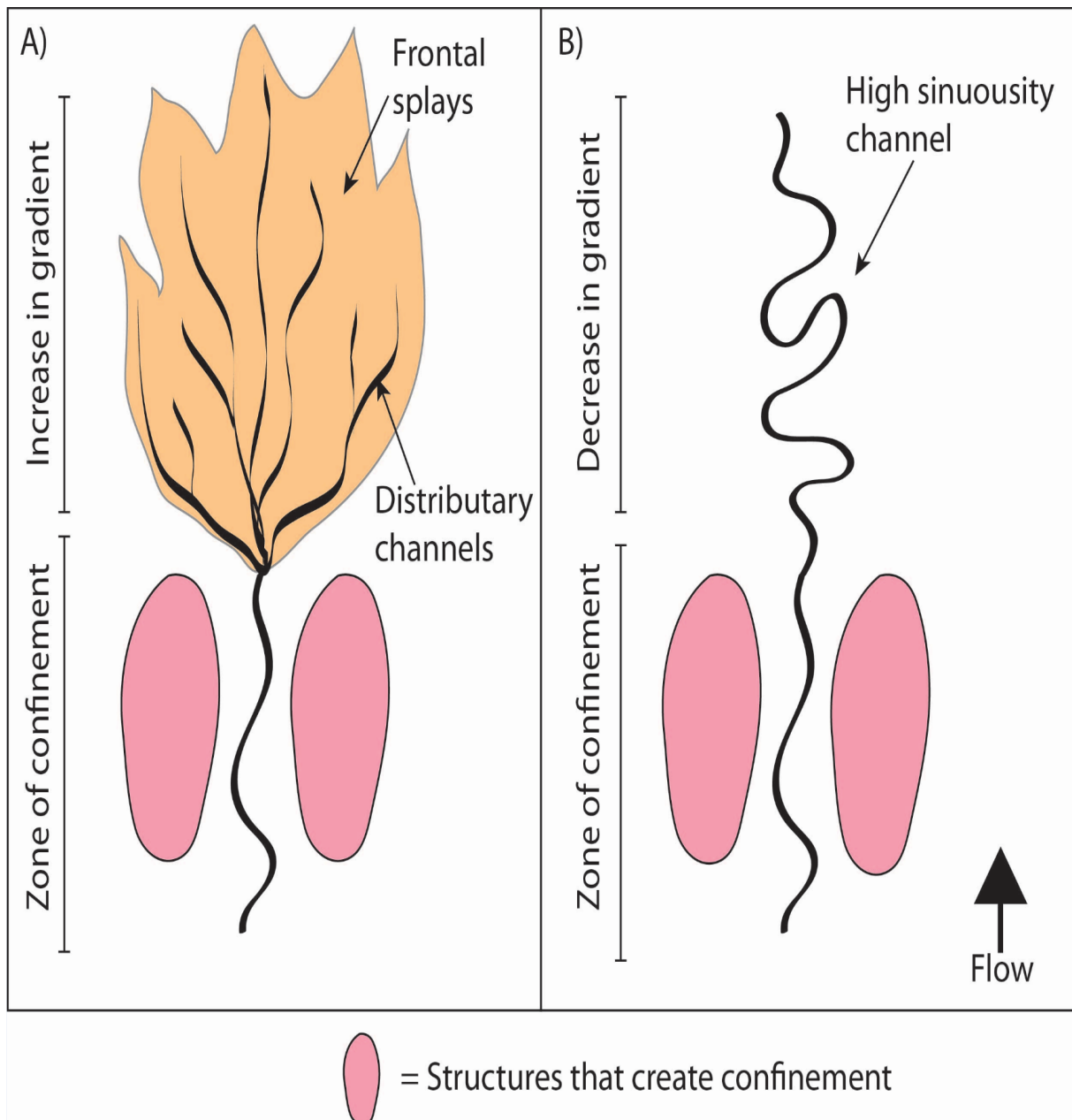
Figure 6.2: *A) Transition from a zone of confinement to a zone of unconfinement in combination with increase in slope gradient results in the transition from channel to frontal splay while B) transition from a zone of confinement to a zone of unconfinement in combination with decrease in slope gradient results at the increase of the sinuosity.*

6.3 Stratigraphic evolution

An idealized depositional sequence in a deep-water setting related cycle of relative sea level change initiates during relative sea level fall and the ends following subsequent the relative sea level rise. The stratigraphy resulting from this consists of mass transport deposits at the base, followed by turbidite deposits subdivided into a lower part consisting of frontal splay deposits and an upper channel levee system. Another mass transport deposit overlain the channel levee complex and the sequence ends with a condensed section of sediments deposited through pelagic/hemipelagic suspension (Posamentier and Kolla, 2003).

The five Units of the Plio-Pleistocene sequence represent different seismic Facies which can be used to describe the evolution of the deep-marine environment through a local point of view that is based on the sea-level fluctuations. The observations are based on the spatial variations of the different facies vertical and lateral with the lack of dating control. All the facies of a sequence representative of an ideal complete cycle of a deep-marine setting have been identified through the Units with the most prominent to be the seismic Facies 1 which seismically is indicated from vertical stacked high amplitude reflectors.

One the main driving forces for incision of submarine valleys of the shelves and the upper slopes is relative sea level fall. During that system tract the basin floor becomes an active depocenter consists of sediments sourced from hinterland and eroded sediments from the upper shelf and middle slope (Posamentier and Walker, 2006). This stage is also characterized from widespread upper slope gravitational instability resulting in mass transport deposits on the basin floor. The mass transport deposits have been described as Facies 3 in the study area and can be observed as seismically low amplitude to transparent with chaotic internal configuration and are located in the Unit 3,4 and 5 with being the dominant facies of the Unit 5.

During the lowstand system tract the sediment flows bypass the submarine canyon and continue to the middle and lower slope with the creation of poorly confined low to moderate sinuosity channels result in the deposition of lobes with reduced down flow sediment supply (Posamentier and Walker, 2006).The depositional lobe during the late lowstand system tract progrades basinwards. These types of deposits have been described as seismic Facies 4 and seismically are illustrated from HARP's and are observed in the Units 1,2,3 and 4 with being more dominant in Unit 4.

During the Transgressive system tract the sediment supply to the deep basin starts to diminish whereas in the middle and lower parts of the slope the channels are characterized by erosive base flanked by well-developed fine-grained levees. The channel themselves are highly sinuous and confined (Pirmez et al., 2000). These types of deposits have been described as seismic Facies 1 for the channels and seismic Facies 2 for the levees and seismically they illustrate HAR's and continuous/discontinuous low to medium amplitude reflector for the channel fill and levee deposits respectively. Seismic Facies 1 and seismic Facies 2 are observed in every Unit of the studied succession.

During the high stand system tract a condensed horizon of hemipelagic sediments is deposited by suspension in the basin when the deposition becomes focused in to the inner and middle shelf the supply from the shelf is shutted off (Posamentier and Walker, 2006). That Facies of low to medium amplitude and parallel reflectors are observed in the Units 1,3,4 and 5 with being dominant in Units 1 and 3.

Based on the type of seismic Facies of each Unit the interaction between vertical evolution of each Unit and the cycles caused by sea-level fluctuations can be described as follows:

The oldest Unit includes the seismic Facies 1, 2, 3 and 5 with the most dominant to be the seismic Facies 5-hemipelagic deposits or sheet like turbidite deposits. The lack of the seismic Facies 4 (HARP's) illustrates an incomplete cycle. The Unit 4 includes all the seismic facies in order that illustrates a complete cycle with the seismic Facies 3 (mass transport deposits on the base overlaid by seismic Facies 4 (HARP's) that are covered from seismic Facies 1 (channel fill deposits) which are surrounded by seismic Facies 2 (levee deposits) and the whole sequence to be covered from seismic Facies 5 (hemipelagic or sheet like turbidite deposits). The Unit 3 includes the seismic Facies 1,3,4 and 5 and the Unit 2 includes the seismic Facies 1,2 and 4. Finally the Unit 1 includes the Facies 1,2,4 and 5 which represent.

Based on the above description is observed that only the Unit 4 illustrates an ideal sequence of a cycle while the rest of the Units represent incomplete vertical successions of Facies with variations in seismic Facies between the Units with the common seismic Facies for all the Units to be the seismic Facies 1. These could be used to suggest that the described from Posamentier and Kolla (2003) sea-level sequence model cannot be applied for the individual Unit with exception of the Unit 4 but it is applicable for the vertical succession of

the Pleistocene sequence (*Figure 6.3*) based on the prominent seismic Facies for each Unit that include seismic Facies 3 (mass transport deposits) for the base consists of the lower Unit 5, passing upwards to seismic Facies 4 (HARP's) in Unit 4, that are overlaid by the seismic Facies 1(HAR's) in Unit 3 which is surrounded from seismic Facies 2 (levees) of the Unit 2 and ending with seismic Facies 5 (hemipelagic or sheet like turbidites) on the top.
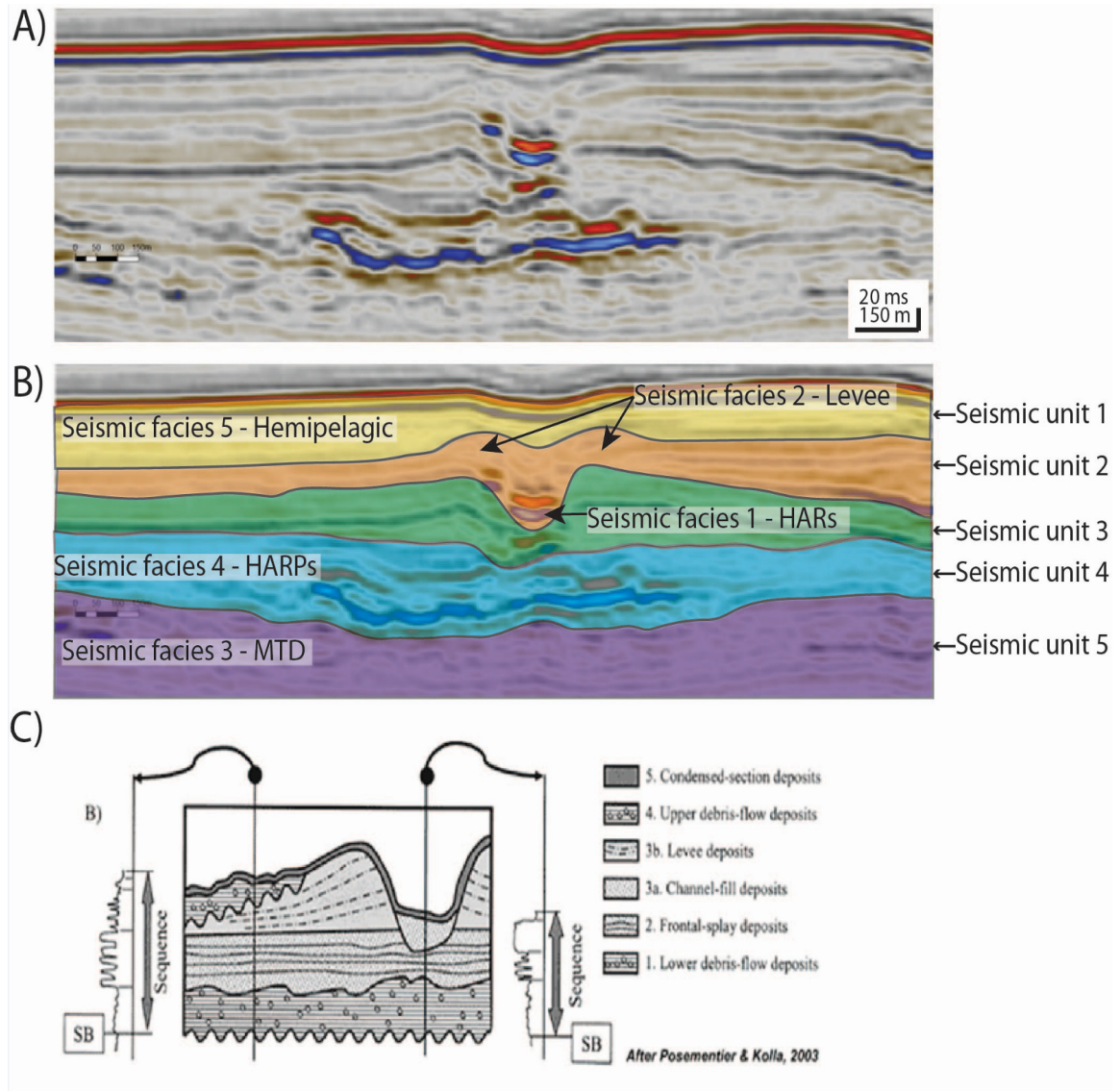
Figure 6.3: A) Seismic section of the Pleistocene sequence and B) its subdivision into the five Units with the prominent seismic Facies of each Unit that fits with C) the model of Posamentier and Kolla (2003).

Another driving force that can be observed from the seismic dataset is the structural control on the development of the seismic stratigraphy with the underlying structures being deformed from the salt movement which creates strike slip faults and subsequent folds. The interaction between the active structures and the stratigraphic evolution can be observed through the onlap of the deposits on the structures and the tilting of the reflectors from the fold crests. The weakly developed onlap on the fold limbs and the thinning of the Units onto the fold crests indicate that the deformation is coeval to the deposition. Based on Cartwright and Jackson (2008) and Folkman and Mart (2008), the main driving force of deformation in the study area is the collapse of the Levant margin to the east combined with gravitational collapse of the Nile Delta to the south-west with the detachment layer to be the Messinian sequence.

7. Conclusions

- Three horizons were mapped for the whole area covered by the dataset that subdivide the Pleistocene Unit into subunits.
- For the area of main focus (southern part of the dataset) six horizons were mapped that subdivide the Pleistocene sequence into five Units with the Base to illustrate the Base Syn-tectonic surface and the top the present day seafloor which represents the Top Syn-tectonic surface.
- The Base of the Syn-tectonic sequence was mapped based on the onlap relation of the internal reflections of the packages that thin onto the fold crests with the fold limbs
- Five seismic Facies identified that reflect a range of depositional environments that include: Facies 1-channel fill deposits, Facies 2- channel levee deposits, Facies 3- mass transport deposits, Facies 4-channelized lobe complexes and Facies 5- hemipelagic or sheet like turbiditic deposits.
- The structures in the area comprise a set of NW-SE trending fold belt, pop-up and pull apart structure created from a set of SW-NE and E-W strike slip faults. The fold structures can be observed on thickness maps from low values because of the thinning of the packages onto the fold crests.
- The deposits that have been mapped include:
  - Channel fill deposits, straight or sinuous illustrated from high amplitude reflectors that are stacked vertically, laterally or both and interact with the growing structures in the following ways: 1) Deflection, when the structural growth is coeval with the channel development which results in the channel laterall migration towards a newly forming topographic low. 2) Diversion, when the structural growth pre-exists the channel development and the channel which results in the channel laterall migration. 3) Confinement where the flow is restricted by the surrounding structures which results in the limitation of laterall migration of the channel. 4) Cases that a flow is confined by structures that deviate large distance, they are characterized from a decrease in sinuosity which is preserved in a moderate level because of progressive diversions and deflections by the pre-existing and coeval growth structures respectively. 5) Cases that the sinuosity of the channel increase because of the passage from a zone of confinement to a zone of unconfinement in combination with a decrease in slope gradient.
    - Frontal splay deposits that are resulted because of the increase in the slope gradient in combination with the passage from a zone of confinement to a zone of unconfinement.
  - The stratigraphic evolution is mainly affected from thin skinned tectonics and an attempt was made during this study for the interaction of the sea-level change which can be applied as the Posamentier and Kolla (2003) for the whole syn-tectonic sequence but not for each Unit individually with exception of Unit 4.

8. Outlook

This study aims to describe the interaction between channel development and structural deformation for the Syn-tectonic Unit of the area covered by the dataset. Previous workers have described qualitatively and quantitatively the interaction between submarine channels and deformed structures for the whole Post Messinian sequence. However the description was mainly focused on the upper parts of the Pleistocene sequence. It should be a matter of further discussion the more detailed analysis of the Pliocene sequence and the top of the Messinian which represents a very interesting set of NW-SE channels that are in different direction of the Pio-Pleistocene channels that are characterized from a NE-SW flow direction.

Another interesting subject for further discussions should be the controls in sequence stratigraphy that can include the climate in terms of the monsoons which act periodically and they assumed to affect the sediment discharge of the river Nile with possible subsequent effects in the stratigraphy of the Levantine Basin.

.

9. References

Almagor, G., (1984). Salt controlled slumping on the Mediterranean slope of Central Israel. Marine Geophysical Research 6, 227–243.

Bellaiche, G., Loncke, L.L., Gaullier, V., Droz, L., Mascle, J., Courp, T., Moreau, A., Radan, S., and Sardou, O., (2002). The Nile deep-sea fan and its channel levees system: Results from the Prismed II and Fanil cruises, *in* Turbidite systems and deep sea fans of the Mediterranean and the Black Sea: International Commission for the Scientific Exploration of the Mediterranean Sea (CIESM) Workshop series 17, 49–52.

Bertoni, C. & Cartwright, J.A. (2007). Major erosion at the end of the Messinian Salinity Crisis: evidence from the Levant Basin, Eastern Mediterranean. Basin Research, 19, 1-18.

Bertoni, C., and Cartwright, J.A., (2006). Controls on the basinwide architecture of late Miocene (Messinian) evaporites on the Levant margin (Eastern Mediterranean). Sedimentary Geology 188-189, 93–114.

Ben-Gai, Y., Ben-Avraham, Z., Buchbinder, B., and Kendall, C.G.StC., (2005). Post-Messinian evolution of the Southeastern Levant Basin based on two-dimensional stratigraphic simulation. Marine Geology 221, 359–379.

Buchbinder, B., Martinotti, G.M., Siman-Tov, R. and Zilbermann, E., (1993). Temporal and spatial relationships in Miocene reef carbonates in Israil. Paleogefraphy, Paleoclimatology and Paleoecology 101, 97-116.

Bouma, A.H., Normark, W.R., and Barnes, N.E. (1985). Submarine fans and related turbidite systems. New York. Springer-Verlag, pp.143-150.

Cartwright, J.A., Jackson, M.P.A., 2008. Initiation of gravitational collapse of an evaporitic basin margin: the Messinian saline giant, Levant basin, eastern Mediterranean. GSA Bulletin 120, 399-413.

Catterall, V., Redfern, J., Gawthorpe, R., Hansen, D., and Thomas, M., (2010). Architectural style and quantification of a submarine channel levee system located in a structuraly complex area: offshore Nile Delta. Journal of Sedimentary Research, 80(11), 991-1017.

Clark, I.R. and Cartwright, J.R. (2009). Interactions between submarine channel systems and deformation in deepwater fold belts: Examples from the Levant Basin, Eastern Mediterranean sea. Marine and Petroleum Geology 26, 1465-1482.

Clark, I.R. and Cartwright, J.R. (2011). Key controls on submarine channel development in structurally active settings. Marine and Petroleum Geology 28, 1333-1349.

Cross, N.E., Cunningham, A., Cook, R.J., Taha, A., Esmaie, E., and El Swidan, N. (2009). Three dimensional seismic geomorphology of deep water slope channel system: The Sequoia field, offshore west Nile Delta, Egypt. AAPG bulletin, 93(8), 1063-1068.

DeVay, J.C., David, R., Scott, E., and Chris, T., (2000). A Mississippi-Sourced, Middle Miocene (M4), Fine-Grained Abyssal Plain Fan Complex, Northeastern Gulf of Mexico. AAPG Memoir 72/Sepm. Special Publications No. 68. 10, 109-118.

Druckman, Y., Buchbinder, B., Martinotti, G.M., Siman Tov, and R., Aharon, P., (1995). The buried Afiq Canyon (eastern Mediterranean, Israel): a case study of a Tertiary submarine canyon exposed in Late Messinian times. Mar. Geol. 123, 167 – 185.

Ferry., J., Mulder, T., Parize, O., and Raillard, S., (2005). Concept of equilibrium profile in deep water turbidite system: effects of local physiographic changes on the nature of sedimentary process and the geometries of deposits. Geological Society, London, Special Publications, 244(1), 181-193.

Fischer, R.V. (1983). Flow transformations in sediment gravity flows. Geology 11, 273-274.

Folkman, Y. and Mart, Y., (2008).Newly recognized eastern extension of the Nile deep-sea fan. The Geological Society of America. Geology 36, 12, 939-942.

Frey-Martinez, J., Cartwright, J.A., and Hall, B., (2005). 3D seismic interpretation of slump complexes: Examples from the continental margin of Israel: Basin Research 17, 83–108.

Gardosh, M.A., Garfunkel, Z.,, Yehezkel Druckman and Buchbinder B., (2010). Tethyan rifting in the Levant Region and its role in Early Mesozoic crustal Evolution. Geological Society 341, 9-36.

Garfunkel, Z., Almagor, G., (1987). Active salt dome development in the Levant Basin, southeast Mediterranean. In: Lerche, I., O'Brien, J. (Eds.), Dynamical Geology of Salt and Related Structures. Academic Press, London, 263–300.

Garfunkel, Z., (2004). Origin of the Eastern Mediterranean Basin: a reevaluation. Tectonophysics 391, 11-34.

Gee, M.J.R. and Gawthorpe, R.L. (2006). Submarine channels controlled by salt tectonics: Examples from 3D seismic data offshore Angola. Marine and Petroleum Geology, 23(4), 443-458.

Gradmann, S., Hubscher, C., Ben-Avraham, Z., Gajewski, D. and Netzeband, G., (2005). Salt tectonics off northern Israel. Marine and Petroleum Geology 22, 597-611.

Gvirtzman, G. & Buchbinder, B., (1978). The Late Tertiary of the coastal plain and continental shelf of Israel and its bearing on the history of the Eastern Mediterranean,

in: Ross, D.A., Neprochov, Y.P. (Eds.), Init. Repts. DSDP, 42 II. U.S Govt. Printing Office, Washington D.C., 1195 - 2220.

Haughton, P, Davis, C., and McCaffrey, W., (2006).Facies Prediction in turbidite Fan Systems – Nature and Significance of 'Linked Debrites' in Sand-Rich Versus Mixed Sand-Mud Systems". Recent Advances in Siliciclastic Facies Models: Implications for Reservoir Characterization II (SEPM), AAPG.

Heezen, B.C., and Ewing, M., 1952. Turbidity currents and submarine slumps, and the 1929 Grand Banks Earthquake: American Journal of Science 250, 849-873.

Higgins, S., Davies, R.J., Clarke, B., 2007. Antithetic fault linkages in a deep water fold and thrust belt. Journal of Structural Geology 29, 1900–1914.

Hirsch, F., Flexer, A., Rosenfield, A. and Yellin-Dror, A., (1995). Palinspastic and crustal setting of the eastern Mediterranean. Journal of Geology 18, 149–170.

Hsu, K.J., Montadert, L., Bernoulli, D., Cita, M.B., Erickson, A., Garrison, R.E., Kidd, R.B., Melieres, F., Muller, and C.,Wright, R.H., (1978). Initial Reports of the Deep Sea Drilling Project, c42(1). U.S. Government Printing Office, Washington D.C., 1249.

Huebscher, C., Netzeband, D., and Gajewski, D., (2006). Structural evolution of Messinian evaporates in the Levantine basin. Marine Geology 230, 249-273.

Huyghe, P., Foata, M., Deville, E., Mascle, G., 2004. Channel profiles through the active thrust front of the southern of the southern Barbaros prism. Geology 32, 429-432.

Kneller, B., and McCaffey, W.D. (1999). Depositional effects of flow non-uniformity and stratification within turbidity currents approaching a bounding slope: Deflection, reflection, and facies variation. Journal of Sedimentary research 69, 980-991.

Kneller, B., and Buckee, C, (2000). The structure and fluid mechanics of turbidity currents: a review of some recent studies and their geological implications. Sedimentology 47,62-94.

Kolla, V., Posamentier, H.W., and Wood, L.J.,(2007). Deep-water and fluvial sinuous channels—Characteristics, similarities and dissimilarities, and modes of formation.Marine and Petroleum Geology 24, 388–405

Lomas, S. A. and Joseph, P. (2004). Confined Turbidite Systems. Geological Society Special Publications 222, 7-328.

Loncke, L., Gaullier, V., Bellaiche, G., and Mascle, J., (2002). Recent depositional patterns of the Nile deep-sea fan from echo character mapping. American Association of Petroleum Geologists Bulletin 86, 1165–1186.

Loncke, L., Gaullier, V., Mancle, J., Vendeville, B. and Camera, L., (2006). The Nile deep-sea fan: An example of interacting sedimentation, salt tectonics and inherent subsalt paleotopographic features. Marine and Petroleum Geology 23, 297–315.

Mahmoud Abu-Zeid, (1983). The river Nile: main water transfer projects in Egypt and impacts on Egyptian agriculture. United Nations University. Long Distance Water Transfer, Chapter 2.

Mart, Y. and Ryan, W. (2007). The Levant slumps and the Phoenician structures: Collapse features along the continental margin of the southeastern Mediterranean Sea. Marine Geophysical Researches 28, 297–307.

Mascle, J., Benkhelil, J., Bellaiche, G., Zitter, T., Woodside, J. and Loncke, L., (2000). Marine geologic evidence for a Levantine-Sinai plate, a new piece of the Mediterranean puzzle. Geology 28, 779-782.

Mayal, M., Lonergan, L., Bowman, A., James, S., Mills, K., Primmer, T., Pope, D., Rogers., L., and Skeene, R. (2010). The response of turbidite slope channels to growth induced seabed topography. AAPG Bulletin, 94(7), 1011-1030.

Meiburg, E., and Kneller, B., (2010). Turbidity currents and their deposits. Annual review of fluid mechanics 42, 135-156.

Meyer L., and Ross, G.M. 92007). Channelized lobe and sheet sandstones of the Upper Kaza group Basin floor turbidite system, Castle Creek South, Windermere Supergroup. AAPG, Studies in Geology 56, 126, 22.

Middleton, G.V., and Hampton, M.A. (1973). Sediment gravity flows: Mechanics of flow and deposition. Turbidites and Deep water sedimentation, pp. 1-38.

Mitra, S., 2002. Fold-accommodation faults. AAPG Bulletin 86, 671–693.

Moscardelli, L., and Wood, L.J., (2008). New classification system for mass transport complexes in offshore Trinidan. Basin Research 20, 73-98.

Mulder, T., and Alexander, J., (2001). The physical character of subaqueous sedimentary density flows and their deposits. Sedimentology 48, 269-299.

Mutti, E., 1977. Distinctive thin bedded turbidite facies and related depositional environments in the Eocene Hecho Group (south-central Pyrenees, Spain). Sedimentology 24, 107–131.

Mutti, E., 1985. Turbidite systems and their relation to depositional sequences. NATO ASI Series C, 148, 65-94.

Mutti, E., and Normark, W.R. (1987). Comparing examples of modern and ancient turbidite systems; problems and concepts Marine Clastic Sedimentology: Concepts and Case Studies, 1-38.

Mutti, E., and Normark, W.R. (1991). An integrated approach to the study of turbidite systems. Seismic Facies and Sedimentary Processes of Submarine Fans and Turbidite systems ,pp. 75-106.

Neev, D., Greenfield, L. and Hall, J.K., (1985). Slice tectonics in the Eastern Mediterranean basin. In: Stanley, D.J., Wetzel, F.C. (Eds.), Geologic Evolution of the Mediterranean basin. Springer-Verlag, 250-269.

Nemec, W., and Steel, R.J. (1984). Alluvial and coastal conglomerates:their significant features and some comments on gravelly mass-flow deposits. Canadian Society of Petroleum Geologists Memoir 10, 1-31.

Netzeband, G.L., Hubscher, C.P. and Gajewski, D., (2006). The structural evolution of the Messinian evaporites in the Levantine basin. Marine Geology 230, 249-273.

Normark, W.R., (1970). Growth patterns of deep sea fans. Am.Assoc.Petrol.Geolo.Bull., v. 54, 2170-2195.

Pirmez, C., Beauboeuf, R, R.T., Friedmann, S.J. and Mohrig, D.C., (2000). Equilibrium profile and baselevel in submarine channels: Examples from Late Pleistocene systems and implications for the architecture of deepwater reservoir. Deep water reservoirs of the world: Gulf Coast Section, 782-805.

Posamentier, H.W., and Kolla, V., (2003). Seismic geomorphology and stratigraphy of depositional elements in deep water settings. Journal of Sedimentary Research, 73(3), 367-388.

Posamentier, H.W., and Walker, R.G., (2006). Deep water turbidites and submarine fans. Facies Models. SEPM, Special Publications 84, 399-520.

Reading H.G., and Richards, M., (1994). Turbidite systems in deep water basin margins classified by grain size and feeder system. American Association of American Geologists Bulletin 78, 792-822.

Richards, M., Bowman, M., and Reading, H.,(1998). Submarine fan systems I: characterization and stratigraphic prediction. Marine and Petroleum Geology 15, 689-717.

Ross, D.A. and Uchupi, E. (1997). Structure and sedimentary history of the Southeastern Mediterranean Sea-Nile cone area. AAPG Bulletin 61 (6), 872-902.

Rowan, M.G., Peel, F.J., Vendeville, B.C., 2004. Gravity-driven fold belts on passive margins. In: McClay, K.R. (Ed.), Thrust Tectonics and Hydrocarbon Systems. AAPG Memoir, vol. 82, 157–182.

Ryan, B.W.F., Stanley, D.J., Hersey, J.B., Fahlquist, D.A., and Allan, T.D., (1970). The tectonics of the Mediterranean Sea. In: Maxwell, A.E. (Ed.), The Sea, 4. Wiley, New York, 387–491.

Saller, A., Werner, K., Sugiaman, F., Cebastianti, A., May, R., Glenn, D. and Barker, C., 2008. Characteristics of Pleistocene deepwater fan lobes and their application to an upper part Miocene reservoir model, offshore East Kalimantan, Indonesia. American Association of Petroleum Geologists Bulletin 87, 541-560.

Samuel, A., Kneller, B., Raslan, S., Sharp, A., and Parsons, C., 2003, Prolific deep-marine slope channels of the Nile delta, Egypt: American Association of Petroleum Geologists Bulletin 87, 541–560.

Schattner, U., Ben-Avraham, Z., Lazar, M. and Huebscher, C., (2006). Tectonic isolation of the Levant basin offshore Galilee-Lebanon-Effects of the Dead Sea fault plate boundary on the Levant continental margin, eastern Mediterranean: Journal of Structural Geology,28, 2049-2066.

Segev, A., Rybakov, M., Lyakhovsky, V., Hofstetter, A., Tibor, G., Goldshmidt, V., and Ben Avraham, Z., (2006). The structure, isostasy and gravity fi eld of the Levant continental margin and the southeast Mediterranean area: Tectonophysics, 425, 137–157.

Shanmugam, G., (2006).Deep-water processes and facies models.Implications for sandstone Petroleum Reservoirs.Handbook of Petr4oleum Exploration and Production 5, 3-48.

Shanmugam, G., (2000). 50 years of turbidite paradigm (1950s-1990s): deep water processes and facies models-a critical perspective. Marine and Petroleum Geology 17, 285-342.

Shanmugam, G., Bloch, R.B., Mitchel, S.M., Damuth, J.E., Beamish, G.W.J., Hodgkinson, R.G., Straume, T., Syvertsen, S.E., and Shields, K.E., (1996). Slump and debris-flow dominated basin floor fans in the North-Sea: an evaluation of conceptual sequence stratigraphic models based on conventional core data. Geological Society Special Publications 103, 145-175.

Smith, R., (2004). Turbidite systems influenced by structurally induced topography in the multi sourced Welsh Basin. Geological Society, London, Special Publications, 222(1), 208-228.

Tibor, G., Ben-Avraham, Z., Steckler, M. and Fligelmann, H., (1992). Late Tertiary subsidence history of Southern Levant Margin Eastern Mediterranean Sea and its implications to the understanding of the Messinian event. Journal of Geophysical Research 97, 17593-17614.

Vidal, N., Alvarez-Marron, J. and Klaeschen, D., (2000). Internal configuration of the Levantine basin from seismic reflection data (Eastern Mediterranean). Earth and Planetary Science Letters 180, 77–89.

Wynn, R.B., Kenyon, N.H., Masson, D.G., Stow, D.A.V., and Weaver, P.P.E.,(2002). Characterization and recognition of deep-water channel-lobe transition zones. AAPG Bull. 86,1441– 1462.